ESCUELA TÉCNICA SUPERIOR DE INGENIERÍA (ICAI)

Aerodynamic design optimization based on Multi-Attribute Structured Hybrid Direct-Search. Application to industrial problems

Author: Isaac Prada y Nogueira
Director: Fernando de Cuadra
Director: Álvaro Sánchez Miralles

Madrid
March 2017

ESCUELA TÉCNICA SUPERIOR DE INGENIERÍA (ICAI)

Optimización del diseño aerodinámico basada en Búsqueda Directa Híbrida, Estructurada y Multiatributo. Aplicación a problemas industriales

Autor: Isaac Prada y Nogueira
Director: Fernando de Cuadra
Director: Álvaro Sánchez Miralles

Madrid
Marzo 2017

Acknowledgement

I thank God for the energy and motivation to have completed this PhD Thesis and for the key people in my life who have made it possible: my girlfriend, my parents, my partner José María Cancer Abóitiz and the team at KeelWit Technology: Dr. Ignacio Serrano, Pablo Cancillo and Enrique Martín.

Agradecimiento

Le doy gracias a Dios por la energía y la motivación para haber completado esta Tesis Doctoral y por haber puesto en mi vida a las personas clave que la han hecho posible: mi novia, mis padres, mi socio José María Cancer Abóitiz y el equipo de KeelWit Technology: el Dr. Ignacio Serrano , Pablo Cancillo y Enrique Martín.

Abstract

The present Thesis tackles the problem of aerodynamic shape optimization, particularly in the case of big changes of geometry. The approach proposed is a **M**ulti-**O**bjective **St**ructured **H**ybrid **D**irect **S**earch and this Thesis presents the MOST-HDS model developed for this purpose. This model is a general, automatic, flexible and robust methodology which is applicable to many different fields of aerodynamic optimization and which combines elements of gradient, genetic and swarm search. MOST-HDS is applied to two relevant and significantly different industrial cases: the design of closed wind tunnels and the inlet duct design of industrial boilers used in combined cycle power plants. The results obtained with the optimization methodology proposed show significant performance improvements over traditional designs and, moreover, innovative and non-conventional designs are obtained for certain cases, which also outperform current design guidelines. A comparison of MOST-HDS and surrogate-based optimization (using response surfaces) is presented and the advantages and limitations of each approach are discussed in detail. Finally, the algorithm developed for this Thesis is also applied to a well-known and challenging mathematical test problem (the WFG test suite) and compared to a popular, advanced Multi-Objective Evolutionary Algorithm, the NSGA-II. The results are very promising and illustrate the potential of MOST-HDS for general optimization purposes, too.

Resumen

La presente Tesis aborda el problema de la optimización aerodinámica, particularmente en el caso de grandes cambios de geometría. El enfoque propuesto es una búsqueda directa híbrida, estructurada y multiobjetivo y esta Tesis presenta el modelo MOST-HDS desarrollado para este propósito. Este modelo es una metodología general, automática, flexible y robusta que es aplicable a muchos campos diferentes de optimización aerodinámica y que combina elementos de búsqueda basada en gradiente, genéticos y enjambre. MOST-HDS se aplica a dos casos industriales relevantes y significativamente diferentes: el diseño de túneles de viento cerrados y el diseño del conducto de entrada de calderas industriales utilizadas en centrales de ciclo combinado. Los resultados obtenidos con la metodología de optimización propuesta muestran mejoras significativas respecto a los diseños tradicionales y, además, se obtienen diseños innovadores y no convencionales para ciertos casos, que también superan las directrices actuales de diseño. Se presenta una comparación de MOST-HDS y la optimización basada en modelos aproximados (utilizando superficies de respuesta) y se discuten en detalle las ventajas y limitaciones de cada enfoque. Por último, el algoritmo desarrollado para esta Tesis también se aplica a un conocido y desafiante problema de prueba matemática (el conjunto de problemas WFG) y se compara con un popular y avanzado algoritmo multiobjetivo evolutivo, el NSGA-II. Los resultados son muy prometedores e ilustran el potencial que MOST-HDS tiene, asimismo, para fines generales de optimización.

Contents

1

Chapter 1 - Introduction. Thesis motivation, objectives and contributions

According to the theory of aerodynamics and wind tunnel testing the bumblebee is unable to fly. However the bumblebee goes ahead and flies anyway—and makes a little honey every day.

Sign in a General Motors Corporation factory.
As quoted in Ralph L. Woods, The Businessman's Book of Quotations (1951).

This chapter introduces a general overview of the field of study of this Thesis and justifies the general motivation for this research work. Moreover, it illustrates the relevance of shape optimization, particularly aerodynamic shape optimization, with real-life examples. Based on this, the Thesis approach is summarized and its main objectives and contributions are presented. Furthermore, the chapter outlines the general structure of the document, to help the reader understand the sequence of the chapters. Firstly, *Section 1.1.* presents a general introduction; *Section 1.2.* puts forward the general motivation of the Thesis; *Section 1.3.* presents a general summary of the objectives and main contributions of this Thesis; finally, *Section 1.4.* describes the general structure of the document, to justify the order of the chapters and to motivate the reader to delve into the whole document.

1.1. Introduction

Complex aerodynamic components are of paramount importance both for the scientific community and for our everyday lives. From a space rocket to a high-speed train, a car or a boat of any kind, aerodynamic design optimization can yield important advantages such as higher speeds, reduced fuel consumption, better stability or a larger operation envelope.

However, aerodynamics has not always been a relevant discipline for the design of these different vehicles. Except in air and spacecraft, for which aerodynamics is the basis, for those bodies intended to travel on land or even on water, the designers did not realize the paramount importance of aerodynamic shape design.

Let us take the example of the automotive sector, highly advanced nowadays in terms of aerodynamic design.

Although during its very first stages (19^{th} century), aerodynamics was not taken into account, quite soon the automobile industry started including aerodynamic considerations in the design phase. However, the main objective was to reduce the Drag coefficient of the vehicle. A lower value of this coefficient means a better penetration of the vehicle in the air, i.e. a lower resistance and therefore a reduced fuel consumption or a higher speed. The mathematical definition for the Drag coefficient is given in the following equation[1]:

$$C_d = \frac{D}{\frac{1}{2} \cdot \rho \cdot V_\infty^2 \cdot A}$$ *Equation 1-1*

where D represents the Drag itself, i.e. the force representing the aerodynamic resistance acting on the vehicle or body along the longitudinal axis, ρ is the air density, V_∞ the air speed of the free stream and A is a reference area (normally the frontal or projected vehicle area). The Drag coefficients for a set of general body shapes are given in Figure 1–1. The strong impact of shape design can be very clearly understood from these values.

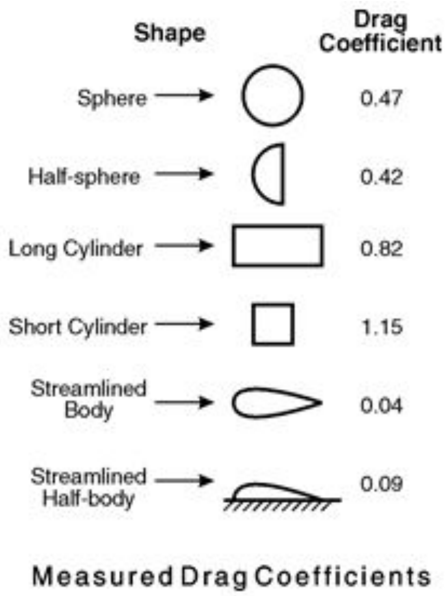

Figure 1–1 - Drag coefficients for general body shapes.

[1] Instead of "d", "x" is sometimes used as the index to refer to the Drag coefficient (C_x).

The aim of the designers was therefore to reduce the value of the Drag coefficient to decrease the value of the longitudinal force that the vehicle had to overcome in order to advance.

For example, as early as 1916, the Peugeot that won the Indianapolis 500 that year had a slightly streamlined, rather than square, rear end, to reduce the Drag of the vehicle (in Figure 1–2, this can be observed, not just in the Peugeot, car 17, but also in the car to the right of the picture).

Figure 1–2 - Darío Resta and his mechanic in the Peugeot car, which won the Indianapolis 500 in 1916.

Nevertheless, the main technical leap occurred when aerodynamic engineers began to worry about the Lift coefficient, analogue to the Drag coefficient but replacing the longitudinal aerodynamic force with the vertical aerodynamic force. More specifically, the goal of the designers was to reduce the value of the Lift coefficient, because it was responsible for the lifting force on a vehicle as its speed increased, and even to make it negative, especially for sports cars (since conventional road cars have positive Lift values, especially near the rear axle). With a negative Lift or downforce the cornering speed you can reach can exceed in more than three times the vehicle's speed without downforce (Katz [2006]).

As an example of the importance of aerodynamics in motorsport, Figure 1–3 illustrates the different trends that have been followed by aerodynamic engineers in Formula 1 throughout its history. Figure 1–4 gives examples of real cars designed following these aerodynamic trends.

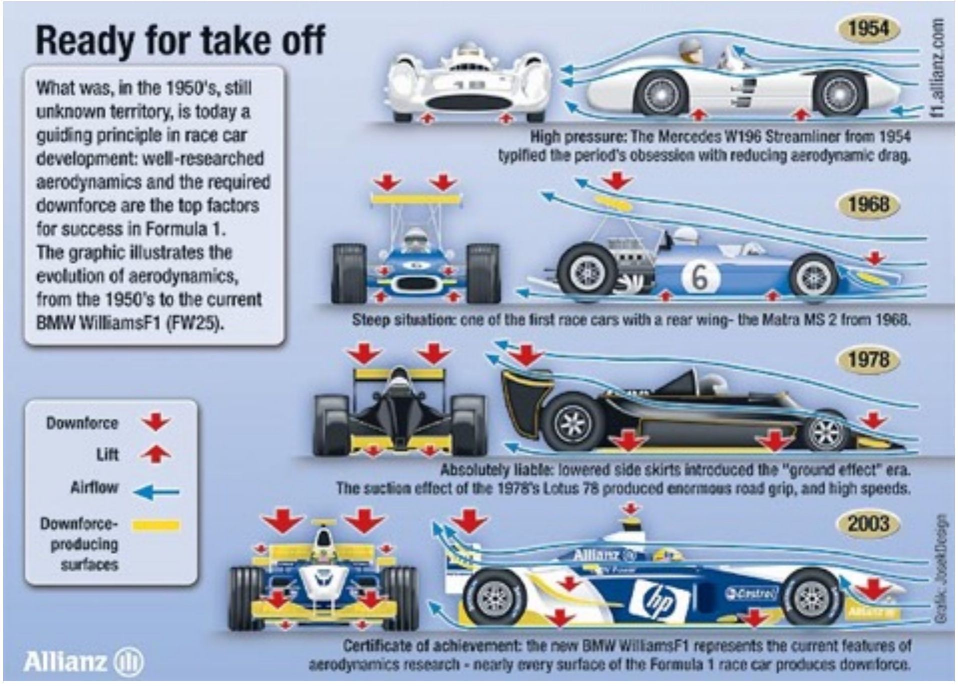

Figure 1–3 - Aerodynamic trend evolution in Formula 1 since the beginning of the competition (1950).

Figure 1–4 - Real examples of the different aerodynamic trends in Formula 1 since the beginning of the competition (1950).

For the purpose of this Thesis, it is very worth highlighting that aerodynamic shape design is not only a case of fine-tuning, but many times of qualitative modifications, as have been shown in Figure 1–3 and Figure 1–4, and even radical, non-conventional or non-intuitive designs, such as those depicted in Figure 1–5. These substantial, qualitative or even disruptive shape design modifications, here referred to as *big geometry changes*, will be taken into account in the shape optimization methodology presented in this Thesis, and this is one of the key differential elements with respect to most of works of the State of the Art.

Figure 1–5 - Examples of disruptive designs in Formula 1, either because of the wing design, or the nose design, or even the introduction of a fan for increased downforce.

In the field of aerodynamics, street cars have inherited numerous elements of the lessons learned in motorsport. Although in general they do not have wings or an aerodynamic bottom, they have incorporated elements and details which allow for a better stability of the vehicle at high speeds, when aerodynamics really counts. Other modifications aim at achieving less aerodynamic noise within the passenger compartment, less accumulation of dirt in long journeys and greater efficiency in aspects such as ventilation or cooling.

The strong evolution in aerodynamic design is by no means exclusive to motorsport or to the automotive sector. The following figures aim at showing the impact of aerodynamics in shape design in a very wide range of sectors.

Figure 1–6 - Aerodynamic design evolution of an example road car, in this case the BMW.

Figure 1–7 - Aerodynamic design evolution in the train sector. A steam high speed train, capable of maximum speeds of 160km/h and average speeds of 130km/h, compared to the most modern Talgo train, the Avril, capable of maximum speeds of 363km/h and average speeds of 330km/h.

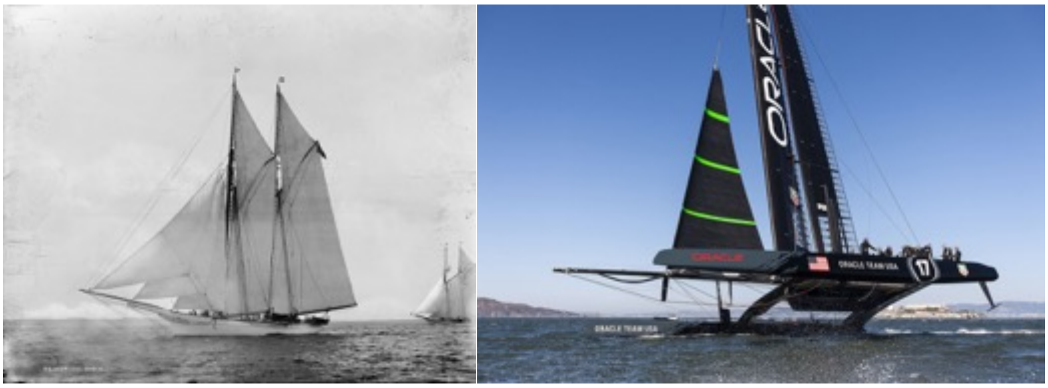

Figure 1–8 - Aerodynamic design evolution in the marine sector, in particular in the America's Cup. To the left the 1871 Defender, the Columbia/Sappho, which won that year. To the right, the 2013 winner, the Defender that year, the 17 Oracle Team USA.

Figure 1–9 - Aerodynamic design evolution in the cycling sector. A set of representative modern racing helmets are shown.

The above figures illustrate how the shape design changes over history in different sectors have been a combination of fine-tuning with qualitative or discrete leaps in design, towards new, more radical or unconventional concepts. These are non-exhaustive examples of what will be referred to as *small* versus *big* geometry changes (Chapter 2), a concept of great importance for this Thesis.

1.2. Thesis motivation

From Section 1.1. above it is clear that aerodynamic shape design is highly relevant in general body design in many different sectors. It is also evident how the design has been moving both in small and in big jumps from one design concept to the following one, up until the present day.

Having said this, it is also worth highlighting that aerodynamics is not a trivial area of research and the governing equations of the different types of flow fields are too complex to be solved analytically. Figure 1–10 depicts the 3D velocity streamlines for an example complex aerodynamic body geometry. Many highly complex flow phenomena (vorticity, flow detachment, backflow, etc.) can be observed and illustrate the complexity of aerodynamic analyses.

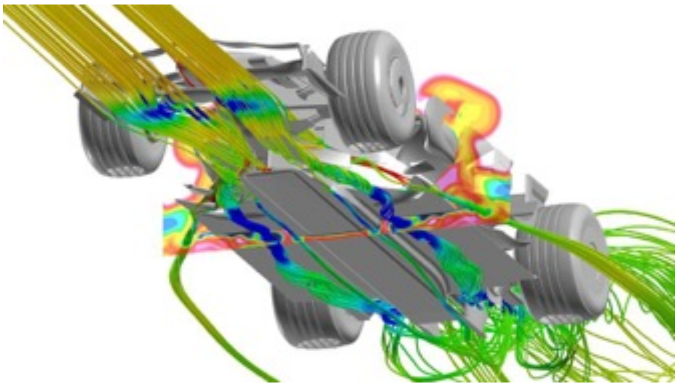

Figure 1–10 - Example 3D velocity streamlines for a complex aerodynamic body, in this case the floor of a motorsports car.

Aerodynamic research has three main tools to evaluate the performance of a particular shape design (for a detailed description of them, for the automotive sector, refer to Joseph Katz [2006]):

1. **Computer analysis**: by means of numerical analysis (Computational Fluid Dynamics, CFD), which can either follow a direct approach of the high-fidelity model[2] (direct simulation) or it can make use of a surrogate (or approximate) model (a good list of the different general surrogate techniques can be found in Robinson et al. [2006]).

2. **Wind tunnel testing**: Figure 1–11 shows three examples of wind tunnel testing for Volkswagen cars of different years.

3. **Testing in the real environment**: this can mean road testing, on-sea testing, flight testing, depending on the body to be tested.

[2] The so-called high-fidelity model, in any case, will also include a set of simplifications of the governing equations, unless performed via Direct Numerical Simulation, which is too time-consuming in most cases.

Figure 1–11 - Wind tunnel testing for three VW cars of different years. Velocity streamlines are simulated with a smoke generator. Changes in the flow field can be observed between the different car models.

Taking all the above into account, the motivation of this Thesis is to propose a general method to optimize shape design with an automatic, flexible and robust procedure which can be applied to many different real industry applications. A strong aspect of this Thesis motivation is the fact that the general method developed should be able to handle not only small, but also big, changes to the body geometry, since they can have an important impact on performance. These big changes are currently handled mostly by trial and error or manual procedures, while computer optimization has been limited to cases of small geometry changes or to fine-tuning (refer to the State of the Art, in Chapter 3).

1.3. Thesis approach, main objectives and contributions

The problem this Thesis deals with is the multi-attribute or multi-objective aerodynamic shape optimization of real geometries in different fields of application, subject to a set of constraints, and taking into account both small and big changes of the geometry of interest.

The approach proposed for the problem described above will be the development of a general method based on a **M**ulti-**O**bjective **St**ructured **H**ybrid **D**irect **S**earch optimization algorithm (referred to as **MOST-HDS**).

1.3.1. THESIS OBJECTIVES

The Thesis main and secondary objectives are the following:

1. Present a structured, detailed and commented review of the applicable State of the Art.
2. Propose how a problem of shape design can be defined in a most suitable way to apply not only advanced optimization schemes in general, but, in particular, multi-attribute/objective, structured, hybrid, direct search (MOST-HDS). This objective includes the following secondary objectives:
    a. Definition of truly independent variables.
    b. Definition of attributes or objectives to be optimized.
3. Design the MOST-HDS algorithm architecture and develop a computer tool to apply it to real problem cases.
4. Validate the MOST-HDS general method presented to show its broad-scope applicability (not only to shape design optimization):
    a. Mathematical validation: test suite benchmark validation
    b. Validate with real industry cases:
        i. Wind tunnel case.
        ii. Industrial boiler case.
5. Compare the proposed method to other methods and approaches used in the State of the Art (surrogate models and other commonly-used optimization algorithms).

1.3.2. THESIS CONTRIBUTIONS

Based on this set of main and secondary objectives, the following is a detailed list of this Thesis contributions, which will be presented again in the conclusions chapter (Chapter 8). They are listed in decreasing order of relevance, from the author's perspective:

1. Development of MOST-HDS, a general model for multi-attribute optimization of aerodynamic shape design which is a contribution because:

    a. It is capable of handling big geometry changes, which is very rarely addressed in literature

    b. It is applicable to a wide range of real life problems, both industrial (shape design optimization) and mathematical (optimization of complex functions modelling real problems). As commented below, the results presented in this Thesis show that the methodology yields performance improvements over currently used optimization algorithms and improved geometry designs, with important reductions of objectives such as energy consumption or material cost.

    c. This model exploits the potential of direct search and, in particular, builds a hybrid direct search architecture, combining genetic, gradient and swarm search intelligence. This approach is novel in itself and, in particular, in the area of aerodynamic shape optimization. Once again, the improvement shown in the results supports the fact that MOST-HDS is an interesting and valuable contribution to the current State of the Art.

    d. The search carried out by MOST-HDS is structured and this is one of the key aspects of the model. This constitutes an additional contribution of this Thesis to the field of aerodynamic shape optimization because such a full use of structured optimization has not been used up to this date.

2. Full implementation of an automatic workflow for optimization of CFD problems. MS Excel and a VBA code (Visual Basics for Applications) are coupled to ANSYS FLUENT for this Thesis, although the optimization methodology can easily be translated to MATLAB, C++, Python or other programming languages (it was considered that the integration with ANSYS would be easier and more efficient using MS Excel). MOST-HDS is thus implemented in a computer tool connected to a CFD solver (ANSYS FLUENT in this case, but it can be a different solver). The MOST-HDS tool controls the optimization process, and calls the solver every time a candidate design point has to be evaluated. This requires finding a smart geometry parameterization to represent body shapes with an efficient set of independent design variables. In every evaluation, these design variables are automatically mapped to other variables in the CFD solver, which are not so intuitive but are understood by the CFD program. This is a contribution to the State of the Art since the automatic workflow is a robust method which reduces a project's cycle time or increases the number of design points which can be evaluated within a fixed time.

3. Application of the MOST-HDS model to two real-life problems: closed wind tunnels, such as those used for testing and leisure, and industrial boilers for combined cycle power plants. This contributes to the State of the Art because the results obtained show that MOST-HDS can yield surprising, non-intuitive and unconventional designs which perform better than traditional concepts.

4. Regarding the industrial boiler optimization, the contribution of this Thesis is twofold: on the one hand, it shows that there is substantial room for improvement in the shape design of the inlet ducts of Heat Recovery Steam Generator (HRSGs), in terms of achieving a lower pressure drop, a higher velocity uniformity and an important cost reduction of the unit; on the other hand, it shows how the application of the MOST-HDS algorithm, applicable in many fields for aerodynamic shape optimization involving big geometry changes, can find these improved designs, which can be quite unconventional and non-intuitive. The results obtained for two HRSG families show that there are optimum trade-off design points with simultaneous reductions in pressure drop of up to 20-25%, in lateral surface of up to 38% and in length of up 16%, while having comparable velocity uniformities to the existing designs.

5. Furthermore, it is also shown in this Thesis that the double angle design of HRSG inlet ducts, which is the current design trend, is not always better than the single angle design, which was the traditional guideline followed.

6. Analysis of the limitations of surrogate models (mainly response surfaces), which are optimization techniques widely used and very popular nowadays. This Thesis shows that MOST-HDS beats surrogate models in the aerodynamic optimization of complex components (wings, high-speed train noses, automotive designs, etc.), especially when big changes of geometry are involved. A detailed comparison is carried out for the specific example of the industrial boiler case. It is difficult in many cases for any surrogate model (be it by means of data fits and response surfaces, or by reduced order models or hierarchical or multi-fidelity models) to be an accurate approximation if the objective function is strongly non-linear, having to represent phenomena such as flow separation, and combining variables of different types (discrete, continuous). This is very much the case when big variable changes are allowed in aerodynamic optimization problems, and when a whole body (wind tunnel, for instance) is optimized, and not only certain parts or components of it.

7. Benchmark results of MOST-HDS when applied to an exhaustive mathematical optimization test suite, in order to compare its performance with other widely used general-purpose optimization algorithms. Hence the potential of MOST-HDS is shown, not only for shape design optimization, but also for other applications. The results show that MOST-HDS can be more competitive than modern optimization algorithms.

8. Exhaustive review of the applicable State of the Art regarding design optimization, with an easy-to-follow structure and relevant highlights on each of the research works included. This can be used in the future by other researchers to have a detailed overview of the State of the Art in this area of expertise.

1.4. Structure of this document

This document aims to present the research work carried out for this Thesis in a rigorous yet comprehensive and easy-to-read manner. Once Chapter 1 has set the foundations for the Thesis, describing its motivation, main objectives and contributions, the rest of the document is organized as follows:

- **Chapter 2 – Problem description and general approach** describes in more detail the problem addressed.

- **Chapter 3 – State of the Art review** is a thorough review of the State of the Art of design optimization, especially in the area of aerodynamics.

- **Chapter 4 – Problem definition** presents the detailed problem definition and the geometry parameterization proposed, for the two industrial examples presented, to illustrate the applicability of the method for widely different fields.

- **Chapter 5 – The MOST-HDS optimization model** offers and in-depth explanation of the general model and optimization algorithm proposed by this Thesis.

- **Chapter 6 – Results obtained** presents the results section and shows the applicability of MOST-HDS for two aerodynamic shape design problems: closed wind tunnels for testing and other purposes, and industrial boilers used in combined cycle power plants. Moreover, it analyses the performance of MOST-HDS as a general purpose optimization algorithm, applying it to a mathematical test suite used for benchmark studies in the State of the Art.

- **Chapter 7 – Comparison to surrogate models** compares the results obtained by MOST-HDS with a very popular optimization approach, surrogate models, used for problems with time-consuming evaluations. This chapter will show the limitations of surrogate models when applied to shape design problems with big geometry changes.

- **Chapter 8 – Conclusions** summarizes the main conclusions, the results obtained, the Thesis contributions, the limitations for MOST-HDS and the future work to be carried out, based on the results of this research.

- **APPENDIXES**
    - **A – Illustration of the MOST-HDS process**
    - **B – Important notes on mesh sensitivity and mesh quality**

List of Figures

Figure 1–7 - Aerodynamic design evolution in the train sector. A steam high speed train, capable of maximum speeds of 160km/h and average speeds of 130km/h, compared to the most modern Talgo train, the Avril, capable of maximum speeds of 363km/h and average speeds of 330km/h.

Figure 1–8 - Aerodynamic design evolution in the marine sector, in particular in the America's Cup. To the left the 1871 Defender, the Columbia/Sappho, which won that year. To the right, the 2013 winner, the Defender that year, the 17 Oracle Team USA.

Figure 1–9 - Aerodynamic design evolution in the cycling sector. A set of representative modern racing helmets are shown.

Figure 1–10 - Example 3D velocity streamlines for a complex aerodynamic body, in this case the floor of a motorsports car.

Figure 1–11 - Wind tunnel testing for three VW cars of different years. Velocity streamlines are simulated with a smoke generator. Changes in the flow field can be observed between the different car models.

2

Chapter 2 - Problem description and general approach

Aerodynamics is for those who don't manufacture good engines.

Enzo Ferrari.

This chapter presents the general problem of aerodynamic shape optimization and the approach followed in this Thesis. It mentions other alternative approaches used by other authors (refer to the State of the Art in Chapter 3 for more detail). In particular, this chapter gives an initial global overview of the hybrid structured direct search approach. Additionally, for the sake of clarity, it defines the concept of small v. big geometry change. Firstly, *Section 2.1.* offers a brief introduction; *Section 2.2.* describes the main problem addressed by this Thesis; *Section 2.3.* outlines the proposed general approach for this work; *Section 2.4.* illustrates the difference between small and big geometry changes, for the purpose of this Thesis, with a real example case which will be presented thoroughly in Chapter 6; and finally, *Section 2.5.* offers a set of final remarks to conclude the chapter.

2.1. Introduction

As Chapter 1 has introduced, the field of aerodynamic shape design in different sectors (automotive, motorsport, aeronautics, high-speed trains, etc.) has undergone different stages of development. At first not well understood, and with an underestimated impact on overall body design, aerodynamics started growing in importance and it is now one of the key areas of engineering design in many fields.

Trial and error has been the common design trend for many decades, based on the designer's experience. Thereafter the aerodynamic performance of each design was at first calculated using either simplified analytical equations or empirical correlations derived from test data. Currently most designs require either Computational Fluid Dynamics (CFD) solvers, or costly wind tunnel tests, or even testing in the real environment.

Shape design optimization has gradually grown in use by designers and engineers, but, in most cases, it starts with a first stage of trial-and-error-based selection of candidates and then a fine-tuning optimization of the best designs. In general, when optimization is used, only small geometry changes are addressed. However, a complete, automatic, flexible and robust methodology for aerodynamic shape design optimization, able to analyze big geometry changes, has not been presented up to date, as far as we know.

This Thesis presents an optimization methodology of this kind, which can be applied to many fields in which aerodynamic design is important.

The main contribution of this chapter is to describe the difference between small and big geometry changes, for the purpose of this Thesis, because there is very little work in the literature focused on shape optimization considering big geometry changes.

2.2. Characterization of the type of problem

The methodology presented in this Thesis is a multi-attribute/objective, structured optimization procedure, based on hybrid direct search (MOST-HDS). Structured refers to the fact that the complete optimization problem will be divided into simpler optimization sub-problems, following a structured architecture. Structured optimization is also referred to as sequential optimization, multi-level optimization, nested optimization or hierarchical optimization (Cuadra [1990], Babu [2014], Held et al. [2006], Robinson et al. [2006], Zhou et al. [2015], Liu and Zhang [2014] or Nuñez et al. [2012]).

The optimization architecture developed here is ideally suited to problems with the following characteristics, as explained for example in Cuadra (1990) and Prada-Nogueira et al. (2015):

1. The number of independent variables (degrees of freedom) is high.
2. The vector of independent variables does not have a fixed dimension; its dimension depends on the value of certain variables.
3. Independent variables are of different mathematical kinds (discrete/continuous), and have a different (stronger or weaker) influence on the final design. These two facts lead to a hierarchy of variables.
4. The number of design constraints is high.
5. There are attributes of interest to the engineer that cannot be reduced efficiently to a single objective function because they are mutually conflictive, or not comparable. Hence, the problem is truly multi-attribute.

6. Complex evaluation methods such as CFD solvers – not only analytical equations – must be used, so the evaluation process (defined by a set of linkage functions) is complex and slow.

In a multi-attribute, structured optimization, the following entities must be thoroughly defined: parameters, independent variables, attributes, linkage functions, constraints, and evaluation process (refer to Chapter 4 for the detailed definition of these elements).

Parameters are quantities of fixed value, being that value fixed either externally by the user or internally by the optimization model within a particular sub-problem. For example, the level of discretization of the geometry model for the aerodynamic body of interest (as will be explained in more depth in Chapter 4), or the stopping criteria (maximum function evaluations, maximum time, etc.). Eres et al. (2014), for instance, present an interesting and novel methodology to introduce customer requirements in the engineering design process, applied to the aerospace sector.

Variables are quantities that can change their value. They may be independent or dependent, but only independent variables are relevant from an optimization point of view, since dependent variables are automatically computed inside a black-box evaluation process. Independent variables (also called degrees of freedom) can take any value among a particular group (positive numbers, binary, etc.); for example, the length of a section of the geometry (continuous variable), or the geometry type of a particular transverse section of the model: circular, rectangular, square, etc. (discrete variable). Explicit constraints may limit their range of values a priori and, of course, other constraints of any kind will bound the feasible search space.

Attributes, or objectives, are special dependent variables which allow for the comparison of one solution to another (i.e. one geometry design to a different design). Here they can refer to cost, size, flow quality, aerodynamic performance, or any other magnitude of interest for the user.

To calculate the values of the various attributes of interest from the values of the independent variables and the parameters, a set of equality constraints or linkage functions is required. This set of functions is structured as an evaluation process, i.e. a black-box process that computes the attributes and constraints for each combination of parameters and independent variables. This Thesis focuses on problems for which the evaluation process is complex and time consuming, because it relies on CFD computations, although the methodology presented can be applied to other problems (refer to Chapter 6 for an example of the results obtained when the methodology is applied to different kinds of problems).

Finally, there will also be a body of inequality constraints, referred to simply as “constraints” in this work. They set the limits for certain variable combinations and hence determine how far off a particular solution is from the space of feasible solutions. In our cases of interest, the constraints are usually variable value ranges or geometry absurdity limitations. It is often useful to define special attributes to quantify the status of constraint violations, i.e., the degree of feasibility of a solution.

2.3. General approach

The approach proposed in this Thesis is a multi-attribute, structured optimization based on hybrid direct search (i.e. direct evaluation of each candidate design and not approximation of its attribute values by any procedure).

The optimization algorithm developed combines genetic, gradient and swarm search intelligence in every iteration, as will be explained in depth in Chapter 5. This novel optimization method allows for an intelligent and efficient direct search in complex aerodynamic problems with big geometry changes. This optimization methodology is applicable to advanced aerodynamic design in cars, aircraft, high-speed trains, etc.

2.4. Definition of small versus big geometry changes

For the purpose of this Thesis, it is important to introduce the difference between small and big geometry changes in the context of aerodynamic shape design optimization. As shown in the whole set of results presented (Chapter 6), the MOST-HDS optimization algorithm can also be applied successfully to problems of small geometry change, and even to other fields quite different to aerodynamic design. However, it is in problems with big geometry changes that MOST-HDS fills a gap present in the State of the Art.

The aim of this section is not to define the terms *small* and *big* in a strict formal way, but rather to illustrate the difference with example figures to help the reader have a clear idea of the meaning of each term.

The concept of big geometry change includes not only a big modification in body geometry, but also a considerable change of position of discrete elements present within the geometry (an engine in the case of an airplane wing, a fan or the test section of a wind tunnel, etc.).

The interest of analyzing big geometry changes stems from the fact that taking this type of changes into account for the optimization can yield improved yet not conventional, or non-intuitive, designs, as will be shown in Chapter 6.

The following figure shows an example transition duct for an industrial application, namely the entrance to a particular kind of industrial boiler, called Heat Recovery Steam Generator (HRSG), which is used in combined cycle power plants. The geometry is quite simple and illustrative and is therefore used as an example. Figure 2–1 represents a possible baseline design for this duct's shape optimization. Figure 2–2 is a sample of possible designs which current commonplace shape optimization techniques would consider (be it by means of direct search, surrogate models, adjoints, etc.). This type of design changes fall within the category of small geometry changes.

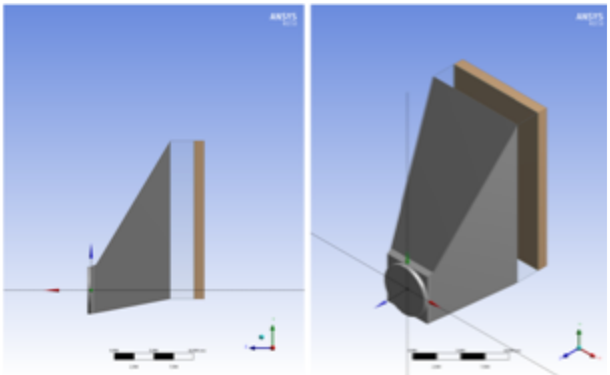

Figure 2–1 - Illustrative example of geometry which represents a possible baseline design, to show the difference between small and big geometry changes for shape optimization.

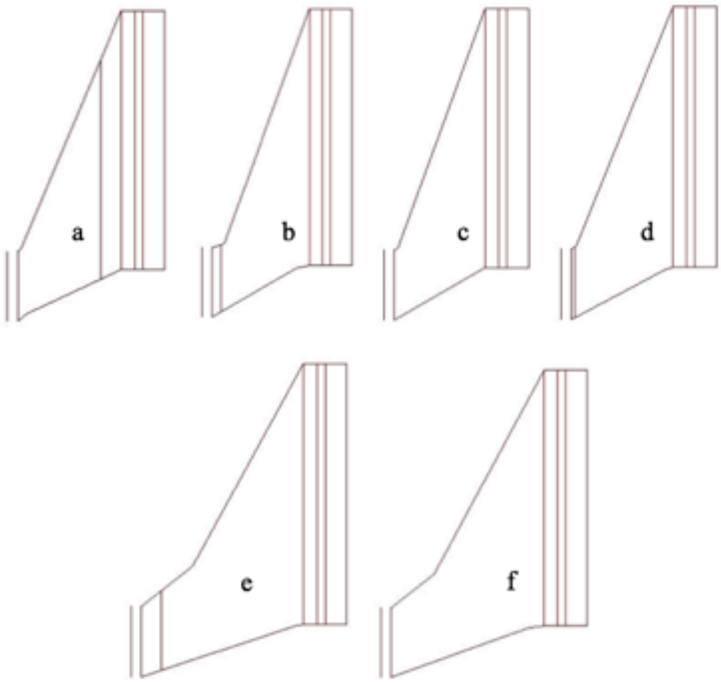

Figure 2–2 - Example designs which are considered small geometry changes with respect to the baseline design (design "a"), shown in Figure 2–1.

Figure 2–3 illustrates a selection of candidate design points which are considered big geometry changes – with respect to the baseline design – for the purpose of this Thesis. Some of these more radical or unconventional designs have proved to yield very good, yet unexpected, results (refer to Chapter 6). Finally, Figure 2–4 shows 3D views of some of these example candidate designs with big geometry changes.

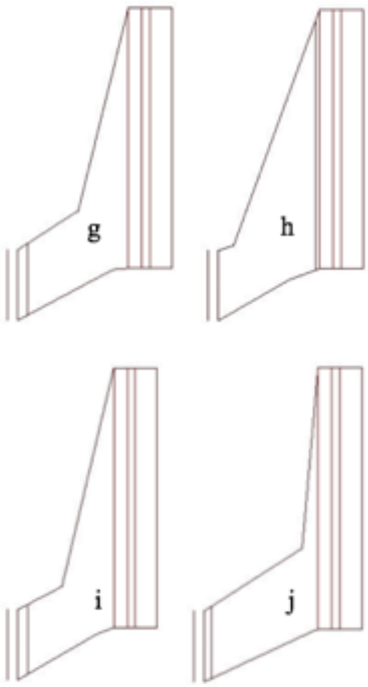

Figure 2–3 - Example designs which are considered big geometry changes with respect to the baseline design (design "a"), shown in Figure 2–1.

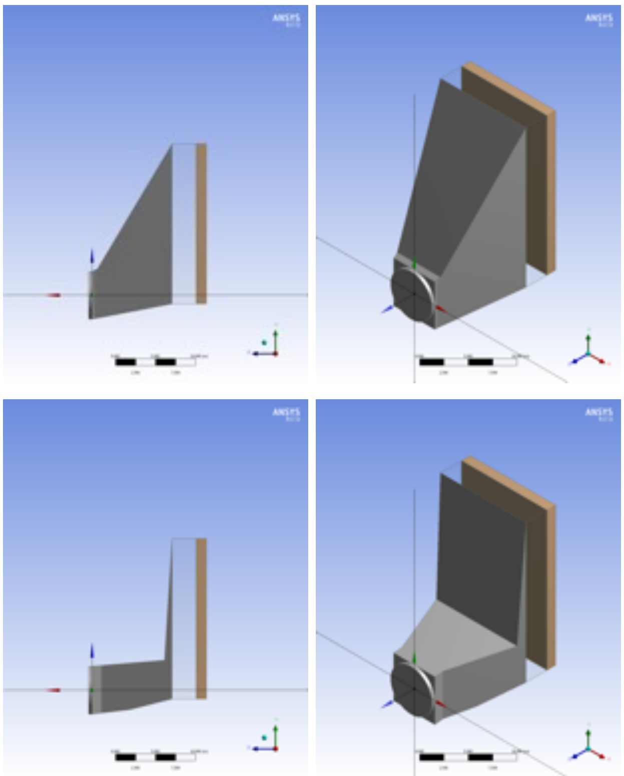

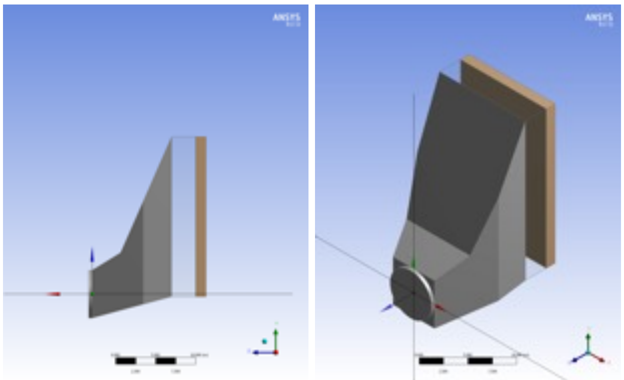

Figure 2–4 - Side views and 3D views of different candidate designs for an example shape-optimization problem with big geometry changes.

2.5. Final remarks

This chapter has characterized the type of problem that this Thesis addresses. Moreover, it has presented a key distinction for the purpose of this research, which is the difference between small and big geometry changes. This distinction if of high importance for this Thesis, since one of its contributions is that it can consider big geometry changes in problems of shape optimization and hence yield optimum designs which are non-intuitive, unconventional, and which have better performance than current designs.

List of Figures

3

Chapter 3 - State of the Art review

If someone tells you there is a rule, break it. It is the only way to move forward.

Hans Zimmer.

This chapter presents a thorough review of the applicable State of the Art. Firstly, *Section 3.1.* presents the structure and classification criteria used for the State of the Art review; *Sections 3.2. to 3.4.* analyze the applicable State of the Art; finally, *Section 3.5.* summarizes the main conclusions regarding the State of the Art review, as well as the location of this Thesis contributions within the State of the Art.

3.1. Introduction and classification criteria

The present Thesis tackles aerodynamic design optimization using the MOST-HDS general model, which proposes a Multi-Objective Structured Hybrid Direct Search for the optimization process.

This chapter will classify the relevant, applicable research work in the existing State of the Art as follows, from a general to a more particular field of study:

1. **Metaheuristic optimization in general**: this section will be less exhaustive, since it covers a much broader spectrum of research. It will discuss papers on optimization approaches which will be compared to the approach followed by MOST-HDS.

2. **Aerodynamic shape or design optimization in general**: this includes papers of different areas of research within general aerodynamic shape design. A special emphasis is made in the comments to clarify whether the different papers take into account only small geometry changes, or if they consider both small and big geometry changes. In particular, the following aspects will be reviewed:

    a. Geometry parameterization techniques: Bézier curves, B-splines and Free Form Deformation.

b. Design of Experiments (DoE) technique used.

c. Advanced meshing: structured v. unstructured meshes, overset meshes, mesh morphing.

d. Evaluation scheme: direct search v. metamodels or surrogate models (Response Surface Methodology (RSM), Reduced Order Models (ROM) or hierarchical modelling).

e. Optimization procedure: structured optimization, gradient-based methods (Adjoint Methods, Sequential Quadratic Programming (SQP), etc.), non-gradient-based methods (Genetic Algorithms (GAs), Simulated Annealing (SA), etc.), hybrid algorithms.

f. General problem complexity: size of space of variables considered for search (i.e. big v. small geometry changes), number of variables, number of constraints, etc.

3. **Aerodynamic shape or design optimization for the industrial cases analyzed**: the different approaches in the area of aerodynamics will be described, specifically for the industrial applications for which detailed results are presented in this Thesis: closed wind tunnels and industrial boilers for combined cycle power plants. In this section it is worth highlighting if the research papers analyzed focus on a local optimization or if they carry out a global optimization of the whole shape of a particular body.

With respect to all these fields of the State of the Art, the specific contributions of this Thesis, which are summarized again at the end of the chapter with a series of scatter plots, are the following:

1. **Metaheuristic optimization in general**: this Thesis presents the MOST-HDS tool, which is highly competitive and can outperform other advanced and commonly-used general-purpose optimization algorithms, as shown in Chapter 6 when applying MOST-HDS to a challenging mathematical test problem.

2. **Aerodynamic shape or design optimization in general**:

   a. This Thesis can handle big geometry changes and can yield very innovative designs, with improved performance. Most of the literature focuses only on small geometry changes or fine-tuning.

   b. The tool developed uses structured optimization, which has not been used so fully up to date in aerodynamics.

c. MOST-HDS follows a direct search approach, which is shown to beat surrogate-based optimization (using response surfaces) for the types of problems addressed by this Thesis.

3. **Aerodynamic shape or design optimization for the industrial cases analyzed**:

   a. **Wind tunnels**: this Thesis considers a wide variety of tunnel configurations, not only 90° corners, rectangular ducts and multi-fan designs. It aims at exploring big geometry changes, which can improve the performance of more traditional design concepts. It focuses on true optimization of the full wind tunnel body, and not only certain parts of it, such as corners or the main nozzle. Moreover, it considers different relative positions of the various elements of the wind tunnel (mainly test section and fan system).

   b. **Industrial boilers**: in this field, the Thesis contributes because it carries out a more extensive design exploration of possible candidate points than the works found in literature. Consequently, it explores unconventional designs which, in some cases, show better performance than boilers designed following traditional trend-lines. Finally, based on the extensive design exploration, MOST-HDS carries out a true and complete optimization. In the State of the Art, most authors limit their work to exploring a reduced set of design candidates. This allows this Thesis to yield important performance improvements (refer to Chapter 6).

3.2. State of the Art of general metaheuristic optimization

The first section of this State of the Art chapter is focused on general optimization research work which is worth analyzing in the context of this Thesis.

Because the MOST-HDS model developed in our research work proposes a multi-attribute, structured optimization based on hybrid direct search, let us analyze the State of the Art of the different aspects involved in the followed approach.

The research on multi-objective optimization is too extensive and covering a wide range of fields and thus we will not aim at presenting a review on this area in this document. Instead, we will commence by focusing on research using structured optimization. The two main concepts of this optimization methodology are: a) hierarchy of variables and b) optimization phases. This approach, including direct search in most cases, has been used in other fields (Cuadra [1990]), but not yet in aerodynamics, or at least not as thoroughly as proposed in this Thesis.

If we only focus on the area of optimization using different phases (or levels) there is relevant research work. In most cases it is combined with the use of highly-detailed and low-detailed models for the different stages (also referred to as high-fidelity and low-fidelity models). A first relevant example is Lyu et al. (2014), which uses a multi-level approach to reduce the computational cost for their problem of optimization applied to the Common Research Model Wing Benchmark. Additional good examples, applied to airfoil shape optimization, are Marduel et al. (2006) and Robinson et al. (2006). This latter explains, for instance, different mapping techniques to find the best set of high-fidelity variables corresponding to a set of low-fidelity variables and vice versa. They propose a methodology of optimization combining low-fidelity and high-fidelity models and they obtain reductions in the number of evaluations of the high-fidelity model of up to 40% using Proper Orthogonal Decomposition (POD) mapping. This paper uses surrogate models and relies on papers such as Eldred et al. (2004) to consider second-order corrections for their surrogate-based optimization.

An area in which optimization divided into phases is widely used is Very Large Scale Integration (VLSI) systems. Babu (2014) describes the different optimization levels whereas Held et al. (2006) states that the traditional methods of hierarchical optimization (divide into optimization subproblems to reduce the search region) are not the best option. They propose a flat methodology, in which they constrain as little as possible the search region of the optimization algorithms.

Other interesting contributions are included here. Zhou et al. (2015), for a method to obtain design alternatives from a pre-existing or base design and for the use of metamodels to switch from a nested optimization structure to a single-loop optimization. Liu and Zhang (2014), for the use of a decoupling strategy to obtain an equivalent single-layer optimization model from their original nested optimization problem. Nunez et al. (2012), in which optimization workflows are analyzed and reformulated.

Regarding sequential – not strictly speaking multi-phase – optimization, Du and Chen (2004) use a decoupling strategy to transform a double-loop optimization problem, typical of optimization with uncertainty, to a single-loop optimization, but they do not decouple the optimization problem itself; they only separate the optimization and probabilistic analyses.

Moving on to the topic of hybrid search strategies and, more specifically, to hybrid direct search, it is worth highlighting the novelty of the proposed MOST-HDS approach. This novelty stems from the fact that MOST-HDS combines elements of all types of algorithms (in particular, genetic, gradient and swarm search techniques) in every phase. In contrast, most other authors switch from one type of algorithm to the other depending on how the optimization is advancing, switching for instance from gradient-based to non-gradient-based algorithms (relevant examples are Guliashki [2008], Hegazi et al. [2002] or Hsiao et al. [2001]).

As opposed to the use of direct search or direct optimization techniques (which rely on the direct evaluation of a full-order model of the problem of interest), surrogate-based evaluation and optimization have become very popular in recent years to reduce the number of evaluations and/or the time consumed for these evaluations. They do so by developing simplified models of the full-order model. These simplified models, as explained very well in Robinson et al. (2006), can be of a data fit type (such as response surfaces) or of a Reduced Order Model (ROM) type or, finally, of a hierarchical model type.

Given the amount of research carried out in this area, and the interest of the debate between direct search and surrogate-based optimization, Chapter 7 of this Thesis is wholly devoted to the comparison of the results of both approaches for one of the industrial cases presented in this research.

Washabaugh et al. (2012) give novel approaches regarding surrogate (in this case reduced order) models, for example. They rely on local instead of global Reduced Order Bases (ROBs), and they obtain better time reductions and improved accuracy. Schaumont and Verbauwhede (2004), on their side, use simplified models of the real model. They call these abstracted models. They also use partial evaluation, i.e. the use of design properties to specialize the simulator. They improve their optimization tools by knowing how the design works, similarly to what is proposed in this Thesis. They also carry out optimization at different levels and with various algorithms.

Other very relevant references in the area of surrogate-based optimization are described next. Su et al. (2016) is a good example of the use of modal-based optimization for the wing shape of highly flexible morphing aircraft. Walton et al. (2013) is especially interesting for their focus on the use of surrogate models for unsteady simulations; in particular, they use a combination of proper orthogonal decomposition and radial basis functions for three-dimensional unsteady compressible inviscid flows over an oscillating ONERA M6 wing, and they report large reductions in computation time without significant losses in accuracy. The work by Krajnovic (2007), for its application to vehicle shape optimization. The paper by Robinson et al. (2006), particularly interesting for its application to airfoil shape design.

In addition, there is also very valuable work in the use of specific alternative evaluators, not necessarily to carry out a computer-based optimization, but rather to merely compare the performance of different solutions, as the work carried out for this Thesis did in its first stages. An area of particular interest for this is game simulation, in particular chess evaluators. Edelkamp and Schroedl (2011) and Fürnkranz and Kubat (2001) offer an interesting insight into the importance of evaluators in game tree search applied to chess.

Optimization problems similar to the one presented in this paper –in general terms- are addressed next. Kelly et al. (2010) introduces a method to quantify user preference of a particular shape design into the objective function (quite different to the method used by Takagi [2001], Interactive Evolutionary Computation, in which evaluations are carried out directly by humans because they relate to feelings or preferences, which cannot be easily quantified). Xiao et al. (2011) or Yoshimura et al. (2013). Goit and Meyers (2015) uses a conjugate-gradient optimization method in combination with adjoint, large-eddy simulations for the determination of the gradients of the cost functional, in order to maximize a wind farm's energy extraction. Sicilia-Montalvo et al. (2015) proposes a multi-objective optimization with ant colony methodologies for the optimum operation of long haul freight transportation. Izraelevitz and Triantafyllou (2014) presents a model-based optimization approach. Finally, Hoffenson et al. (2015) introduces sustainability and environmental impact quantification of design alternatives.

Moreover, this Thesis presents the benchmark results of the application of MOST-HDS to one of the most challenging -as well as comprehensive- mathematical test problems found in literature (Huband et al. [2006]) and the comparison to the results obtained with a well-known Multi-Objective Evolutionary Algorithm (MOEA), NSGA-II, to this same test problem. Very interesting observations are made in Chapter 6. This helps support the potential of MOST-HDS for general-purpose optimization and it shows its advantages and limitations, as well as those of NSGA-II.

In the field of test problems, some major examples that can be found in literature include:

1. *ZDT*: 6 real-valued problems from Zitzler et al. (2000)
2. *DTLZ*: 5 unconstrained, scalable real-valued problems from Deb et al. (2001)
3. *LZ*: 9 real-valued problems from Li and Zhang (2009)
4. *CEC2009*: 13 unconstrained and 10 constrained real-valued problems from the Congress on Evolutionary Computation (CEC 2009) competition
5. *WFG*: 9 scalable, real-valued problems by Huband et al. (2006)
6. *BBOB-2016*: 55 bi-objective problems from the Black Box Optimization Benchmarking (BBOB) workshop hosted at the Genetic and Evolutionary Computation Conference (GECCO 2016)
7. Others, such as knapsack, NK-landscapes, etc.

Among the researchers having used the WFG test frame, it is worth mentioning here the Thesis by Zhao (2007) and the work by Bradstreet et al. (2007), for their comparison of the performance of various algorithms when applied to the WFG test problems.

Concerning the most modern MOEAs that can be found in literature, one of the largest libraries available currently, the MOEA framework[3] presents Table 3–1. This table is included, given the great amount of work and the popularity of MOEAs for many fields of optimization. It can prove a valuable review of MOEAs for authors interested in this area.

MOEA	DESCRIPTION
AbYSS	Multiobjective Scatter Search
Borg MOEA	Adaptive Multioperator Search with ε-Dominance and ε-Progress Triggered Restarts
CellDE	Cellular Genetic Algorithm with Differential Evolution
CMA-ES	Covariance Matrix Adaption Evolution Strategy
DBEA	Improved Decomposition-Based Evolutionary Algorithm
DE	Differential Evolution (Single Objective)
DENSEA	Duplicate Elimination Non-dominated Sorting Evolutionary Algorithm
ECEA	Epsilon-Constraint Evolutionary Algorithm
ES	Evolution Strategies (Single Objective)
ε-MOEA	ε-Dominance-based Evolutionary Algorithm
ε-NSGA-II	NSGA-II with ε-Dominance, Randomized Restarts, and Adaptive Population Sizing
FastPGA	Fast Pareto Genetic Algorithm
FEMO	Fair Evolutionary Multi-objective Optimizer
GA	Genetic Algorithm with Elitism (Single Objective)
GDE3	Generalized Differential Evolution
HypE	Hyper-volume Estimation Algorithm for Multi-objective Optimization
IBEA	Indicator-Based Evolutionary Algorithm
MOCell	Multi-objective Cellular Genetic Algorithm
MOCHC	Multi-objective CHC Algorithm

[3] www.moeaframework.org (last verified on February 2017).

MOEA/D	Multi-objective Evolutionary Algorithm with Decomposition
MSOPS	Multiple Single-Objective Pareto Sampling
NSGA-II	Non-dominated Sorting Genetic Algorithm II
NSGA-III	Reference-Point-Based Non-dominated Sorting Genetic Algorithm
OMOPSO	Multio-bjective Particle Swarm Optimization
PAES	Pareto Archived Evolution Strategy
PESA2	Pareto Envelope-based Selection Algorithm
Random	Random Search
RSO	Repeated Single Objective Algorithm
RVEA	Reference Vector Guided Evolutionary Algorithm
SEMO2	Simple Evolutionary Multi-objective Optmimizer
SHV	Sampling-Based Hyper-volume-Oriented Algorithm
SIBEA	Simple Indicator-Based Evolutionary Algorithm
SMPSO	Speed-Constrained Multi-objective Particle Swarm Optimization
SMS-EMOA	S-Metric Selection MOEA
SPAM	Set Preference Algorithm for Multi-objective Optimization
SPEA2	Strength-based Evolutionary Algorithm
VEGA	Vector-Evaluated Genetic Algorithm

Table 3–1 - List of most relevant MOEAs as provided by the MOEA framework library (www.moeaframework.org).

Many of the authors working in optimization have also carried out extensive research of performance indicators, to compare their algorithms to the State of the Art. Among the most important indicators, the following can be highlighted (as per the MOEA framework): Hyper-volume, Generational Distance (GD), Inverted Generational Distance (IGD), Additive ε-Indicator, Contribution, Maximum Pareto Front Error, Spacing, R1 Indicator, R2 Indicator and R3 Indicator.

Only a review of research using the hyper-volume will be included here, for its popularity and potential in multi-objective optimization.

The hyper-volume indicator, as explained in Bader and Zitzler (2011), is the only single set quality measure known to be strictly monotonic regarding Pareto dominance. This means that when a Pareto set approximation entirely dominates another one, the indicator value of the dominant set will be better, too. This property is highly interesting and relevant for problems involving a large number of objective functions.

Some relevant works on the use of the hyper-volume indicator are described next, apart from the mentioned Bader and Zitzler (2011). The PhD Dissertation by Bader (2009) provides a thorough theoretical basis for hyper-volume optimization. Auger et al. (2012) presents two different approaches: one is the optimization of multiple objectives simultaneously (traditional approach) and another is an indicator-based optimization, which maximizes hyper-volume (weighted, in this case), or other indicators, for a set of underlying objectives. Bradstreet (2011); Azevedo and Araújo (2011), include the comparison among different performance indicators. Minella et al. (2008) is particularly interesting for its comparison of two performance indicators: hyper-volume and unary epsilon. Two web references are also provided here, with worthwhile selections of hyper-volume-related literature [4,5].

To conclude this section of the State of the Art of general metaheuristic optimization, it has been deemed of interest to distinguish between exact, heuristic, metaheuristic and hyperheuristic methods, to clarify why the method developed in this Thesis is classified as metaheuristic.

In the first place, exact algorithms guarantee they will find the optimum in a finite amount of time. However, for most real optimization problems, this finite amount of time is usually too lengthy.

As opposed to exact methods, heuristics do not have mathematical proof that they will find the optimum. At most, they have a high probability of obtaining a good solution within a reasonable time. Strictly speaking, heuristic algorithms are problem-dependent, i.e. they are adapted to a particular optimization problem.

Metaheuristics, on the other hand, offer problem-independent techniques, although they still have a set of parameters which must be fine-tuned for each particular problem.

Finally, hyper-heuristics go beyond meta-heuristics, and they refer to methods that either select the best heuristics for a particular problem or generate adapted heuristics (Burke et al. [2013]). Additional works of interest relative to hyper-heuristics are Pillay (2016), which offers a recent review of hyper-heuristics applied to combinatorial optimization, in particular to the educational timetabling problem, and Branke et al. (2016), which offers a review of hyper-heuristics, in this case for the field of production scheduling.

[4] https://ls11-www.cs.uni-dortmund.de/rudolph/hypervolume/start (last verified on February 2017).
[5] https://hpi.de/en/friedrich/research/hypervolume.html (last verified on February 2017).

3.3. State of the Art of general aerodynamic shape design optimization

For the purpose of this Thesis, and in order to serve as a general review of the research work in this field, it is important to highlight the most representative or interesting work carried out in advanced aerodynamic optimization in general (not only for wind tunnels and HRSGs). Moreover, it is also useful to put the problem in a wider context, and so to indicate some relevant works on design optimization in general.

Firstly, there are interesting results, following a more traditional approach, such as, for instance, the work of Montenegro-Johnson and Lauga (2015), J. Wild (2008), or the general overview on optimization presented in Koziel and Yang (2011).

However, the most recent approach in the specific area of aerodynamics consists of the following steps, as can be seen in Forti and Rozza (2014), Hicken and Zingg (2010), Krajnovic (2007), Mengistu and Ghaly (2008), Okumura et al. (2013) or Paniagua (2014):

1. Geometry parameterization, normally using Bézier curves.
2. Metamodels or surrogate models, to approximate the real objective function with a more simplified one, by means of Design of Experiments (DoE) and metamodels such as Response Surface Methodology (RSM), Radial Basis Functions (RBF) or others.
3. Optimization, using either non-gradient-based methods (Genetic Algorithms (GAs), Simulated Annealing (SA), etc.), or gradient-based methods (Adjoint Methods, Sequential Quadratic Programming (SQP), etc.). Most of the work in this area carries out multi-objective optimization, for instance determining Pareto optimal fronts.

Consequently, we will structure the State of the Art review in this section according to the above steps.

In the first place, the initial step deals with geometry parameterization techniques. In current literature, either Bézier curves, B-splines or Free Form Deformation (FFD) are used.

In the present Thesis, Bézier curves will be selected. These curves are chosen because they are robust, they can easily be controlled to avoid absurd tunnel shapes, and they have good mathematical behavior and optimum aerodynamic performance. Bézier curves are used extensively in aerodynamic optimization (a good illustrative example is Paniagua [2014]).

In other cases, B-splines are used as a generalization of Bézier curves to avoid problems such as the Runge phenomenon, or other effects, which mean higher order polynomials can have higher interpolation errors than lower order polynomials. In our case, the Bézier curves are not used as an approximation to a real function, but as a method of generating good aerodynamic surfaces. Cubic Bézier curves (and not higher order ones) are hence chosen in our analyses. They represent an optimum trade-off between the number of control points and the capacity to represent a very wide range of geometries for the tunnel. Splines, for instance, could yield absurd geometries, which must be avoided; they also introduce much more complex mathematics, and they are better suited for cases of real function approximations and not so much in aerodynamic shape generation.

Lee et al. (2017) offers an interesting comparison on two of the most widely used geometry parametrization techniques commented: B-splines and FFD. B-spline surface control is often found to result in slightly better performance. Nevertheless, both methods perform equally well in general. FFD provides a more general approach to problem setup, decoupling geometry control from parameterization. Overall, the results presented suggest that B-spline surface control is better suited for simple geometries such as wings, whereas FFD is better adapted for complex geometries, such as unconventional aircraft, and for implementation with multi-start algorithms and adaptive geometry control approaches.

The above-mentioned work by Hicken and Zingg (2010) also uses B-splines. Another very relevant work in the area of aerodynamic shape optimization is Jing et al. (2013), on the optimization of the position of a nacelle and pylon assembly for aeronautics. It is very interesting because it combines geometry parameterization, using adapted FFD and NURBS curves, mesh-morphing with Delaunay triangulation, Particle Swarm-search Optimization (PSO) for the optimization and Kriging for the response surface. Consequently, this paper will be highlighted various times in this section of the State of the Art.

Moving on to the DoE techniques used, which was not one of the objectives of the present Thesis (it will be part of the future work), we only mention here the work by Krajnovic (2007) and its recommendation to study the use of Latin Hypercube Sampling (LHS) and Orthogonal Arrays (OA).

The next step to be carried out in aerodynamic shape optimization, once the geometry has been parameterized or modelled, is the meshing process. In the State of the Art, work can be found both on structured and unstructured meshes, but a very interesting approach is the use of overset meshes (Kenway et al. [2017]), which develops an overset meshing procedure that performs very well with respect to common structured or unstructured meshes. Other relevant pieces of research on the topic of advanced meshing are the already mentioned works by Hicken and Zingg (2010), on mesh movement; and Jing et al. (2013), which uses mesh morphing with Delaunay triangulation. Mesh morphing is undoubtedly a very relevant topic for shape optimization and geometry deformations.

Regarding the evaluation scheme, of particular importance in problems of costly evaluation (for example those requiring CFD evaluations), two approaches can be found in mainstream literature: direct search (originally defined formally in Hooke and Jeeves [1961]) and meta-models or surrogate models (Response Surface Methodology (RSM), Reduced Order Models (ROM) or hierarchical modelling). Prada-Nogueira et al. (2015), and especially Prada-Nogueira et al. (2017 (a), 2017 (b)) offer good examples of direct search applied to aerodynamic optimization. References of direct search and hybrid direct search applied to other fields, other than aerodynamics, are included in Section 3.2 of this chapter.

A review on the most relevant and recent references in the area of surrogate-based evaluation will be commented below (and in Section 3.2), when referring to works on surrogate-based optimization.

A wide variety of approaches is found in current literature about optimization procedures. It is usual to label them as:

1. gradient-based methods, such as Adjoint Methods or Sequential Quadratic Programming (SQP)
2. non-gradient-based methods, such as Genetic Algorithms (GAs), Simulated Annealing (SA), or Particle Swarm Optimization (PSO)

but there are also other optimization schemes or features such as structured search or hybrid algorithms, which are the core of the algorithm developed for this Thesis.

The references included aim at offering a relevant selection of the most innovative research approaches that can be found in the State of the Art, instead of an exhaustive coverage of more traditional optimization schemes, of which there is a wide range of examples.

For problems in which there is a risk of the optimization process being trapped in local minima, gradient-based methods need to be revised or enhanced to be able to perform well. Arreckx et al. (2016) offers an example of how the limitations of gradient methods can be overcome. It proposes a matrix-free optimization to avoid the calculation of Jacobian and Hessian matrixes, for a close-to-gradient-based optimization of engineering problems with thousands of variables and constraints. It has been especially applied to Multidisciplinary Design Optimization (MDO) for aero-structural problems.

Fabiano et al. (2016) use adjoints for MDO in a time-dependent situation, applying adjoint-based optimization to a different field of aerodynamic design, in this case helicopter rotor blades. This reference offers a very valuable insight into the State of the Art of the use of adjoints in the field of unsteady aerodynamic problems.

The authors state that there are many works on the use of adjoints for steady-state shape optimization, whereas there are not so many for unsteady flow problems. It were the works by Mani and Mavripilis (2009) and by Rumpfkeil and Zingg (2010) that initially demonstrated unsteady discrete adjoint-based shape optimization in the context of two-dimensional problems. Mavripilis (2007) offered a preliminary demonstration of the method's feasibility in three-dimensional problems. Thereafter, a full implementation and application to large scale problems concerning helicopter rotors and fighter jets was performed by Nielsen et al. (2010 (a), 2010 (b)).

Based on the works of these papers in the field of adjoint-based optimization, the next step is to extend the use of adjoint methods to multidisciplinary simulations, using the calculated sensitivities to perform MDO. In the domain of fixed and especially rotary wind aircraft, aeroelastic coupling effects can be very significant and must be considered in the context of a successful optimization procedure, according to Fabiano et al. (2016).

To conclude on the references concerning the use of adjoints, the already commented paper by Hicken and Zingg (2010) is also a very good example.

With respect to references regarding surrogate-based optimization, Section 3.2 offers an interesting set of relevant research works. Worth highlighting here are the ones described next. Once more, the work by Jing et al. (2013), which is a very complete example of aerodynamic shape optimization, from geometry parameterization and mesh morphing, to the use of the Kriging response surface method for the optimization. Poole et al. (2017) contributes to the State of the Art for several reasons: (1) its use of proper orthogonal decomposition to derive aerofoil design variables, (2) its method to obtain an efficient and reduced set of orthogonal design variables, (3) the application of a constrained global optimizer to aerodynamics, and (4) its illustration that with only six variables an aerofoil optimization can be carried out successfully. Finally, Allen et al. (2016), for its use of modal-derived variables and gradient-based optimization.

The last topic to be commented, concerning shape optimization in the field of aerodynamics, is the complexity of the problem solved in the different works analyzed. Some aspects of special relevance are the size of the space of variables considered for the search process (i.e. big or small geometry changes), the number of variables, and the number of constraints.

Given that one of the key aspects of the method developed for this Thesis, MOST-HDS, is that it is able to handle big geometry changes, it is worth mentioning that there is very little work on the topic of truly big deformations in aerodynamics, which can lead to innovative and very new designs. Most of the papers analyzed focus on aerodynamic shape design involving small fine-tuning of the geometry, or at least not changes of the extent of those considered in this Thesis.

Example research on big geometry changes includes the very good paper by Hicken and Zingg (2010). It is very worth describing this paper in detail here. The authors present an efficient gradient-based algorithm for aerodynamic shape optimization, which consists of several components, including a novel integrated geometry parameterization and mesh movement, a parallel Newton-Krylov flow solver, and an adjoint-based gradient evaluation. In order to integrate geometry parameterization and mesh movement, they use generalized B-spline volumes to parameterize both the surface and the volume meshes. The work shows that the volume mesh of B-spline control points mimics a coarse mesh. Thereafter, a linear elasticity mesh-movement algorithm is applied directly to this coarse mesh and the new mesh is regenerated algebraically. The authors claim mesh-movement time is reduced by two to three orders of magnitude relative to a node-based movement. They state that the mesh-adjoint system also becomes smaller, and hence complex-step derivative approximations can be applied successfully. When solving the flow-adjoint equations using restarted Krylov-subspace methods, a nested-subspace strategy is also shown to be more robust than truncating the entire subspace. In this paper, optimization is accomplished by the use of a sequential-quadratic-programming (SQP) algorithm. The effectiveness of this complete algorithm is proved using a lift-constrained induced-drag minimization that involves big changes in geometry. The extent of these geometry changes can clearly be seen in the figures presented in their work.

The dissertation by Paniagua (2014) also considers big (or at least moderate) changes of geometry in the case of the shape optimization of a high-speed train nose.

Lund et al. (2003) is another good, yet older, example of shape optimization with large geometry change. It uses gradient-based optimization and it involves big changes of geometry in Fluid-Structure Interaction (FSI) problems.

Moving on to other aspects of problem complexity, the paper by Arreckx et al. (2016) mentioned above, deals with problems involving thousands of variables and constraints, which are handled efficiently thanks to the use of matrix-free optimization.

After going through all the relevant steps of shape optimization and offering a selection of relevant research works for each step, this section will be concluded with useful, yet more general, research examples, also of interest within the domain of aerodynamic shape optimization.

First of all, there is a very considerable amount of research on CFD shape optimization applied to the NASA Common Research Model Wing. Relevant examples are the following papers.

Lyu et al. (2014) uses a gradient-based optimization algorithm in conjunction with an adjoint method that computes the required derivatives. The objective is to minimize the drag coefficient, subject to lift, pitching moment, and geometric constraints. The authors apply a multilevel technique in order to reduce the computational cost. In the first place, a single-point optimization is solved with 720 shape variables using a 28.8-million-cell mesh and reducing the drag by 8.5%. Secondly, a more realistic design is achieved through a multi-point optimization. The geometries obtained differ by only 0.4% of the mean aerodynamic chord. Moreover, the effect of varying the number of shape design variables is examined.

Liem et al. (2017) offers an interesting contribution because they use aircraft operational data as basis for their optimization. An additional reference of interest is the already indicated work by Kenway et al. (2017).

Other interesting works are described next. Courty and Dervieux (2006) uses some of the abovementioned aspects, but applied to the so-called CAD-free aerodynamic optimization problems. Chao et al. (2013), for their parameterization of complex geometries (in the order of 250 variables), the use of an evaluator & optimizer architecture and the comparison of the panel method and CFD as solution evaluators. Van Rees et al. (2015) investigates solutions in the speed-energy space, laying the foundations for the design of high-performance, artificial-swimming devices. Miralbés-Buil and Ranz-Angulo (2015), for their multidisciplinary optimization of vortex generators, taking into account aerodynamic, structural, ergonomic or manufacturing aspects. Quinn et al. (2015) employs experimental gradient-based optimization to maximize the propulsive efficiency of flexible underwater propulsors.

To conclude this section on the State of the Art of general shape design optimization, it is important to mention the work by Eschenauer et al. (2012), which is a very valuable reference book for shape design optimization in various fields, mostly focused on structural components of diverse applications.

3.4. State of the Art of aerodynamic shape design optimization for the industrial cases analyzed

A review will be presented of the research work carried out specifically for the areas of the two industrial cases analyzed in this Thesis, which are two very different examples of aerodynamic shape design: closed wind tunnels for testing and leisure activities and industrial boilers for combined cycle power plants.

WIND TUNNELS

Regarding the topic of tunnel design optimization there are two different approaches found in literature. The first approach focuses on the optimized design of particular sections of the tunnel (in most cases the contraction or nozzle just before the test section and the turning vanes and corners of the wind tunnel). The second approach is the general optimization of the whole tunnel design. It is this second approach that the research presented in this Thesis wants to address. However, both approaches will be analyzed in this section in order to have a better overview of the State of the Art in wind tunnel design optimization.

In the area of research focusing on particular tunnel sections, it is important to highlight the work carried out by Borger (1976), on the optimization of tunnel contractions for the subsonic range. Borger carries out an extensive survey on other works on contraction design methods.

The homogenization of the velocity profile at the exit of a contraction is shown to be dependent on the contraction ratio and not on the contraction contour. Furthermore, his definition of the velocity index in the test section (as the difference between the maximum and minimum velocity values over the average velocity) is more stringent than the more common version used by other authors. Regarding the definition of the contraction shape itself, Borger claims that the position of the inversion point is much more important to determine the contraction length than the definition of the correction geometry at the exit section of the contraction. A program code is included in his work to compute the optimum contraction length and contour for a set of given constraints. As a result, a number of optimized contours are shown for several example cases.

Mikhail (1979) describes the optimum contraction ratio and length of wind tunnel nozzles for an optimum design. First, he states that the optimum contraction ratio is a key trade-off between tunnel shell size (this affects material cost, which is lower as tunnel size is reduced) and power consumption (lower if tunnel is bigger, up to a certain point, because of lower power losses and reduced need for flow conditioning devices). Next, the minimum length must be determined to satisfy the contraction ratio and the flow quality requirements in the test section. The length of the exit section of the nozzle is determined on the basis of achieving 0.25% flow uniformity at a point on the test section center-line one local radius downstream from the contraction exit. An optimum shape for the contraction curvature distribution is defined, which permits the design of contractions half as long as those employed when his paper was published. The contraction, as expected, can be made shorter for higher Reynolds number applications. For low Reynolds number applications, a problem might be encountered regarding boundary-layer re-laminarization towards the exit end of the nozzle. It is also shown that shorter contractions can be used whenever a thinner boundary layer exists at the contraction inlet.

A more recent work by Doolan and Morgans (2007) offers a comparison of optimization methods applied to the design of tunnel contractions. They compare Sequential Quadratic Programming (SQP), DIRECT and Efficient Global Optimization (EGO). They conclude that SQP was able to solve the optimization problem efficiently, but not robustly; DIRECT provided a robust global optimization at the expense of function evaluations; and EGO is robust and always gave acceptable solutions, but its efficiency depended on the initial random sampling. In some cases, it was competitive with SQP, and the authors claim that with further research it should become an attractive algorithm for global optimization of low speed wind tunnel contractions.

Other works can also be found on the topic of tunnel contraction optimization: Jordinson (1961), Morel (1975, 1977), Downie et al. (1984) and Vieira and Aparecido (1999). The main conclusions of these papers, as far as this Thesis research is concerned, have already been outlined and are included mostly in Doolan and Morgans (2007), but also in Borger (1976) and Mikhail (1979).

Furthermore, Hoghooghi et al. (2016) offers an interesting contribution, as they use the ball-spine inverse design method to improve the performance (outlet velocity uniformity) of a nozzle of reduced contraction ratio (to reduce its cost), yielding reasonably similar results to nozzles with higher contraction ratios. Ardekani (2013) also offers an interesting insight into the reduction of nozzle length, in this case for vertical wind tunnels.

Concerning research work carried out on wind tunnel turning vanes and corner design optimization, the following are among the most relevant papers for the purpose of the present research.

The first one is the well-known work by Friedman and Westphal (1952). They tested the performance of a diffusing bend with different boundary layers, simulating the flow that would be encountered in a bend situated downstream of different ducts and objects. They state that the use of diffusing corners does not have such a negative impact on pressure losses while having the benefit of reducing overall tunnel length. They highlight the key importance of boundary control systems to reduce pressure losses.

Eckert et al. (1982) gives recommendations for the design and implementation of several flow control devices used for internal flow applications. Among the key recommendations, the authors propose chord-to-gap ratios of 2.5-3 for turning vanes in 45-90° corners. They highlight the impact of a number of factors on the pressure loss introduced by turning vanes: basic vane contour, total turning angle and tail deflection angle, chord-to-gap ratio (as already mentioned) and hinge-gap seals. This paper recommends thin vanes with a sealed hinge-gap, with respect to multi-arc circular vanes (even those with tail).

Lindgren et al. (1998) offers an interesting and in-depth study of turning vane performance in expanding bends (diffusing bends, as Friedman and Westphal called them). These bends are of particular interest to reduce tunnel overall dimensions. According to Lindgren et al., in closed wind tunnels the requirement of attached flow in the various diffusers is often a major factor in determining the total length of the circuit. Therefore, the optimum design of the combination of diffusers and corners (or bends) is of paramount importance to reduce or optimize the total size of a particular wind tunnel. Space restrictions can be a serious limiting factor and thus expanding corners with optimized turning vanes can be a promising solution. For instance, vanes of an optimized profile can offer three dimensional total pressure loss coefficients up to four times smaller than conventional ¼ circle-shaped vanes with prolongation at the trailing edge.

However, it is not always the minimum pressure loss that is best, because flow quality must also be considered, especially in the corner upstream of the settling chamber. The wind tunnel design proposed by the authors achieves a total contraction ratio of nine. This is achieved with a quite moderate need of diffusers, yet with an expansion ratio of about 1.32 in each corner. The results show that this can be achieved with very small losses in the corners, and a good quality of the flow exiting those corners. The MISES code, developed by Youngren and Drela to analyze turbo-machinery design, is used to optimize turning vane design using an inverse method: the user inputs the desired pressure-distribution along the vane and the program will yield the vane design. Further information on the MISES code can be found in: Giles and Drela (1987), Youngren and Drela (1991) or Drela and Youngren (1995).

Moreover, Lindgren et al. also recommend inspecting the CP evolution along the upper and lower surfaces of the vanes to check where separation occurs and if a further optimization is possible. Finally, given that the total pressure loss coefficient is inversely dependent on the lift-to-drag ratio of the entire corner (not just of a single vane), it is important to maximize this ratio for every single vane, and also to reduce the number of vanes.

Jeong et al. (2004) use the Kriging model and Genetic Algorithms (GAs) to optimize the design of an airfoil and the position of a flap on a multi-element airfoil, which is applicable to wind tunnel turning vane design. As pointed out by the authors, it is very interesting that the Kriging model reduces the computation time required to find an optimum. It is well suited for aerodynamic problems (thanks to the use of GAs). Also worth highlighting in this work is the fact that a variance analysis is carried out to determine the influence of the different variables on the objective function (sensitivity analysis).

Calautit et al. (2014) can also be highlighted, because it offers a design method for closed-loop subsonic wind tunnels, and many of its conclusions are focused on turning vane and corner design improvements. However, unlike the present Thesis, it does not carry out a full optimization procedure.

Finally, we will present the most relevant papers relating to the optimum design of the whole wind tunnel circuit. The first paper worth highlighting for our purpose in this area is the work carried out by Eckert et al. (1976). In this case, formulae for the pressure losses in each tunnel section are presented (very similar to the impressive empirical work by Idel'Cik [1969], where the pressure loss coefficient of most commonly used geometries in hydraulics and aerodynamics can be found). Interesting formulae among those found in the work by Eckert et al. refer, for example, to the pressure loss in meshes. This paper minimizes total pressure losses along the whole wind tunnel. The necessary structural strength of the tunnel walls is taken into account. A computer program is hence developed to obtain the optimized tunnel design and check its performance. Some additional interesting points are the explanation of the impact of inaccurate estimations of pressure losses and fan efficiency on the power required by the tunnel and the velocity in the test section, and a final description of the main tunnel types considered.

Abbaspour and Shojaee (2009) focus on the whole-tunnel design, but they follow an interesting approach, for instance, in the nozzle design. Their objective is to develop a multipurpose tunnel for the R&D department of the Islamic Azad University (Iran). They claim that only the nozzle section and certain parts of the test section have to be modified to be able to use the tunnel for three main applications: environmental, subsonic or climatic tests. This is a good example of a modular wind tunnel concept. These authors change approximately half of the nozzle to adapt it to these different applications and thus the first half is always the same and the second half is exchanged depending on the test to be carried out (changing the whole nozzle would be much more difficult). In the case of the design of the nozzle, they use a fifth order polynomial as those presented in Bell and Mehta (1988).

The final paper included in the context of full wind-tunnel design optimization is a very valuable work by González et al. (2013). Although it only optimizes a traditional wind tunnel configuration, the work is very complete and interesting, and the authors suggest somewhat non-conventional solutions such as a diffuser upstream of the fan system, instead of a nozzle geometry. They also propose a further diffuser in the section before the corner upstream of the test section and their design includes a considerably long nozzle. A detailed Excel spreadsheet is developed and can be found in their website6. This spreadsheet allows for the modification of many tunnel parameters and, for the input values, it will yield an optimized design. However, it is not an automated computer optimization tool.

Furthermore, this work states that in the case of wind tunnels for civil or industrial applications, a contraction ratio between four and six may be sufficient. With a good design of the shape, the flow turbulence and non-uniformity levels can reach the order of 2.0%, which is acceptable for many applications. Nevertheless, the authors claim that with one screen placed in the settling chamber those levels can be reduced up to 0.5%, which is a very reasonable value even for some aeronautical purposes. For more demanding aeronautical applications, when the flow quality must be better than 0.1% in non-uniformity of the average speed and longitudinal turbulence level and better than 0.3% in vertical and lateral turbulence level, a contraction ratio between eight and nine is more desirable. This ratio also allows installing two or three screens in the settling chamber to ensure the target flow quality without high pressure-losses through them. The authors state that the old-style contraction shape with a small radius of curvature at the wide end and a large radius at the narrow end to provide a gentle entry to the test section is not the optimum. There is a risk of boundary-layer separation at the wide end, or perturbation of the flow through the last screen. Good practice is to make the ratio of the radius of curvature to the flow width about the same at each end. However, an excessively large radius of curvature at the upstream-end leads to slow acceleration and therefore increased rate of growth of boundary-layer thickness, so the boundary layer, if laminar as it should be in a small tunnel, may suffer from Taylor-Goertler ‘centrifugal’ instability when the radius of curvature decreases.

[6] http://www.aero.upm.es/LSLCWT (last verified on February 2017).

Regarding the power plant design or fan system, this work by González et al. proposes using a multi-fan matrix, instead of a more standard single-fan configuration, stating that this reduces the cost of this component by roughly one order of magnitude. The paper, however, does not optimize the location of this power plant along the tunnel circuit and this has important effects on pressure loss and tunnel performance.

To conclude the State of the Art review on wind tunnel design optimization, the contributions of our Thesis in this area are now commented.

The work covered by our research aims to take into consideration also other tunnel configurations, not only 90° corners, rectangular ducts and multi-fan designs. In particular, it aims at exploring big geometry changes and therefore non-conventional or non-intuitive designs, which may improve the performance of more traditional design concepts. It focuses on true optimization of the full wind tunnel body, and not only certain parts of it, such as corners or the main nozzle. Besides, different tunnel wall materials will also be considered (in future research), as well as different relative positions of the various elements of the wind tunnel, mainly test section and fan system.

HEAT RECOVERY STEAM GENERATORS (HRSGS)

Over the decades, the design of HRSG inlet ducts has largely remained unchanged. In this Thesis we will focus on the shape design optimization of the inlet duct of different HRSG families, thanks to the application of the proposed MOST-HDS algorithm.

Generally speaking, there are two current design trend-lines for an HRSG inlet duct: single-angle (more traditional) and double-angle. Most manufacturers have used both over the decades. However, some manufacturers, such as ALSTOM, have recently tried somewhat unconventional variations of the double-angle inlet duct design, using a second angle of close to 90°, as shown in Chapter 4. Anyhow, extensive design analyses have not been performed, as far as we know, to compare the different inlet duct designs alternatives thoroughly.

There are a number of works in the area of CFD modelling of an HRSG's inlet duct, but to our best knowledge, a complete shape optimization analysis of this critical element has never been addressed. The aim of these works is to analyze the flow distribution of a particular design, or the effects of elements introduced in the inlet duct to improve the flow distribution, such as Ameri and Dorcheh (2013) and Lee et al. (2002).

The following are general works in the field of CFD analyses, of relevance for the purpose of this Thesis, and useful for future authors working in the area of shape design optimization of HRSGs.

Galindo et al. (2014) is a very valuable work because it develops a more complex CFD model of the whole HRSG body to include an accurate model for the real geometry of the tube bundles, moving on from the more traditional approach of modelling the tube bundles as porous media. Aslam Bhutta et al. (2012) offers a review of CFD applications in various types of heat exchangers. Galindo et al. (2012), for the development of CFD models of the whole HRSG to offer a better comprehension of the flow inside the unit and of its performance for plant operators. Shi et al. (2009) and Hedge et al. (2007) for their general CFD modelling of HRSGs. Sundén (2007) for the work on CFD modelling for R&D on the field of heat exchangers in general. And finally Daiber (2006) for his work on the analysis in particular of the gas side of an HRSG flow design.

The contribution of this Thesis, regarding HRSG inlet-duct shape-design optimization, is twofold. On the one hand, it shows that there is substantial room for improvement in the shape design of the inlet ducts of HRSGs, in terms of achieving a lower pressure drop, a higher velocity uniformity and an important cost reduction of the unit. On the other hand, it shows how the MOST-HDS algorithm is applicable in diverse fields for aerodynamic shape optimization involving big geometry changes, finding improved designs that can be quite unconventional and non-intuitive. The results obtained for the two HRSG families presented illustrate the interest for the State of the Art of the work presented in this Thesis.

Furthermore, this Thesis performs extensive design analyses to compare the different inlet-duct design alternatives thoroughly. As far as we know, this kind of analyses have not been performed before.

3.5. Concluding remarks and Thesis mapping to the State of the Art

As an important concluding remark to this chapter on the applicable State of the Art, and as it will be commented further on in this Thesis, MOST-HDS has certain similarities with the Nelder and Mead simplex method for function minimization presented in Nelder and Mead (1965). The Nelder-Mead algorithm, or simplex search algorithm, is one of the best-known algorithms for multidimensional and unconstrained optimization without derivatives.

The main contributions of the Thesis in the area of optimization in general include the use of structured optimization in the field of aerodynamic shape design, the definition of a novel hybrid direct search technique and the development of the MOST-HDS model as a whole. MOST-HDS is a general, automatic, robust and flexible tool for shape design optimization, as it will be shown throughout this document.

The particular mapping (or location) of the Thesis within the applicable State of the Art is illustrated in the following scatter plots, for a better general perspective.

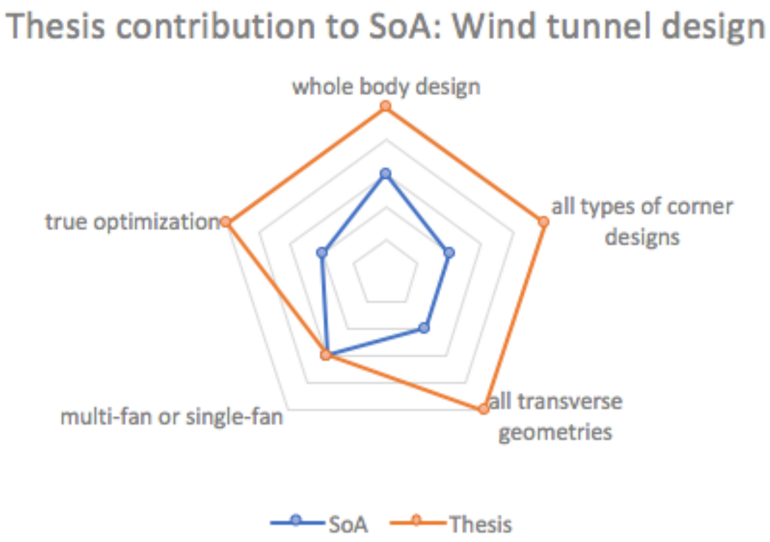

Figure 3–1 - Scatter plot of Thesis contributions to State of the Art (SoA) of wind tunnel design optimization.

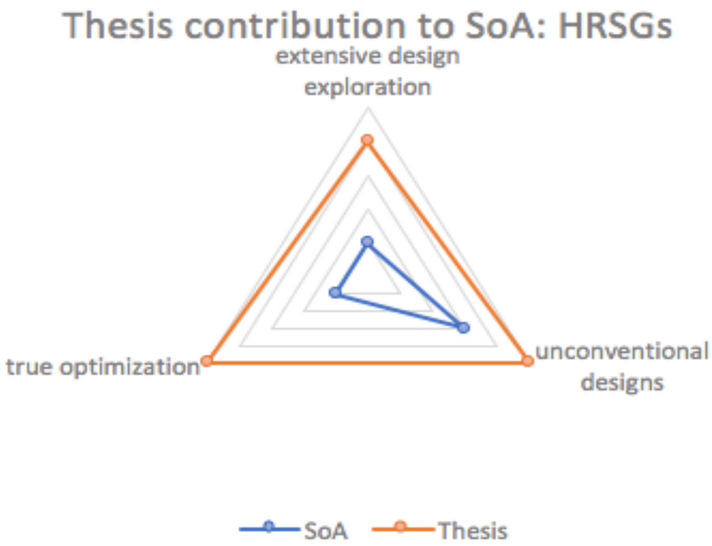

Figure 3–2 - Scatter plot of Thesis contributions to State of the Art (SoA) of HRSG inlet duct design optimization.

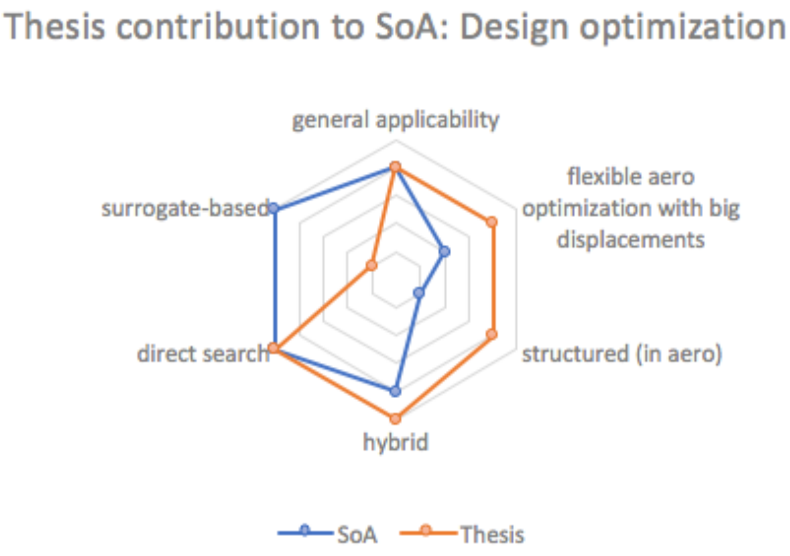

Figure 3–3 - Scatter plot of Thesis contributions to State of the Art (SoA) of general design optimization.

List of Figures

List of Tables

4

Chapter 4 - Problem definition

If I had an hour to solve a problem I'd spend 55 minutes thinking about the problem and 5 minutes thinking about solutions.

Albert Einstein.

This chapter defines the general problem addressed by this Thesis in an efficient way in order to apply automated (i.e. computer-based) optimization techniques. It defines the main elements of this kind of problem statement: variables, attributes and parameters, as well as a crucial aspect for shape design optimization: the geometry parameterization approach. All concepts are applied to the two industrial examples which will be presented in Chapter 6: closed wind tunnels and industrial boilers for combined cycle electricity generation plants. Firstly, *Section 4.1.* puts forward the need for a robust problem definition; *Section 4.2.* defines the main elements; *Section 4.3.* presents the geometry parameterization scheme; and finally *Section 4.4.* summarizes a set of final remarks.

4.1. Introduction

The final objective of this Thesis is to develop an optimization architecture which can be applied to aerodynamic shape design optimization problems. One of the first steps is to present a general way to define any, or at least most, of the problems a designer can face in the field of shape optimization, so that the optimization model can handle them in a more efficient and comprehensive manner. This means that the way attributes, parameters and, mainly, variables are defined is not to be underestimated. It will lay the foundations for an easy-to-follow optimization process.

Variables condition the way the geometry is parameterized and this has to be done with care to ensure the parameterization is clear and intuitive, since this will highly facilitate the development of the strategy to control the optimization algorithm. Furthermore, it will make easier the revision, maintenance and future developments of the program source-code.

Consequently, the contribution of the Thesis in this chapter is the proposal of how a problem of shape design can be defined in a most suitable way to apply not only advanced optimization schemes in general, but, in particular, multi-attribute/objective, structured, hybrid, direct search (MOST-HDS). This is shown for two example cases of very different industrial fields, to illustrate that the approach and method are general.

This contribution includes the following related contribution: definition of an efficient set of truly independent variables. This includes defining variables which are easy to understand and are intuitive enough to let the designer check how the optimization proceeds. These variables must then be translated to the variables used by the CFD solver, which are normally not as easy to handle or interpret.

A final contribution worth highlighting in this chapter is the geometry parameterization proposed for the wind tunnel case. There are very rare examples of a full wind tunnel parameterizations in literature, more so using Bézier curves (18-20 are used in this Thesis for a real full wind tunnel).

4.2. Problem definition

This section will be divided into two parts: one focused on closed wind tunnels and another one focused on industrial boilers, since we will be applying the problem definition to these two real examples throughout this Thesis.

WIND TUNNELS

In the nineteenth century, the Wright brothers started a systematic process to study flight technology, based on the work of their predecessors, such as Da Vinci, the German Otto Lilienthal or the American Samuel Langley. Thanks to their strong effort, both the Wright brothers and Santos Dumont bear the title of pioneers of aviation. One of their main contributions was the design and development of the first-known wind tunnel. Since then, many bodies subject to wind are tested in wind tunnels: aircraft, vehicles, civil structures, sports goods, etc. All wind tunnels share two key elements: the air-moving device (fan system) and a testing section to place the prototypes analyzed.

In wind tunnels, an airflow is generated around the objects tested. The objects themselves are equipped with various kinds of sensors to obtain the relevant aerodynamic data (mainly pressure distributions and forces acting on the prototypes). The airflow quality itself (turbulence and velocity indexes) must also be accurately measured to ensure the test is as close to real conditions as possible. All of these data allow for the prediction and analysis of the aerodynamic performance and the forces that will appear on the tested object when used in its real-life conditions.

Wind tunnels can be classified according to different criteria. One of the most important classifications divides wind tunnels into open-loop and closed-loop tunnels.

In open-loop wind tunnels, ambient air is suctioned by the fan, it flows through the test section, and then through an open outlet and into the atmosphere again.

However, in order to have a better control of the airflow's quality and conditions (temperature and humidity) and to reduce energy consumption, closed-loop wind tunnels were developed. In these tunnels, the same air is re-circulated once and again through a closed ducting, commonly moved by some kind of fan system. The air flows through the test section and back to the fan for a new cycle. The higher quality airflow and reduced energy consumption, main advantages of closed-loop wind tunnels, usually outweigh their main drawbacks: considerable space requirement for their construction and high cost. Moreover, the fact that these tunnels are closed allows for the use of other gases, different from air, and this fact contributes to a better density control and broader applicability of this type of equipment.

This Thesis focuses on closed wind tunnels, since they are much more extensively used, but the model can be applied to open wind tunnels, too.

Figure 4–1 illustrates a representative variety of types of wind tunnels.

Figure 4–1 - Different types of wind tunnels. From right to left and top to bottom: Replica of the Wright wind tunnel; Closed wind tunnel at the Ferrari Formula 1 Team; Open wind tunnel at NASA Ames Research Center; A2 open wind tunnel for testing of various kinds (including vehicles and professional cyclists and skiers); and vertical wind tunnels for scientific testing of aircraft spins, helicopter blades, and parachutes: at NASA Langley Research Center (first ever built vertical wind tunnel, 1940) and the TsAGI Vertical Wind Tunnel T-105 in Russia (1941).

For any kind of wind tunnel, an optimum aerodynamic design is required to ensure adequate performance and cost at all test conditions. This means minimal energy consumption, minimal cost (including investment, operation and maintenance), and best possible emulation of real conditions.

In order to reach an optimized wind tunnel design, an optimization model architecture must be built. This model will need two types of inputs: parameters and variables, and it will have two main outputs: the values of each of the attributes and the so-called state of the constraints vector (which can be considered as a special type of attribute).

Table 4–1 and Table 4–2 show the generalized list of parameters (i.e. designer input) and attributes proposed, respectively, for the study of closed wind tunnels. It is worth noting that some of the parameters may be left blank; for example, cooling may not considered, or convection or radiation may be neglected. Attributes can be grouped into different categories for the sake of clarity, in groups such as cost attributes, geometry/flow attributes and thermal attributes. Note that the groups of attributes do not have to be disjoint; for instance, power consumption should be part of the cost group (energy cost), but it may also be considered a category by itself, for environmental reasons.

PARAMETER	**Explanation**
1. N_{WT}	Number of sections or modules for wind tunnel discretization
2. AR_{MIN}	Minimum frontal cross–section area ratio in test section (i.e. $A_{TEST\ SECTION}/A_{MODEL}$)
3. $Z_{MAXMODEL}$	Maximum height of models to be introduced in test section
4. $Y_{MAXMODEL}$	Maximum width of models to be introduced in test section
5. D_{MINTS}	Minimum distance in z and y directions between model and test section walls
6. L_{MINTS}	Minimum required length for test section
7. HA	Horizontal arrangement for horizontal closed wind tunnels (1: purely horizontal, 2: recirculating duct runs on top of main duct)
8. $\Delta T_{MAX}/s$	Maximum allowed temperature increase of air inside wind tunnel per second
9. T_{AMB}–time	Ambient air temperature versus time of air surrounding tunnel for a representative 24h day, for convection modelling
10. G_{SOLAR}–time	Solar radiation versus time for a representative 24h day, for radiation modelling

Table 4–1 - Proposed general set of parameters for closed wind tunnels.

ATTRIBUTE	**Explanation**
1. P_{TOT}	Total power consumption
2. C_{FIXED}	Fixed cost (i.e. investment)
3. C_{VAR}	Variable cost (operation & maintenance)
4. L_{TOT}	Total length
5. W_{TOT}	Total width
6. H_{TOT}	Total height
7. V_{TOT}	Total volume
8. $\bar{v}_{TS}$	Average velocity in test section

9. v_{INDEX}	Velocity index in test section
10. t_{INDEX}	Turbulence index in test section
11. $Z_{MAXREAL}$	Maximum achieved height of models that can be introduced in test section (the value will normally be the same as $Z_{MAXMODEL}$, but it may be higher)
12. $Y_{MAXREAL}$	Maximum achieved width of models that can be introduced in test section (the value will normally be the same as $Y_{MAXMODEL}$, but it may be higher)
13. AR_{REAL}	Achieved value of area ratio in test section (the value will normally be the same as AR_{MIN}, but it may be higher)
14. L_{REALTS}	Achieved value of length of test section (the value will normally be the same as L_{MINTS}, but it may be higher)
15. $\Delta T_{REAL}/s$	Achieved value of temperature increase of air inside wind tunnel per second (the value will normally be the same as $\Delta T_{MAX}/s$, but it may be lower)

Table 4–2 - Proposed general set of attributes for closed wind tunnels.

In the case of wind-tunnel design, the following independent variables, presented in Table 4–3, were already defined in Prada-Nogueira et al. (2015) and they constitute an efficient set of truly independent variables (independent in a strict sense, i.e., none of them can be computed univocally from the others). This set of variables is capable of representing most wind tunnel configurations, and it is appropriate to build an optimization tool based on them. Figure 4–2 explains graphically the meaning of each of these variables. This set gives an example of how variables should be defined for other aerodynamic components. Recommendations on how to define an efficient variable set will be given at the end of this section, after the explanation on the industrial boiler case.

VARIABLE	**Explanation**
1. w_{TUNNEL}	Width of tunnel
2. l_{TS}	Length of test section
3. w_{TS}	Width of test section
4. $\alpha_{F/TS}$	Relative position of fan and test sections
5. d_F	Fan diameter
6. $geom_{TS}$	Test section geometry
7. $profile_{DUCT\ 1}$	Profile shape of the different parts in which we divide the ductwork which joins the test section to the fan (duct 1: it comprises diffuser 1, corner 1, diffuser 2, corner 2 and fan nozzle).
8. $profile_{DUCT\ 2}$	Profile shape of the different parts in which we divide the ductwork which joins the fan to the test section (duct 2: it comprises corner 3, diffuser 3, corner 4 and nozzle 1).
9. $a_{DUCT\ 1}$	Area distribution for the wind tunnel sections along duct 1
10. $a_{DUCT\ 2}$	Area distribution for the wind tunnel sections along duct 2
11. $geom_{DUCT\ 1}$	Transverse geometry for the wind tunnel sections along duct 1
12. $geom_{DUCT\ 2}$	Transverse geometry for the wind tunnel sections along duct 2
13. n_{FANS}	Number of fans

14. Other	Other variables include: length of diffuser and nozzle sections, length of fan section, angles of diffuser and nozzle sections, offsets in corner sections

Table 4–3 - Proposed general set of variables for closed wind tunnels[7].

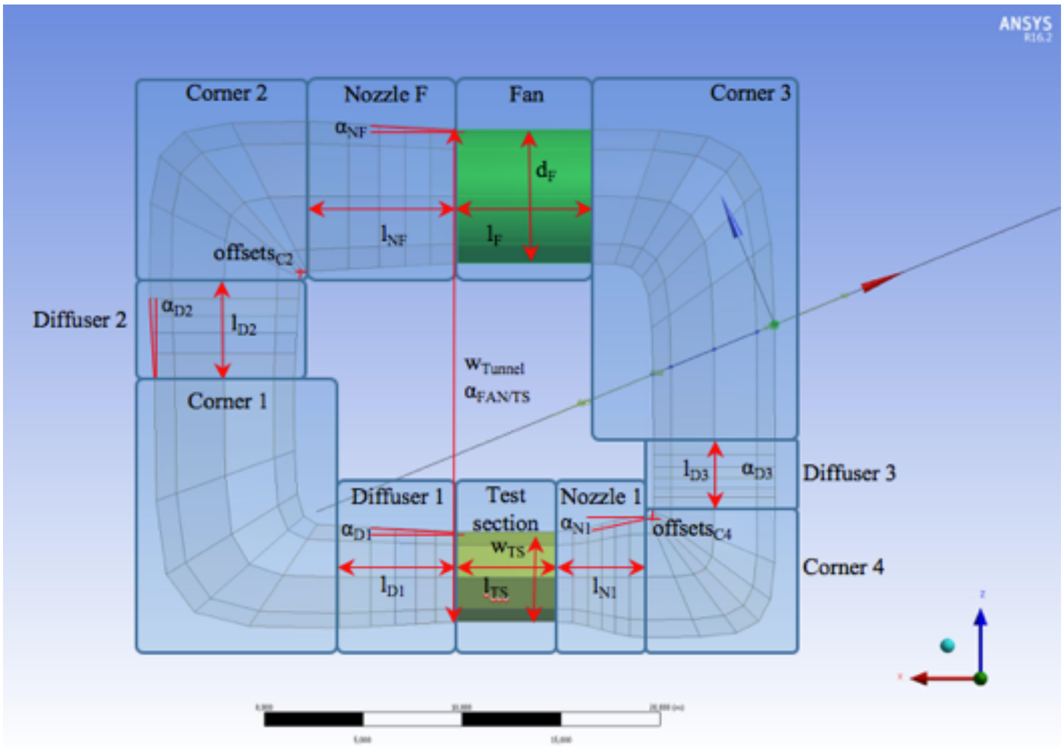

Figure 4–2 - Proposed set of independent variables which yield an efficient representation of most wind tunnel configurations and are adequate for the application of computer-based optimization methodologies.

INDUSTRIAL BOILERS: HEAT RECOVERY STEAM GENERATORS (HRSGS)

Heat Recovery Steam Generators (HRSGs) for combined cycle power plants are a key industrial equipment in the power generation sector. They are designed and manufactured by big engineering companies and they are both expensive, large in size, and crucial to the performance of the power plant. However, the design of certain critical components, such as the inlet duct, has remained largely unchanged for many decades. The performance of the inlet duct is mainly measured in terms of pressure drop throughout the unit, gas flow velocity uniformity and heat transfer capacity.

[7] Note that parameters and attributes are represented with uppercase names and variables are represented with lowercase names.

In an HRSG, the hot exhaust gases of a gas turbine flow through a set of tubes (normally finned tubes) through which water is pumped. The heat of the gas flow is transferred to the water flow, which is transformed into steam. This steam can be used directly for industrial applications, or for electricity generation in a steam turbine, or for both (in the so-called co-generation plants). Figure 4–3 shows an example layout of a combined cycle power plant and an example of a real HRSG.

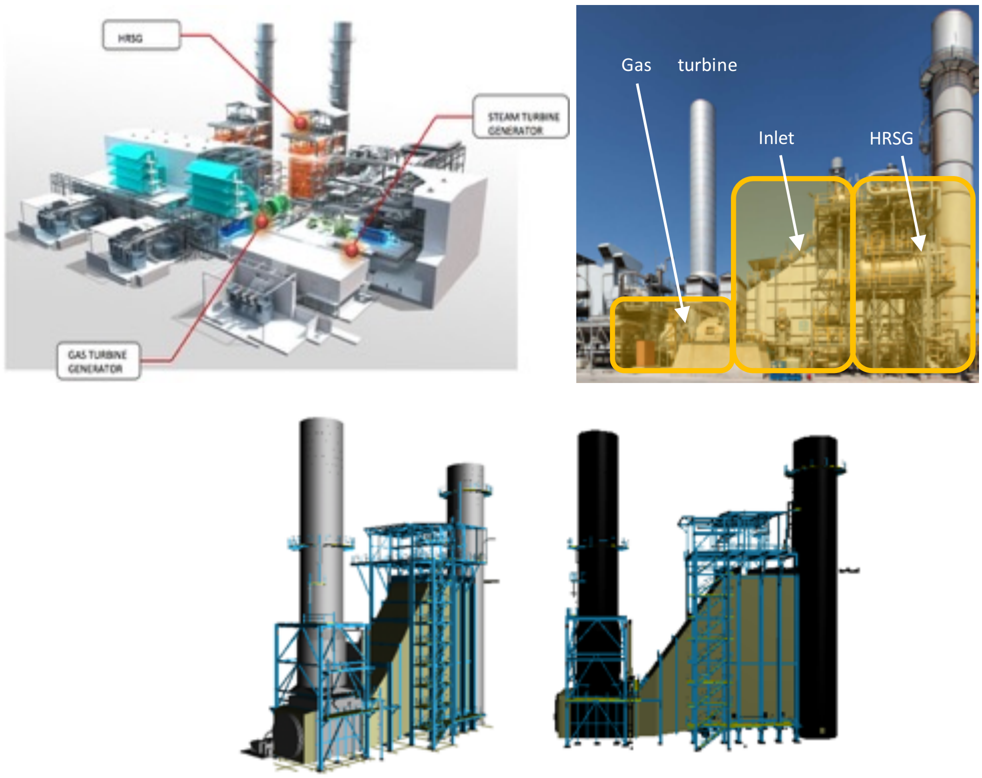

Figure 4–3 - Example combined cycle power plant layout and real and render versions of an example HRSG.

The main challenge in this application is that the exhaust gas flow exiting the gas turbine has to flow into the HRSG, which has a much bigger cross-sectional area, through a critical section, the so-called inlet duct. This introduces flow detachment and hence turbulence and velocity non-uniformity, which can be observed in Figure 4–4. The velocity profile exiting the gas turbine greatly influences flow performance depending on its velocity uniformity, swirl and other characteristics.

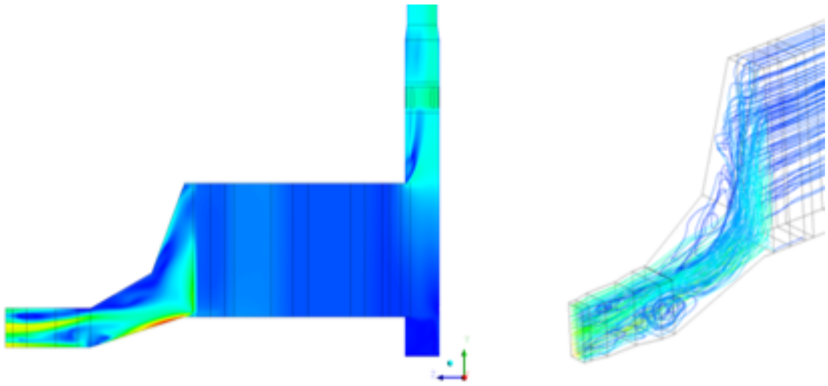

Figure 4–4 - Side view of velocity contours in the mid-plane of a typical HRSG (left). Detailed isometric view of velocity magnitude streamlines in the inlet transition duct (right).

Despite this, all manufacturers try to make this inlet duct as short as possible, to make their whole units shorter and more compact, while gas pressure drop and gas velocity profile are maintained within certain limits. This is because reducing the size of the inlet duct facilitates its integration into the power plant layout, and it can reduce manufacturing costs considerably, since it is built of very costly stainless steel.

For the purpose of this Thesis, MOST-HDS will be applied to the shape design optimization of the inlet duct of several HRSG families, to show its applicability to an industrial example of a completely different field to wind tunnels.

The optimization problem is multi-attribute or multi-objective, since the final goal is to obtain the inlet duct designs which minimize two attributes: total pressure drop across the inlet duct and velocity non-uniformity in the outlet plane of the inlet duct[8].

The pressure drop is measured as the difference in mass weighted average of the total pressure between the inlet and the outlet of the inlet duct.

[8] The problem is defined with two objectives to be able to present the optimization results more simply. The problem can be defined with a higher number of objectives. Magnitudes of importance such as material cost and total length are calculated throughout the optimization, but are not used directly as optimization attributes.

The velocity non-uniformity is defined as the difference between the velocity area-weighted average and the mass-flow-weighted average. This definition is simply one of the possible ways of measuring velocity non-uniformity. Other alternative definitions would be, for example, checking the difference between the maximum velocity, the minimum velocity and the average velocity (as is done for velocity indexes, for instance); or comparing the maximum and minimum velocities, etc. However, these alternative definitions, involving the maximum and minimum velocity values, can be misleading, since minor mesh irregularities, inevitable in most CFD simulations, can yield false values of maximum or minimum velocities. These values are acceptable numerical errors and can be easily discarded by the engineer when evaluating the results one by one and manually, but cannot be detected as easily by the CFD code when launching an automatic optimization. Therefore, the indicated definition of velocity non-uniformity is used. It must be noted that, strictly speaking, by velocity non-uniformity we are not only referring to the fact that velocity values are uniform in the outlet plane of the inlet duct, but to the fact that the mass flow must also be distributed as evenly as possible and the “combination” of velocity and mass flow uniformity is given by the difference between the velocity area-weighted average and the mass-flow-weighted average[9].

Both attributes are handled in per unit magnitude. The optimum designs are those which minimize both attributes.

Regarding the independent variables used for this case, the following set is proposed: two angles for the top wall, two angles for the lateral wall (identical on both lateral walls), two more for the bottom wall and the total length of the inlet duct. These variables take into consideration the design modifications which are feasible in terms of manufacturing and assembly in real power plants. For example, curved walls or more than two intermediate angles are not considered of interest and they are consequently not included in this analysis. These variables are listed in Table 4–4.

VARIABLE	**Explanation**
1. α_{1T} (A16)	First angle top plane
2. α_{2T} (A17)	Second angle top plane
3. α_{1B} (A18)	First angle bottom plane
4. α_{2B} (A27)	Second angle bottom plane
5. α_{1S} (A6)	First angle side plane
6. α_{2S} (A7)	Second angle side plane
7. l_{TOT} (V31)	Total length

Table 4–4 - Proposed general set of variables for HRSGs. The names in brackets refer to ANSYS names for the variables.

[9] Other definitions for velocity non-uniformity used by manufacturers in industry include the determination of the percentage of velocity values which lie within a 10% of the RMS value of a particular plane, or within 15%.

The width and height of the HRSG and the elevation difference between turbine and boiler floor are kept constant for all simulations and are therefore included as parameters.

The set of variables for the inlet duct is shown in **Error! Reference source not found.** and an example inlet duct 3D geometry is included in Figure 4–6.

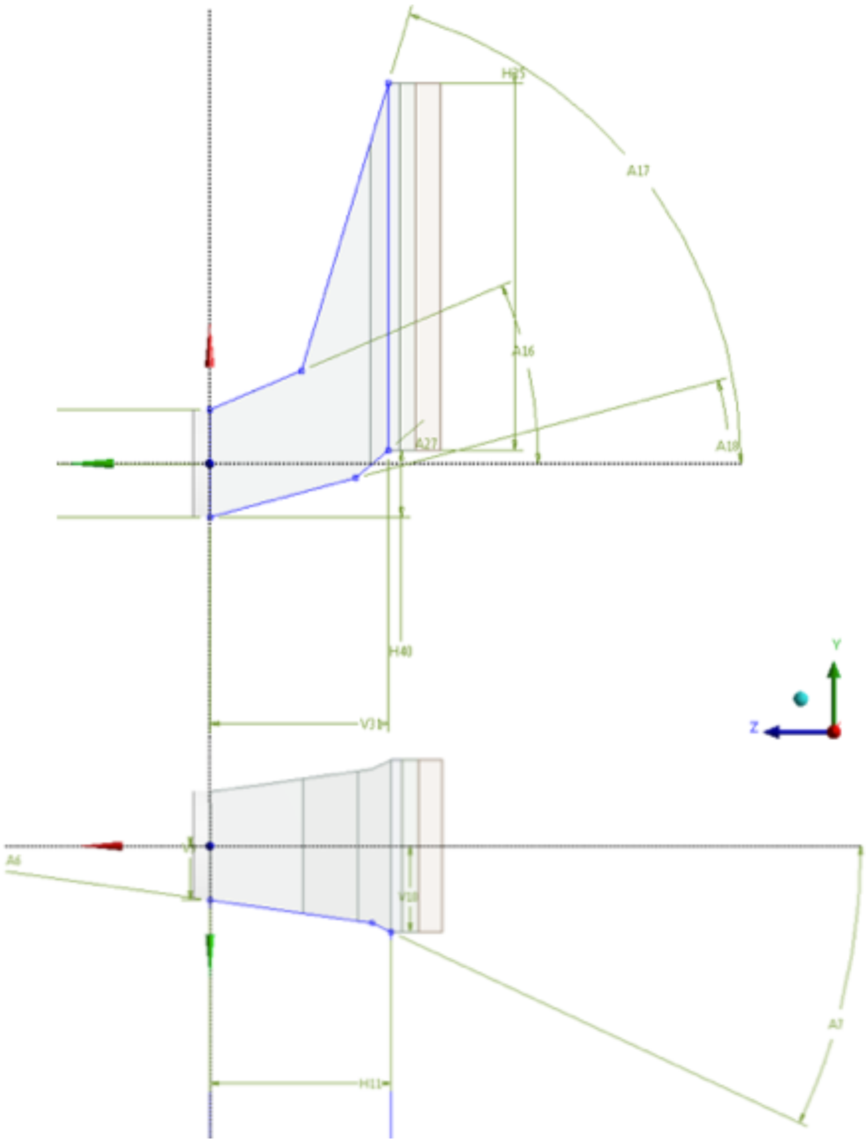

Figure 4–5 - Variables used to parameterize a general inlet duct for different HRSG families (x-axis and y-axis views).

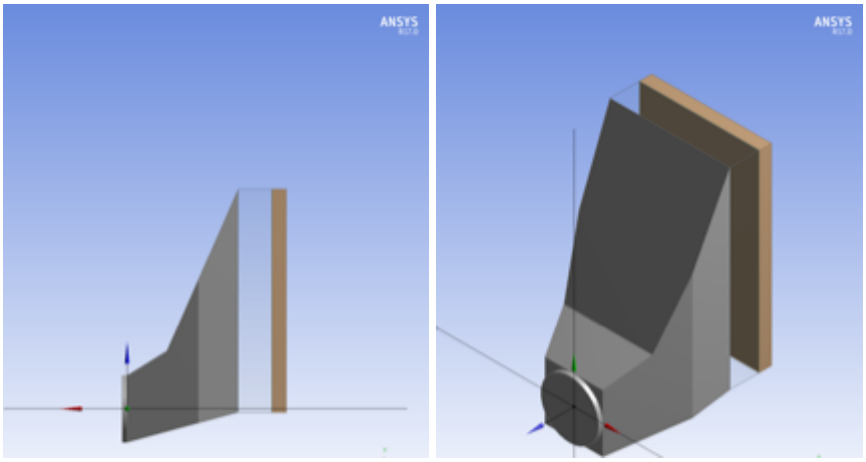

Figure 4–6 - Side and 3D views of an example HRSG inlet duct geometry, generated with the proposed geometry parameterization.

RECOMMENDATIONS FOR AN EFFICIENT VARIABLE SET DEFINITION

This section offers a general outline on some of the observations or recommendations to be taken into account when defining a variable set for a problem to which we are going to apply automatic optimization tools:

1. Check thoroughly that any variable set is truly independent, i.e. the value of each variable is independent from the value of the rest of the variables.

2. The variable set has to be defined to be as simple and intuitive as possible. In the case of shape design optimization, a useful way of thinking is to define the variables you would need to sketch a drawing of the body geometry. Additionally, each variable should represent visual aspects of the geometry, such as a particular dimension, or curvature, or relative position. Avoid variables which may be used to define the geometry but which are not clear geometrical magnitudes that any non-expert person can understand. As explained in point 3, the optimization algorithm and the CAD program may use completely different sets of variables to define the same geometry.

3. The CAD or CFD programs used to generate the body geometry require a variable set used to define or parameterize that geometry, but it may not be an efficient variable set for the optimization process. It is very worth highlighting this, as will be explained in detail in Chapter 5. It is useful to bear in mind that the variable set used for an optimization process will be more efficient if independent changes in each of the variables are feasible, visual, and directly generate different design candidates. Note that all the algorithm-embedded intelligence will act directly on the variable values. If changes to these values are intuitive, it is more efficient for algorithm checking, maintenance or improvement. For instance, using the relative position of two elements of the geometry is better than using the base point position of the planes containing each of the elements.

4. The variables used should allow for an easy formulation of the constraints. In the case of shape design optimization, a very important type of constraints is geometry absurdity checks (negative volumes, intersecting parts, absurd curvatures, etc.).

5. Despite all the above, there is normally nothing such as the best and unique variable set for a particular problem. These are merely general guidelines applicable to most geometries, for shape design optimization purposes.

4.3. Geometry parameterization

In order to carry out a full optimization of a body's shape design, this body's geometry has to be parameterized in a CAD program (or CAD module of a CFD program, in our case). Although referred to as "parameterization", this step really defines the variable (and not the parameter) set used by the CAD program to represent the geometry univocally.

As has been highlighted in the previous section, the efficient variable set defined for the optimization process will in most cases not be the same as the variable set defined to parameterize the geometry. The latter will depend on the CAD program used and the way the designer generates the geometry. This variable set will generally not be the most efficient, intuitive, illustrative or high-level enough so as to use directly for the optimization process (the variables may not even be independent). Throughout the section a number of concrete examples will be given so that the reader understands this aspect fully. Once again, for the sake of clarity, the section will be divided in two: wind tunnel and HRSG geometry parameterization.

Figure 4–7 represents a general closed wind tunnel of the traditional type (most current wind tunnels are qualitatively of this design). The present work aims at proving that alternative designs (different corner geometries, cross-section types, etc.) can prove interesting and better for certain applications.

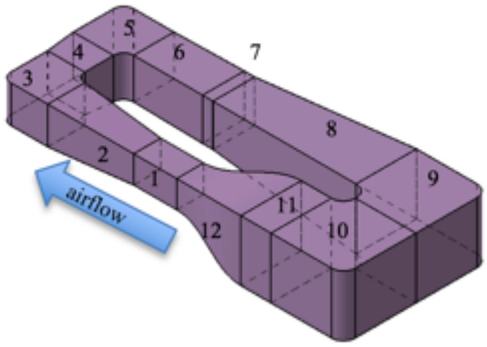

Figure 4–7 - Sections of a general closed wind tunnel of the 'traditional' type. Section 1 is the test section and, following the airflow direction, the sections are: 2. diffuser, 3. corner, 4. diffuser, 5. corner, 6. straight section, 7. fan section, 8. diffuser 9. corner, 10. corner, 11. settling chamber and 12. nozzle.

The wind tunnel geometry parameterization is carried out by a discretization of the tunnel into a number of transverse sections. The number of these sections is selected by the user as one of the input parameters to the model. Each section is parameterized with a number of segments and angles (see Figure 4–8). For this work eight segments of equal length are used, but this can be generalized to any number which creates a closed polygon.

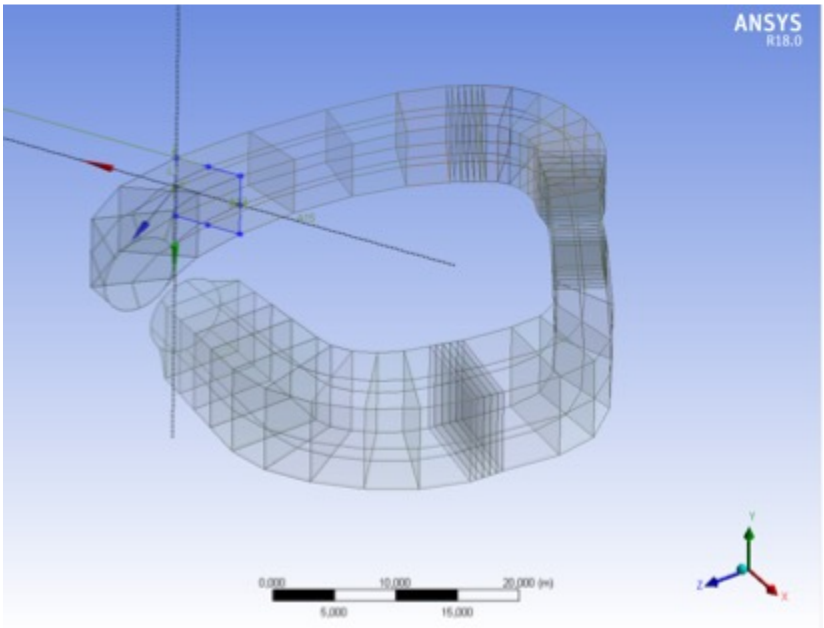

Figure 4–8 - Wind tunnel geometries are generated by means of a discretized set of transverse parameterized sections. An example plane containing one of these transverse sections is shown.

The polygon for each transverse section can have any geometry, thus being able to represent most wind tunnel designs. The area of each of these sections can also be varied as one of the model variables. For instance, the angles of the segments of each polygon are variables used in the CAD module to generate the geometry and are not very intuitive variables to be used for the optimization[10]. The geometry shape (rectangle, circle, regular polygon or others), which is much more visual, is used instead, and the values of the angles are adjusted automatically by the tool developed for this Thesis so that the CAD module can generate the geometry.

Finally, the sections are generated along the points of a set of Bézier curves. These curves are chosen because they are robust, they can easily be controlled to avoid absurd tunnel shapes, and they have good mathematical behavior and optimum aerodynamic performance. Bézier curves are used extensively in aerodynamic optimisation (a good illustrative example is Paniagua [2014]). In other cases, B-splines are used as a generalization of Bézier curves to avoid problems such as the Runge phenomenon, or other effects, which mean higher order polynomials can have higher interpolation errors than lower order polynomials. In our case, the Bézier curves are not used as an approximation to a real function, but as a method of generating good aerodynamic surfaces. Cubic Bézier curves (and not higher order ones) are hence chosen in our analyses. They are an optimum trade-off between number of control points and capacity to represent a very wide range of geometries for the tunnel. Besides, splines, for instance, could yield absurd geometries, which must be avoided.

[10] Stricty speaking, for an octagon, only the angle for six sides must be specified, and not for all eight, in order not to over-constrain the geometry parameterization.

Depending on the complexity of the designer requirements for the wind tunnel model representation, more or less Bézier curves can be used for the geometry definition. An optimum trade-off must be reached between level of detail and computational load.

A set of 18-20 Bézier curves provides a highly-detailed model, able to represent most wind tunnel geometries. The representation with this number of curves is depicted in Figure 4–9.

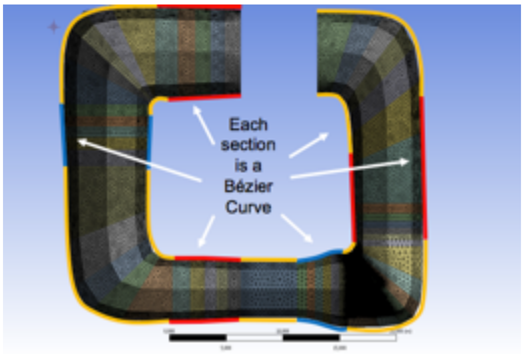

Figure 4–9 – Highly-detailed representation of a generalized wind tunnel design, able to represent most tunnel geometries (18-20 Bézier curves are needed).

In this Thesis, this highly-detailed representation will be used to apply the MOST-HDS algorithm and obtain results for a real industrial case. However, to better explain certain aspects of the optimization process and to analyze the way the algorithm works, a simpler geometry model will be used as well for the wind tunnel example.

This simpler version, shown in Figure 4–10, uses only four Bézier curves: two for the ductwork between the test section and the fan section (referred to in this work as duct 1) and two for the ductwork from the fan section back to the test section (duct 2), all defined in the direction of the airflow (Figure 4–7).

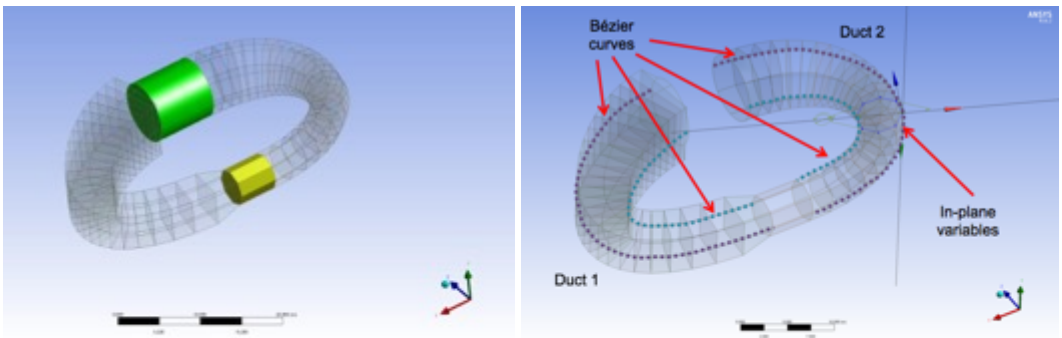

Figure 4–10 - Low-detail representation of a wind tunnel design, used to better illustrate certain aspects of the optimization methodology presented in this work. Only four Bézier curves are used. Fan and test sections are both shaded in this figure (left). An example plane containing one of the transverse sections used for the tunnel geometry discretization is also shown (right).

In the case of the inlet duct of HRSGs, which is a much simpler geometry than that of closed wind tunnels, the variables commented in Section 4.2. are used to parameterize the geometry (Figure 4–5). For this industrial example, the geometry is quite straightforward, and the variable set used for the optimization process is the same as that used to generate the geometry in CAD.

4.4. Final remarks

This chapter has explained how this Thesis proposes to define shape design optimization problems of a wide range of fields. It includes real industrial examples of a simple case in terms of number of variables, parameters and geometry parameterization (HRSGs) and an example of a complex case (wind tunnels). Very especially, the way variables are defined and the proposed geometry parameterizations allow for an efficient and easy-to-follow optimization process, as is analyzed in the following chapters.

List of Figures

List of Tables

5

Chapter 5 - The MOST-HDS optimization model

Insanity: doing the same thing over and over again and expecting different results.

Albert Einstein.

This chapter describes in detail the MOST-HDS model and the optimization algorithm developed for this Thesis. It highlights the differential aspects between this approach and the current State of the Art. Firstly, *Section 5.1.* presents a general introduction. *Section 5.2.* explains the main elements of the structured optimization approach proposed by MOST-HDS. The fact that the search carried out by MOST-HDS is structured is one of the key aspects of the model and a contribution of this Thesis to the field of aerodynamic shape optimization. *Section 5.3.* describes the MOST-HDS model. *Section 5.4.* illustrates the architecture of the model implementation. This architecture contributes to the State of the Art because it carries out a full implementation of an automatic workflow for an optimization-simulation environment based on direct search, applicable to CFD problems of a wide range of fields. Finally, *Section 5.5.* outlines a set of final remarks on MOST-HDS, to summarize the most important aspects of this chapter.

5.1. Introduction

The approach proposed by this Thesis for the aerodynamic shape design problems, able to handle both small and big geometry changes, is the development of a general method based on a **M**ulti-**O**bjective **St**ructured **H**ybrid **D**irect **S**earch optimization algorithm (referred to as **MOST-HDS**).

Extensive research has been carried out over many years in all aspects of optimization, applied to a very wide range of fields. This Thesis focuses on a very particular area, aerodynamic design. Many interesting contributions to optimization in this field can also be found (refer to the State of the Art, Chapter 3).

The novel aspects and contributions of the MOST-HDS model are:

- Firstly, that it is an automatic, flexible and robust implementation of structured optimization in an area (aerodynamic shape design) to which this approach has not been applied, as far as we know.

- Secondly, the contribution to the concept of hybrid direct search, used by other authors. In this regard, MOST-HDS combines genetic, gradient and swarm search intelligence in a way no other author we are aware of has proposed.

- Moreover, the fact that MOST-HDS is able to cope smoothly with big geometry changes or modifications of the shape design means that it can produce non-conventional or non-intuitive designs. Such designs would never have been tried manually by the designer or explored by other optimization algorithms focused on small geometry changes (see Chapters 1 and 2 for the importance of big geometry changes in the field of aerodynamic design).

- The relevance of direct search for problems of aerodynamic shape design with big geometry changes is compared to other approaches, mainly surrogate models, which are shown not to perform as well for cases in which a big geometry change means a qualitative change in the flow regime around the body of interest (refer to Chapter 7).

- Finally, the applicability of the MOST-HDS model is shown for two real industrial examples in Chapter 6 (closed wind tunnels and industrial boilers for combined cycle plants) to illustrate that it is a substantially general optimization model. Besides, its performance is also compared to an extensively used general purpose optimization algorithm by applying MOST-HDS to a relevant mathematical test suite which is commonly used for benchmark analyses of optimization algorithms (Huband et al. [2006]).

5.2. Structured search: Variable hierarchy and optimization phases

Two of the fundamental concepts of this optimization methodology are the hierarchy of variables and the optimization phases. This approach – including direct search in most cases – has been used in other fields (Cuadra [1990] is a very good reference example), but not yet in aerodynamics, or, at least, not as thoroughly as proposed in this work.

Hierarchy of variables

Hierarchy of variables refers to the fact that the independent variables which define each possible design of the aerodynamic body are not all of them of equal importance in terms of their impact on attributes and constraints. This is one of the aspects for which the engineer's know-how is of paramount importance.

As an example, in the particular case of wind tunnel design optimization, the following main independent variables were already defined in Prada-Nogueira et al. (2015) and presented in Chapter 4:

1. Width of the tunnel.
2. Length of the test section.
3. Width of the test section.
4. Relative position of fan and test sections.
5. Fan diameter.
6. Test section geometry.
7. Profile shape of the so-called ducts 1 and 2.
8. Area distribution for the wind tunnel sections.
9. Transverse shape for the wind tunnel sections.
10. Number of fans.

For this design problem, we propose, based on our experience, the following hierarchy of variables for the optimization model:

1. <u>High importance variables</u>: width of the tunnel, length of the test section, width of the test section, relative position of fan and test sections, fan diameter and geometry of the test section.
2. <u>Medium importance variables</u>: profiles for ducts 1 and 2, area distribution and shape of sections in ducts 1 and 2.
3. <u>Low importance variables</u>: number of fans.

This hierarchy reflects the importance the engineer assigns to each variable. Treating variables differently, according to their hierarchy (i.e. their importance on the value of the attributes considered), allows for a more efficient optimization process, as will be explained below.

It must be noted that the hierarchy of variables for this particular case, or for any other, is not unique and it must suit the purpose and experience of the designer. This is where the engineer plays a key role in ensuring the best set-up for the optimization problem. A bad selection of the hierarchy can result in less efficient optimizations.

Optimization phases

The second key aspect of the optimization architecture presented, after variable hierarchy, is the concept of optimization phase. Figure 5–1 summarizes the optimization model structure and introduces the concept of optimization phase for two example set-up configurations.

Figure 5–1 - Optimization model structure, illustrating the optimization phases, for two example set-up configurations. The arrows and equal signs indicate magnitude of change for each type of variable in each phase.

The main difference between phases is the level of change of the various variable hierarchies (as well as the search techniques employed by the model). Figure 5–1 depicts how the variable value-changes are considered in the different phases for two example configurations (a big arrow stands for gross changes, a small arrow for medium changes or even fine tuning and an equal sign means that variables of that hierarchy are kept constant or derived from others). The number of phases depends on the particular problem and the accuracy and time constraints.

Figure 5–1 illustrates how MOST-HDS, after a design exploration phase (Phase 0, not included in this figure because it is not an optimization phase), will implement different types of change for each variable, depending on the hierarchy of that variable and the optimization phase.

For the initial phases, given that the designer has a reasonable idea of where in the search region the optimum designs could lie, a certain variation will be allowed for the high importance variables, those with a stronger impact on the value of the attributes. However, this variation range allowed will not be gross, otherwise the search region will be too large and the total computing time too long. It is important to note that, for discrete variables, a small change may already imply a qualitative change in design.

For medium importance variables, the model allows the highest level of change. This is so since it is normally for this type of variables that the designer cannot rely on his intuition or experience alone, or for which he cannot take all the mutual interactions into account, to know beforehand which designs can be better than others. It is thus important that the optimization explores big changes in these variables.

Regarding low importance variables, they are not modified for the first stages of the optimization. The reason behind this is that their impact on the value of the attributes is weak and therefore it makes no sense trying to fine-tune the design at this very early stage of the optimization.

As the optimization proceeds, the variation of the high importance variables and medium importance variables is gradually reduced from their initial levels, and it is the low importance variables that suffer gross changes, because it is in these final stages of the optimization that the designs have to be fine-tuned.

The whole architecture and levels of change for each phase and type of variable (Figure 5–1) can of course be adapted to each particular problem if the designer wishes to do so.

A naïve example of the difference between variables of different hierarchies and between gross and fine changes can be the selection of a vehicle to purchase. The high importance variables would be the type of vehicle, and gross changes would be either selecting a car or a truck, while a low importance variable would be vehicle color and a small change would be changing the tone of green chosen, for example. This example is illustrated in Figure 5–2, Figure 5–3 and Figure 5–4.

Figure 5–2 - Gross and fine tuning example for high importance variables. In this example the high importance variable is the type of vehicle. In the upper line, gross changes, and in the bottom line, for the selected vehicle type (car), fine tuning of the particular model.

Figure 5–3 - Gross and fine tuning example for medium importance variables. In this example the medium importance variable is the type of fuel: diesel or gasoline. In the upper line, gross changes (diesel or gasoline), and in the bottom line, for the selected fuel (gasoline), fine tuning of the particular gasoline type.

Figure 5–4 - Gross and fine tuning example for low importance variables. In this example the low importance variable is the color of the vehicle. In the upper line, gross changes, and in the bottom line, for the selected color (green) fine tuning of the tone.

Variable hierarchy and optimization phases are at the core of a structured optimization model. Their importance stems from the fact that the number of evaluations of the objective function can be reduced in a robust and efficient manner if the selection of variables in each hierarchy level and the particular gross and fine tuning levels are well selected by the expertise of the designer.

Furthermore, the optimization algorithms, evaluation methods or tools used can differ from phase to phase to better exploit the types of variables to be modified in each phase (discrete/continuous), their hierarchy, or the level of change they suffer (gross, fine or none). Besides, the areas of the search region to focus on can also be changed during the optimization process. This is done automatically by MOST-HDS, based on its embedded intelligence and metaheuristics, as will be explained later on in this chapter.

To further illustrate the optimization phases, the detailed optimization architecture is shown in Figure 5–5, for each proposed phase. The example application is the wind tunnel design optimization, subject to a set of constraints.

For this particular case, the approach of Figure 5–1 is followed, with some specific adaptations. Some of the high importance variables (width of the tunnel and length and width of the test section) are left constant from the very beginning, while the rest of the high importance variables suffer medium changes. This is so to limit the number of designs for the exploration phase (Phase 0) to a manageable number of 32, in order to present and analyze the results for this Thesis with more clarity. It also stems from the fact that the experienced tunnel designer will acknowledge that the variables set as constants are usually constraints of the project and so no modifications (or only minor ones) are allowed.

As commented above, this methodology, with the appropriate modifications – it is the job of the designer/engineer to adapt the method (variable hierarchies and number of phases) – can be used for other problems of advanced aerodynamic design of complex systems. In this Thesis a second example, the application of MOST-HDS to the shape optimization of a critical part of industrial boilers, will also be presented.

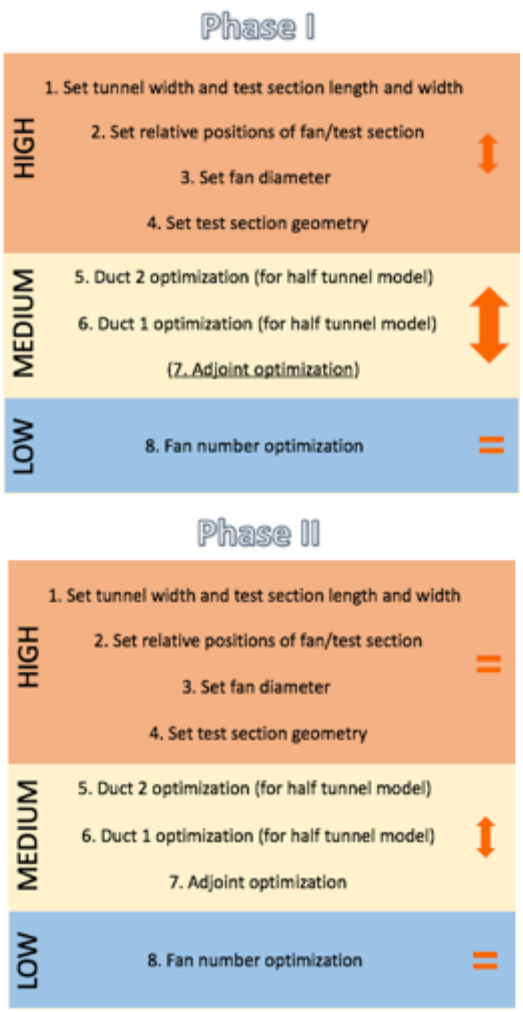

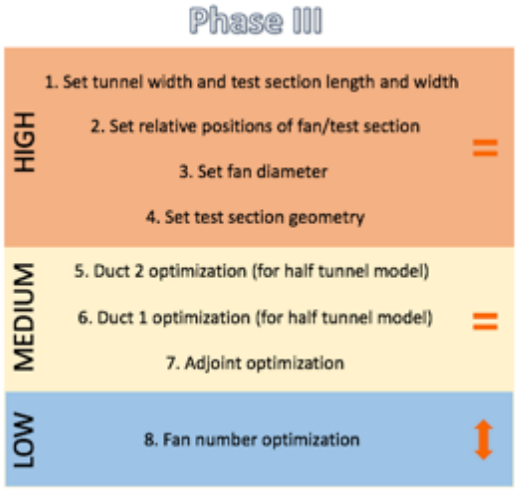

Figure 5–5 - Proposed detailed optimization architecture for the example case of a wind tunnel design optimization and for one possible problem configuration.

As the optimization proceeds, the algorithm will keep the best solutions it finds, and it will calculate the new design points taking the architecture shown in Figure 5–5 (or the particular one set by the designer) into account for each phase. Consequently, in the first phases it will allow for changes in the variables of higher importance but, gradually, it will focus on the areas of the search region which are yielding better results and, for those designs, it will reduce the magnitude of the modifications for variables of higher importance and it will focus on the optimization of the lower importance variables.

5.3. Description of the MOST-HDS algorithm

The optimization algorithm needs a set of embedded metaheuristic rules to determine how to move throughout the search region, for the different variable hierarchies, variable types (discrete or continuous) and optimization phases. This section will give an overview of these rules.

1. Phase 0: Initial design set evaluation (design exploration phase)

The initial phase or Phase 0 performs an initial evaluation of a set of design points within the search region. Design points in this initial set will usually have various different values for the high and medium importance variables and fixed values for the low importance variables, in accordance with Figure 5–1 and Figure 5–5, but it is a phase previous to those shown in these figures, since it is not an optimization phase in itself, but a mere design exploration.

In defining this initial evaluation to be performed, the experience of the engineer is critical, since it must be broad enough to explore the whole area of the search space where optimum points could be found. The optimization algorithm will then refine the search in each optimization phase, but a poor initial evaluation set, as happens with most optimization algorithms, will increase the computing time required to find the optimum solutions or may make convergence more difficult. However, using a very broad evaluation set is only recommended in cases in which there is a high uncertainty on where the optimum may lie, because a very high number of initial points will also increase the computation time considerably. The ideal situation is to generate an initial evaluation set which is both limited in the number of points and which covers the whole search space well, or the area where the optima are known to lie. This situation is common to most algorithms currently used.

In the real industrial cases presented in Chapter 6 we will use initial evaluation sets which work well for this kind of problems, based on our experience. In one of the examples, the wind tunnel design optimization, this set is generated as all the possible combinations of all maximum and minimum variable values for the whole set of variables defined. Thus the first phase explores the values of the attributes for design points on the limits of the search space and will then, based on these results, move into the search space. In the second example, the industrial boiler inlet duct, the initial evaluation set is generated by Design of Experiments (DoE).

For computer-based design optimization, as is our case, DoE schemes such as Latin Hypercube Sampling (LHS) or Orthogonal Arrays (OA) are recommended in literature (refer to Krajnovic [2007] or, even better, to the survey work in Simpson et al.[2001]).

However, for other cases, such as the problem of the application of MOST-HDS to a mathematical test function (also presented in Chapter 6), the initial set is purely a random generation of the minimum number of points which is considered necessary to have a good coverage of all the search space.

In any case, the way MOST-HDS performs has been designed to reduce the dependency of the results and of the convergence rate on the initial evaluation set as much as possible. Anyhow, extensive work on this topic is part of the future work to be performed.

Let us illustrate Phase 0 for the wind tunnel example case. In this problem, the initial evaluation set is generated according to the following steps:

1. Two values are chosen for the relative position of the fan and test sections.
2. Two fan diameters are selected (one below and one above a nominal recommended diameter).
3. Two geometries for the test section shape are set (square or circular).
4. Two possible profile shapes are used for duct 1 (one nearly circular and one skewed). Duct 1, as explained in Chapter 4, is the duct which joins the test section and the fan and which is downstream of the test section.
5. Finally, two shapes (square or circular) are set for the transverse sections of duct 1.

It is important to note that duct 2 is kept constant to a baseline design geometry for this example case, once more to keep the number of design points for Phase 0 to 32[11].

This yields a tree of 32 wind tunnel design points (Figure 5–6). These design points are evaluated using the CFD software ANSYS FLUENT v17. The tree is designed in this manner, in order to minimize the points to be evaluated, while covering the search region adequately.

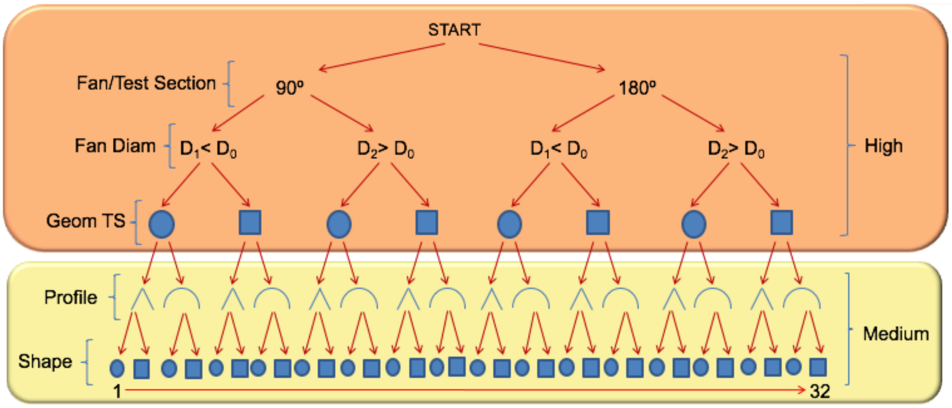

Figure 5–6 - Example initial evaluation set for Phase 0 (in this case, 32 wind tunnel designs).

Once the initial search is set in Phase 0 of the optimization, the different candidate design points are evaluated using CFD, in the case of aerodynamic optimization problems, or using any particular evaluation function in other cases.

Based on the results of Phase 0, which is a mere design exploration, the algorithm must decide how to proceed to the optimization itself. This means that the algorithm must decide:

1. How to use the information from the previous phase to set up the search problem of the current phase.
2. How to perform an optimization search in successive steps, seeking design improvements at a minimum computing cost.
3. When to stop searching and give way to the next optimization phase.

The following subsections explain the general strategy proposed for the optimization search. The scheme proposed exploits a mix of gradient, genetic and swarm search concepts.

[11] The industrial boiler case will illustrate a much larger number of design points for the exploration phase.

2. Pareto tolerance threshold

Given a set of evaluated solutions, some of them must be rejected, while the rest are kept for further analysis.

The first step is to calculate the Pareto front for the solutions of the initial search on the evaluation set. The Pareto front groups the optimum solutions in a multi-objective optimization. Any solution on that front improves at least one objective at the expense of sacrificing the value of at least another objective, with respect to the rest of the points on the Pareto front.

Because the solutions on the Pareto front may not be the only designs worth considering for the subsequent optimization phases, a tolerance threshold is defined. An example threshold is depicted in Figure 5–7. Designs within this area of the search region could potentially evolve to be optimum designs, yielding even better results than those solutions initially on the Pareto front, because this Pareto front is only the result of a first-step exploration.

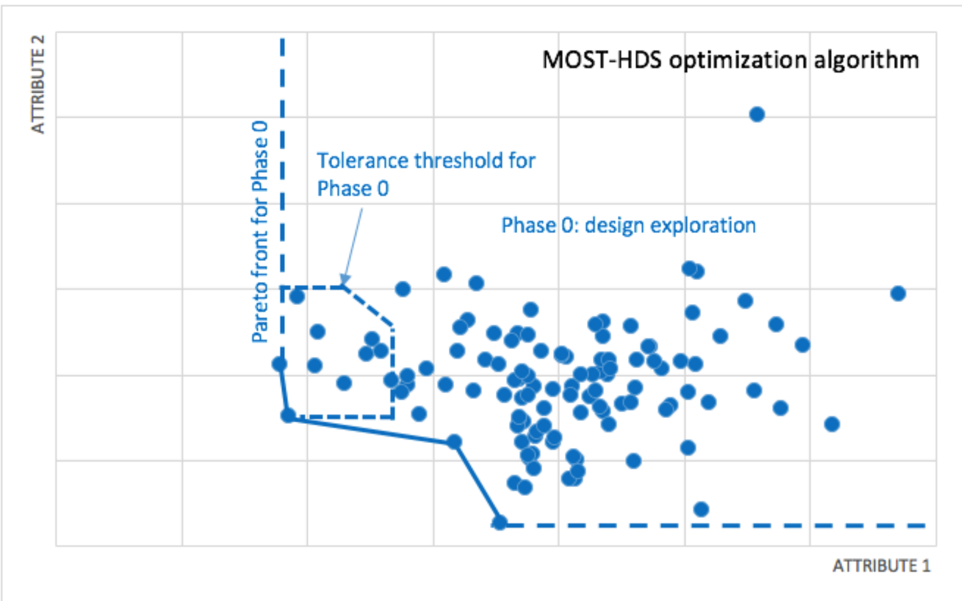

Figure 5–7 - Illustration of the Pareto front and the tolerance threshold for Phase 0 of the MOST-HDS optimization algorithm.

The threshold is defined in terms of allowed tolerances for each selected attribute. For instance, a possible threshold definition can be:

$$f_{i,j,k}^{Threshold} = f_{i,j-1,k}^{Pareto} + \delta_{i,j,k} \qquad \textit{Equation 5–1}$$

where *i* represents the particular attribute considered, *j* the next phase of the optimization, *k* represents each solution on the Pareto front, $f_{i,j-1,k}^{Pareto}$ represents the value of attribute *i*, for phase *j-1* (the current phase), at point *k* along the Pareto front, $\delta_{i,j,k}$ is the value of the particular threshold assigned and, finally, $f_{i,j,k}^{Threshold}$ is the threshold value that will be considered for attribute *i* and optimization phase *j* at the Pareto point *k*.

For cases such as the wind tunnel, the threshold can simply replicate the shape of the Pareto front (refer to Chapter 6). The threshold of Figure 5–7, however, offers a more general example. In this case the threshold does not replicate the Pareto front, but is focused on a very particular area of the search space to which the designer wants to limit the optimization search from this phase onwards. This is the type of threshold used for the industrial boiler inlet duct, as will be explained in Chapter 6. An alternative threshold definition, which can easily be introduced in the model, would be to limit the number of points selected for the next phase to a maximum amount, so only the best 10 or 100 or 1000 points would be kept, for instance.

Regarding this tolerance definition, for problems which are evaluated using CFD codes, it is worth commenting that the best values for the tolerance on each of the attributes depend on the number of solutions explored in the current phase, the accuracy of the CFD solver (the level of precision increases in general from phase to phase) and the trade-off between computing time and accuracy stated by the designer. Special care must be taken, for instance, if the accuracy of the CFD solver (for example in terms of mesh coarseness) does not yield a systematic error in the results. However, the more the engineer uses this optimization tool, the more experience he will have to select appropriate tolerance values.

Once the tolerance threshold area is defined, as shown in Figure 5–7, all the solutions that lie between this curve and the Pareto front are potential candidate solutions kept for the next optimization phase. Neither strict dominance nor significant dominance criteria are used, to keep some additional and potentially interesting designs (see Cuadra [1990] and Schweppe and Merril [1986] for a discussion on these dominance criteria).

However, among all the solutions that lie within the tolerance threshold, not all will be used as baseline for the following optimization phase. Given that the CFD evaluations are very time consuming, candidate solutions to be kept have to be selected efficiently. The selection methodology is explained in detail in *Step 3. Selection of search directions*.

3. Selection of search direction(s)

Firstly, the algorithm will search for the closest solutions on the Pareto front to each candidate design. These are potentially good search directions to continue the optimization and it is one of the main novel aspect of MOST-HDS. The designer must choose the number of closest solutions to be used to determine the search direction(s) from a particular candidate design. He can select to use the closest solution on the Pareto front, or the two closest, or more (this can also be selected automatically by the algorithm). The higher the number of directions to consider, the higher the probability of reaching a good optimum, but also the analysis will be more time consuming, so a trade-off must be reached.

It is worth noting that, for the particular case of solutions on the Pareto front of the previous optimization phase, the algorithm will follow search directions along the Pareto front itself.

Once the search directions for all candidate solutions have been determined, the reduced set of solutions that will really be used for the next optimization phase must be selected.

The selection method is as follows:

1. The algorithm groups all the candidate solutions depending on their search direction (i.e. the point(s) on the Pareto front towards which they would move).

2. Among those solutions which would move towards the same Pareto point(s), both the distance between designs in the space of variables and in the space of attributes must be determined.

3. Space of variables: the metric to measure the distance in the space of variables is the relative distance between two designs, for each variable, with respect to the maximum range of that variable in that particular optimization phase. Then, to add up all the distances for the different variables, different weights are applied to the distance for each variable, depending on the hierarchy of that variable and the phase.

4. The metric to measure the distance in the space of attributes is analogous to that of the space of variables, except that the weight of all the attributes is the same (unless the user wants different weights).

5. When a number of designs that would move towards the same Pareto point(s) are close both in the space of attributes and in the space of variables (i.e. below certain preset maximum distance thresholds), then a representative for that subset of designs will be selected, to prevent the algorithm from evaluating very similar designs. This representative selection will be carried out by means of a clustering algorithm (the k-means algorithm, in our case, as originally explained in Hartigan [1975] and as currently coded in MATLAB). This is similar to the work carried out on swarm search methodologies (a good reference example of enhanced swarm search is Shi and Eberhart [1998]).

6. However, if various solutions are close in the attribute space, but far apart in the variable space, all must be kept, because they represent different designs and they enrich the search process (a similar approach is proposed in Cuadra [1990]).

The discarded solutions of intermediate optimization phases will, anyhow, not be eliminated completely and will be kept, in case the algorithm decides they can still be interesting candidates to analyze in any of the subsequent optimization phases.

4. Selection of search variable(s)

Based on the search direction(s) defined, the algorithm will determine the variable changes needed to move each model towards its Pareto target model(s). It will run through the variable values for each selected point and compare those values to the values of the target Pareto point(s). Search variables for each candidate point will be those for which the point and its target Pareto point(s) have different values.

5. Calculation of the increment to be applied to each variable

Once the search directions for all points have been determined and the variables to change have been picked up, the algorithm will determine the amount each variable has to be changed. In order to do this, the algorithm will check the type of variable (i.e. hierarchy) and the optimization phase and it will introduce value changes to each of the variables, following the guidelines of Figure 5–1. For example, if the variable to be changed is of high importance, for optimization Phase I the changes introduced would be small, towards the value of the target point on the Pareto front. However, this is only the general approach followed by the algorithm. The detailed procedure is detailed below and shown in the flow diagram of Figure 5–10.

For continuous variables the changes are clear to understand. For instance, in Phase I, a big change can imply moving towards the target point 2/3 of the difference between the value of each variable for the design point considered and the value of that same variable for the target point. A small change, on the other hand, can mean moving 1/3 of the distance in that variable. The particular increment factors are calculated by the algorithm dynamically as explained below.

For discrete variables, however, the algorithm will jump from one discrete value to the next one – for instance, from a circular to a square shape. For these variables, small and big changes may therefore coincide, depending on their range of values.

These increment factors are modified by the algorithm depending on the hierarchy of variables, the particular variable, the optimization phase and, most importantly, the results of the optimization process. This method of increments follows a very similar approach to the extensively used method developed originally in Nelder and Mead (1965). The possible changes of values explained in that work (namely reflection, expansion and contraction) are also used here, with some modifications, and using not the centroid point of the set of points defining the simplex, but the closest point(s) on the Pareto front.

It is worth noting that MOST-HDS will use increment factors below or above unity. Hence the exploration moves are both within the search region already explored and also outside of it.

6. Evaluation of the new design points

Once steps 1-5 have been performed for all the selected designs within the Pareto threshold of the previous optimization phase, the new candidate solutions will be evaluated (in our case simulated using CFD) and a new Pareto front will be determined.

7. Further optimization phases

To move to further optimization phases, the algorithm repeats steps 1-6 until the stopping criteria defined are met.

The user can select a maximum number of evaluations (or alternatively maximum calculation time) and the algorithm can estimate the number of phases and solutions to be kept for each phase to match that time target as closely as possible, as well as other internal aspects such as mesh refining criteria for each phase (in the case of CFD evaluation), etc. Another possible stopping criterion is the maximum percentage of the current set of design points that is in the best Pareto front (as soon as the optimization reaches that threshold value it will stop).

Moreover, the algorithm is able to change mesh coarseness, for example, depending on the optimization phase. Extensive results on the impact of mesh coarseness (mesh sensitivity analyses) will be presented in future work. For the purpose of this Thesis, mesh size has been varied in each case until a good trade-off between accuracy and computing time is found.

8. Final optimum design fine-tuning: the adjoint method

For an enhanced fine-tuning of each solution on the Pareto fronts found for the last optimization phases, the use of the adjoint method (a good classical reference is Giles and Pierce [2000]) is proposed, as mentioned in Figure 5–1. This method allows for the determination of the sensitivities of one or more particular attributes to local modifications in the geometry of the body of interest. One of the most relevant research works on the application of adjoints to advanced aerodynamic optimization is Paniagua (2014), for the case of high-speed train nose optimization.

In the following sections, important remarks on the MOST-HDS algorithm are highlighted. For a detailed illustration of the optimization flow diagram and metaheuristics behind MOST-HDS, refer to Figure 5–10.

The MOST-HDS optimization procedure in short

In the following sections, important remarks on the MOST-HDS algorithm are highlighted. For a detailed illustration of the optimization flow diagram and metaheuristics behind MOST-HDS, refer to Figure 5–10.

A brief summary of how MOST-HDS proceeds is included here for the reader's comfort. Figure 5–8 illustrates the main steps followed:

1. Phase 0 is the design exploration phase, in which a number of design points are generated and computed to have an initial representation of the space of attributes (i.e. the performance space). These points can be generated by means of any Design of Experiments (DoE) technique, or other methods.

2. A first Pareto front can be computed, to represent the optimum designs for Phase 0. The Pareto front is a very useful tool for true multi-attribute optimization problems.

3. A tolerance threshold is automatically generated, based on the expert's settings, to group the candidate points that will be selected for the next phase. Clustering can be applied to select representative points among a group of very similar design points (both in the space of variables and in the space of attributes).

4. A crossover is performed between each selected design point and its closest point(s) on the Pareto front. The crossover is controlled by the so-called increment factors, which are automatically tuned to improve the optimization speed and final result.

5. A new set of design points is hence generated. These points constitute Phase I.

6. A new Pareto front is computed. The optimization has proved successful if the new Pareto front improves the Pareto front of the previous phase.

7. This procedure can be repeated as many times (i.e. phases) as set by the expert, or as controlled internally by the algorithm based on a set of stopping or convergence criteria.

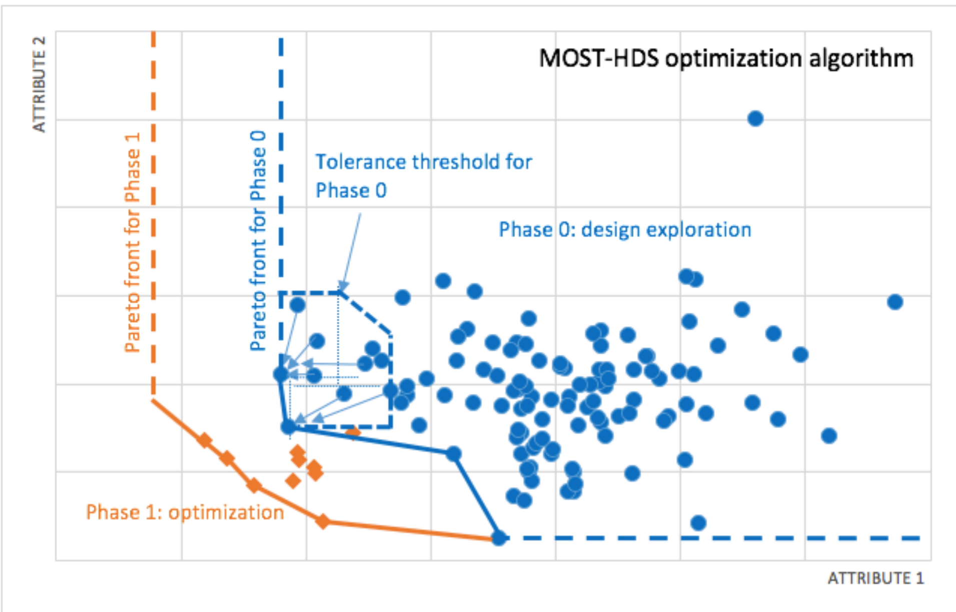

Figure 5–8 - Illustration of the procedure followed by the MOST-HDS optimization algorithm for the optimization in each phase.

Final remarks on the MOST-HDS optimization model

MOST-HDS aims to prove an original, general methodology based on multi-attribute, structured optimization and following a hybrid direct search approach. It combines genetic, gradient and swarm search intelligence in every iteration, as will be explained in this section.

Besides being multi-attribute, because it has been developed specifically for problems with more than one objective to be optimized (although it could also be used for single-attribute optimization), MOST-HDS exploits the concept of structured optimization, making use of two key differential aspects: hierarchy of variables and optimization phases. These concepts have been used in other fields (refer to the State of the Art in Chapter 3), but have not been used, as far as we know, in aerodynamic shape optimization.

Furthermore, MOST-HDS proposes a novel hybrid direct search approach. In the first place, according to the extensively cited paper by Hooke and Jeeves (1961), the term direct search is used, as they state literally, "*to describe sequential examination of trial solutions involving comparison of each trial solution with the "best" obtained up to that time together with a strategy for determining (as a function of earlier results) what the next trial solution will be. The phrase implies our preference, based on experience, for straightforward search strategies which employ no techniques of classical analysis except where there is a demonstrable advantage in doing so.*". In other words, direct search will imply direct evaluation of each candidate solution (in our cases using CFD) and a search strategy to proceed with the optimization, avoiding the use of any other methods, such as surrogate models or any kind of approximation or alternative to the direct evaluation of each candidate point[12].

Regarding the search strategy developed for MOST-HDS, besides following a structured optimization approach, it is a combination of genetic, gradient and swarm search intelligence, hence a hybrid direct search. Its novelty stems from the fact that, as opposed to most other authors who have combined gradient-based and non-gradient-based algorithms (relevant examples are Guliashki [2008], Hegazi et al. [2002] or Hsiao et al. [2001]), MOST-HDS does not switch from one type of algorithm to the other depending on how the optimization is advancing, but it benefits from elements of all these types of algorithms in every phase.

To illustrate this better, an example of the search strategy, showing the most relevant cases which can occur, is presented in Figure 5–9. This figure is also very important because it clarifies the difference between the space of variables and the space of attributes, for a simplified example of 2 variables and 2 attributes. The terms search space and fitness space are also used to refer to the same concepts (a good example emphasizing the difference between both spaces is Huband et al. [2006]).

[12] Of course it can always be argued that CFD evaluation, unless computed using Direct Numerical Simulation, or even only because it uses space and time discretization, is not a direct evaluation of the problem either. However what we mean by direct search is the use of the most approximate evaluation method available, avoiding the use of further simplifications or approximations.

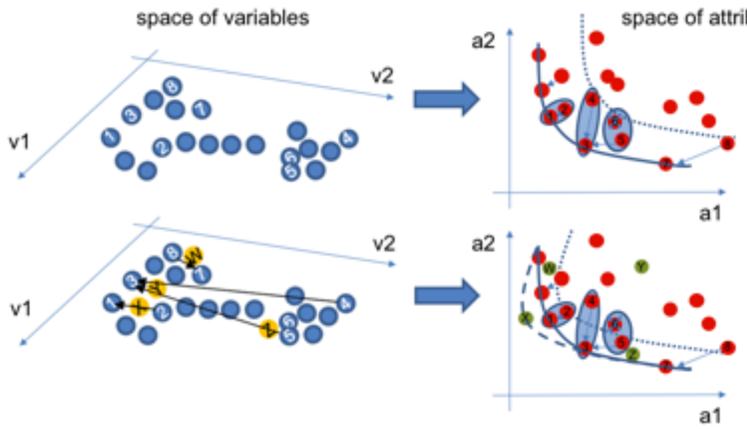

Figure 5–9 - Conceptual explanation showing how the hybrid optimization algorithm proposed proceeds, combining genetic, gradient and swarm-search intelligence for a multi-attribute, structured optimization. The figure depicts the Pareto front and threshold for the current phase and the new Pareto front and threshold obtained for the next phase.

After a particular phase has been computed, the solutions to be used for the next optimization phase are picked only from within the Pareto tolerance threshold, as has been explained. This is the fitness criterion (in genetic algorithm terminology). Moreover, once the distance between design points, both in the variable and attribute spaces, is calculated (because both distances are important), clustering may further eliminate design points which are close to others in both spaces (for instance design point 6, in the example of Figure 5–9), so this step is also part of the fitness evaluation of each candidate solution.

For the following phase, the new design points obtained will be the crossover of the design points selected in the current phase. The crossover process (i.e. determining how the child solution is obtained from both parents) can change from phase to phase, and depending on the type of variable and its hierarchy.

One of the key aspects of noting the conceptual difference between space of variables and space of attributes is that, for an efficient search process, certain parent design points can be kept or discarded for the crossover process, depending on their relative distances in both spaces. As can be seen in Figure 5–9, the child design points obtained from the most relevant crossover combinations, compared to their parents, can be:

1. Close in the space of variables and close in the space of attributes. Example: parent solutions 1, 2 and their child solution X. The crossover of this type of parent points will generally yield a very predictable design, such as X, very similar to its parents. Therefore this type of crossover can be discarded to reduce the number of evaluations. Clustering can obtain a representative design point from a group of points which are very close (i.e. below preset distance thresholds) in both spaces and only cross them with points which are not so close in either spaces, to explore other regions of potentially better designs.

2. Close in the space of variables and far apart in the space of attributes. This implies a critical region of design, in which performance is very sensitive to small changes in the variables. Example: parent solutions 7, 8 and their child solution W. The crossover of this type of parent points, which are very close in their variable values and yet far apart in their attribute values can produce original or non-conventional design points, such as point W, which is also close in the space of variables but in a different area of the space of attributes. Thus the search can produce innovative or disruptive designs, showing that the results are not intuitive and illustrating the importance of applying automatic optimization schemes.

3. Far apart in the space of variables and far apart in the space of attributes. Example: parent solutions 3, 4 and their child solution Y. The crossover of this type of parent points is worth exploring, since its result will also normally be far apart in the space of variables and in the space of attributes, so it should produce quite novel designs, which could improve the attribute values obtained up to this point of the optimization.

4. Far apart in the space of variables and close in the space of attributes. Example: parent solutions 3, 5 and their child solution Z. The crossover of this type of parent points is also worth exploring, because it means that results are not intuitive, at least in some parts of the search region, given that very different designs can yield very similar performances.

In conclusion, the MOST-HDS optimization algorithm is hybrid in the sense that it uses a gradient-based approach to define the Pareto front and tolerance threshold, and to select the search direction; thereafter, variable increment (crossover strategy) is defined depending on the hierarchy of the variables to be changed, their type, the current phase and the results obtained up to this point of the optimization, in order to obtain child solutions from their parents, so it follows a genetic approach (which may perform the crossover of very different designs or yield very original designs, as commented above). Swarm search aspects are used, as mentioned, mainly whenever clustering is applied and, to a certain extent, to focus on certain areas of the search region (either in the space of variables or in the space of attributes) based on the results of the search process for groups of design points in different parts of the search region.

In the proposed algorithm there is no mutation, as opposed to most genetic algorithms, since all child solutions are obtained from two parents. It could be included, however, if deemed convenient.

In general terms, on the one hand, the genetic approach introduces the randomness needed to produce sufficiently novel design points which cover well both the space of variables and the space of attributes. On the other hand, gradient search is used when the movement of a design point improves and it seems to follow a gradient reasoning (local improvements). Finally, swarm search intelligence is used at all moments to control how the global performance in the different areas of the search region is progressing. All these elements are key to handle the optimization of challenging functions or real-life problems.

The intelligence embedded in the MOST-HDS model has proved successful, as shown in Chapter 6, not only for the type of problems it was initially aimed at, namely aerodynamic shape design optimization with big geometry changes, but also for more general optimization problems.

Detailed flow diagram of the metaheuristics behind the MOST-HDS algorithm

The following figure shows the detailed flow diagram of the MOST-HDS optimization algorithm developed in this Thesis.

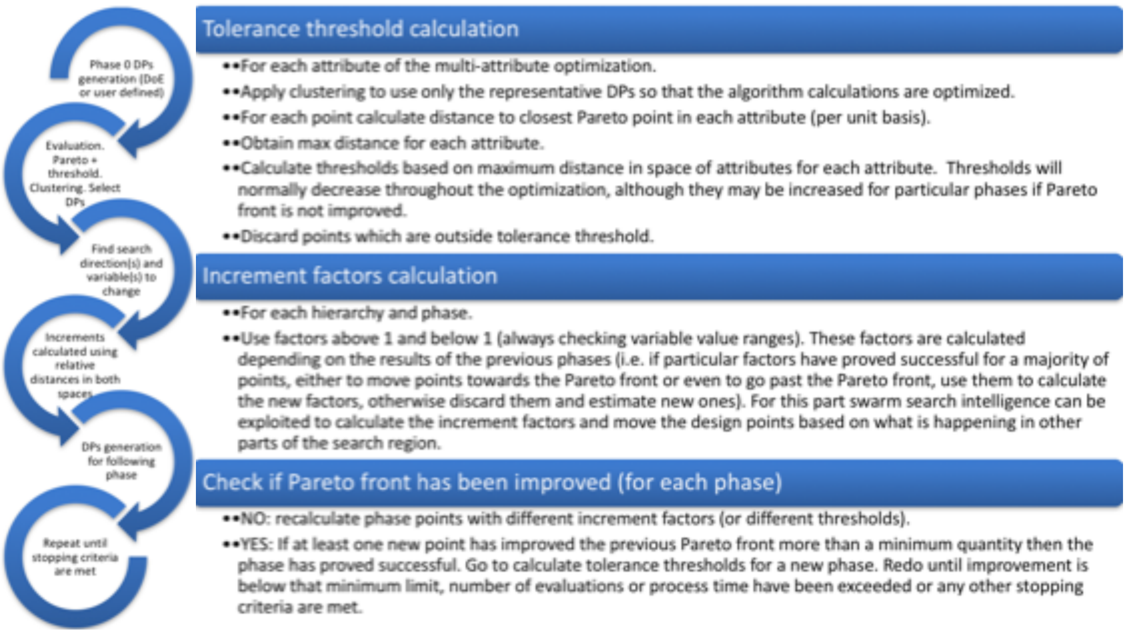

Figure 5–10 - Flow diagram and detailed notes describing the optimization procedure followed by the MOST-HDS model. DPs stands for Design Points.

5.4. Implementation of the MOST-HDS algorithm

The architecture of the model implementation is illustrated in this section. This architecture contributes to the State of the Art because it carries out a full implementation of an automatic workflow simulation environment for optimization of CFD problems, based on direct search, for a wide range of fields. In particular, Microsoft Excel and a CFD solver (ANSYS FLUENT in this case) are coupled and a Visual Basics for Applications (VBA) code is developed to implement the MOST-HDS solver, which controls the optimization process from Excel (externally to ANSYS). The MOST-HDS algorithm is coded in VBA and not in other programming languages (C++, Matlab, etc.) because it was considered that the integration to ANSYS would be easier and more efficient. In any case the code can easily be adapted to these alternative programming languages, to make the MOST-HDS algorithm even more broadly usable.

The model architecture is presented in Figure 5–11. It is worth highlighting that the architecture for the MOST-HDS model has been designed with the objective of making this tool as general as possible. The initial goal of the model was the aerodynamic shape optimization of complex geometries with big geometry changes (for these cases an external CFD solver is required). Nevertheless, the tool has also been applied to a commonly used benchmark mathematical function, not only to show its applicability for very different and challenging optimization purposes, but also to illustrate how general the model is. To give an example, for this general purpose mathematical optimization problem (presented in Chapter 6), the architecture is valid and the only difference would be that, given that an external evaluator is not required (all the evaluations can be performed internally in Excel), and because there is no need for variable translation, the module *Translation of optimization variables to solver variables* would not be called.

Figure 5–11 - Schematic diagram of the module architecture of the MOST-HDS model implementation for a fully automatic optimization workflow, coupling Microsoft Excel VBA and an external solver or evaluator, if required (in this case ANSYS was used for the CFD evaluations).

5.5. Final remarks

This chapter has presented in detail the MOST-HDS optimization model. Before moving on to Chapter 6 and the results of the application of this tool to industrial problems and to a mathematical benchmark function for optimization algorithms, the following is a summary of the main highlights of this model:

1. The MOST-HDS model is a **M**ulti-**O**bjective **St**ructured **H**ybrid **D**irect **S**earch optimization algorithm.

2. A first contribution of this model is to apply a structured optimization approach, and its two main elements (variable hierarchies and optimization phases), to aerodynamic design optimization problems.

    a. The structured architecture allows for a scope, level of detail and search schemes which are modified or adapted automatically in each phase of the optimization.

b. The concept of hierarchy of variables as a method to feed into the model the stronger or weaker influence of a particular variable on the attributes is very interesting for industrial optimization problems, as will be shown in Chapter 6. The optimization process handles the variables differently among the various hierarchies defined. This, alongside other key features of MOST-HDS, allows for an efficient search process in a type of problems which is characterized by considerably time-consuming design point evaluations.

3. The difference between the variables used by the optimization algorithm and the variables used by the evaluator (in this case a CFD solver) is once again noted (as in Chapter 4). Consequently, a translation module is required to transform the optimizer's variables into those used in the CFD solver for geometry parameterization.

4. The hybrid direct search scheme proposed by MOST-HDS is an efficient approach which, thanks to the combination of genetic, gradient and swarm search aspects, can move through the search region in a smart and adaptive manner.

5. The model developed is a fully automatic, robust and highly flexible optimization tool which, once set-up by an expert engineer, can be used by any non-expert person.

6. The model architecture developed, which is highly general and applicable to other domains of optimization, is also an important contribution of the MOST-HDS tool.

7. The concepts of space of variables and space of attributes (also referred to in literature as search space and fitness space) are clarified, so that it can be seen that the search process has to take the position of each design point in both spaces into account.

8. Due to the way the optimization is carried out, the MOST-HDS model paves the way for non-intuitive and quite disruptive designs, which will often outperform more conventional designs, as will be seen in Chapter 6.

List of Figures

Figure 5–3 - Gross and fine tuning example for medium importance variables. In this example the medium importance variable is the type of fuel: diesel or gasoline. In the upper line, gross changes (diesel or gasoline), and in the bottom line, for the selected fuel (gasoline), fine tuning of the particular gasoline type.

Figure 5–4 - Gross and fine tuning example for low importance variables. In this example the low importance variable is the color of the vehicle. In the upper line, gross changes, and in the bottom line, for the selected color (green) fine tuning of the tone.

Figure 5–5 - Proposed detailed optimization architecture for the example case of a wind tunnel design optimization and for one possible problem configuration.

Figure 5–6 - Example initial evaluation set for Phase 0 (in this case, 32 wind tunnel designs).

Figure 5–7 - Illustration of the Pareto front and the tolerance threshold for Phase 0 of the MOST-HDS optimization algorithm.

Figure 5–8 - Illustration of the procedure followed by the MOST-HDS optimization algorithm for the optimization in each phase.

Figure 5–9 - Conceptual explanation showing how the hybrid optimization algorithm proposed proceeds, combining genetic, gradient and swarm-search intelligence for a multi-attribute, structured optimization. The figure depicts the Pareto front and threshold for the current phase and the new Pareto front and threshold obtained for the next phase.

Figure 5–10 - Flow diagram and detailed notes describing the optimization procedure followed by the MOST-HDS model. DPs stands for Design Points.

Figure 5–11 - Schematic diagram of the module architecture of the MOST-HDS model implementation for a fully automatic optimization workflow, coupling Microsoft Excel VBA and an external solver or evaluator, if required (in this case ANSYS was used for the CFD evaluations).

6

Chapter 6 - Results obtained

Don't be trapped by dogma - which is living with the results of other people's thinking.

Steve Jobs.

This chapter presents a detailed overview of the most relevant results obtained with the application of the MOST-HDS model to different problems. Firstly, it analyzes two industrial problems of shape design optimization of very different fields. The results shown are very positive and are a strong contribution to the State of the Art of shape design optimization for real, industrial problems. The first of these two problems is the shape optimization of the inlet duct to industrial boilers (in particular Heat Recovery Steam Generators, or HRSGs) which are used in combined cycle power plants. The second case study is the shape optimization of closed wind tunnels, a facility which is used for testing and for leisure purposes. After both cases have been presented, a short section illustrates the results of the application of the adjoint method to the final fine-tuning of the optimized geometries. To conclude, and to offer a better perspective on the applicability of MOST-HDS, the model is applied to a well-known mathematical test suite used for benchmark of general-purpose optimization algorithms. Although the initial focus of MOST-HDS was the aerodynamic shape design optimization of geometries, including small and big geometry changes, it was considered that this last benchmark section could prove relevant to show the general validity of the proposed optimization search scheme. *Section 6.1*. is the introduction to the chapter. *Section 6.2.* analyzes the results of the case of the inlet duct of a set of HRSG families. *Section 6.3.* presents the results for the closed wind tunnel case. *Section 6.4.* comments on the results of the application of the adjoint method to both industrial cases. *Section 6.5.* studies the results for the benchmark of MOST-HDS when applied to the WFG mathematical test suite. Finally, *Section 6.6.* indicates the final remarks which summarize the most important conclusions which can be drawn from this chapter.

6.1. Introduction

The previous chapters have gradually presented how the MOST-HDS model has been developed: motivation and objectives, problem definition, overview of the State of the Art and a detailed description of how the model works. This chapter aims at showing clear applications of the model for real industrial problems and thus illustrate that it is a general model for shape design optimization and for certain problems of general optimization. The improvements obtained in performance for the different cases presented are quantified and the model results are validated with real measurements taken in validation cases. Furthermore, some of the optimum designs obtained are clearly unconventional, go far beyond traditional design guidelines, and would rarely have been tried out by most designers. This occurs because MOST-HDS can work with big geometry changes, which is not the case for most research works in the literature. These are some of the key contributions of this Thesis, that will be presented throughout this chapter.

6.2. Industrial boiler inlet duct shape design optimization

A particular kind of industrial boilers, referred to as Heat Recovery Steam Generators (HRSGs), are used in combined cycle power plants to recover part of the heat of the exhaust gases of a gas turbine, in order to generate steam for a steam turbine. Ever since the use of HRSGs for power plants, the shape design of the inlet duct at the entrance to these units, one of their most critical components, has followed greatly unchanged design guidelines. The contribution of this Thesis in this section is twofold. On the one hand, it shows that there is substantial room for improvement in the shape design of the inlet ducts of HRSGs, in terms of achieving a lower pressure drop, a higher velocity uniformity and an important cost reduction of the unit. On the other hand, it shows how MOST-HDS algorithm can find improved designs that may be quite unconventional and non-intuitive, in fields like aerodynamic shape optimization involving big geometry changes. The results obtained for the two HRSG families presented show that there are optimum trade-off design points with simultaneous reductions in pressure drop of up to 20-25%, in lateral surface of up to 38% and in length of up 16%, while having comparable velocity uniformities to the existing designs.

VALIDATION CASE FOR THE ANSYS CFD SOLVER FOR INDUSTRIAL BOILER SIMULATIONS

In the first place, as will also be done for the closed wind tunnel case, a brief section is presented on the validation of the results of the CFD solver used (ANSYS v17.0) for the evaluation of HRSGs.

The following table presents the comparison of the pressure losses provided by the manufacturer and the pressure losses obtained from the CFD simulation for each one of the tube banks which are located throughout an HRSG and through which water is pumped to generate steam. This is a typical comparison to validate any CFD simulation applied to HRSGs. For clarity, the tube banks are shown for an example simulation in Figure 6–1.

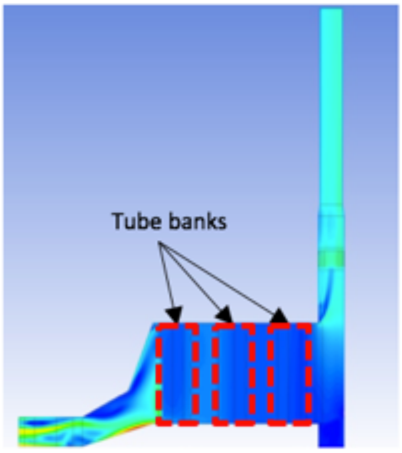

Figure 6–1 - Side view of velocity contours in the mid-plane of a typical HRSG to illustrate the position of the different tube banks.

Tube bank	**Error [%]**
#1	9
#2	9
#3	7
#4	3
#5	5
#6	1
#7	2
#8	4
#9	5
#10	5
#11	4
#12	4
#13	4
#14	4
#15	5
#16	5
#17	5
#18	5
#19	6
#20	8

Table 6–1 – Relative error between the pressure losses as provided by the manufacturer and as obtained from the CFD analysis for the tube banks of an example HRSG.

According to the previous table, there are certain errors between the values provided by the manufacturer for the pressure losses and the values obtained from the CFD simulation. These differences are mostly due to the non-uniformity of the velocity distribution at the entrance of each one of the tube banks (simulated as porous media), whilst the porous media equations assume a homogeneous velocity profile. Besides, the pressure losses provided are point measurements and their values are affected by the exact position of the reading within each tube bank's inlet/outlet plane (it must be noted that the tube banks are of considerable size).

In any case, the errors are very acceptable, given the application and the absolute pressure values, which mean that the absolute errors are of very few Pascals. Refining the CFD mesh may have slightly reduced the errors (if the sensor readings are accurate enough), but it would have increased the computation time considerably, so it was not deemed necessary. Consequently, the CFD solver is considered reliable to use as an evaluator for the optimization process carried out by MOST-HDS[13].

RESULTS FOR THE SHAPE OPTIMIZATION OF THE INLET DUCT OF HRSGS

Over the decades, HRSG inlet ducts have been designed following largely the same design trend lines. Broadly speaking, the design of an HRSG inlet duct has up to date always been of one of the two types shown in Figure 6–2.

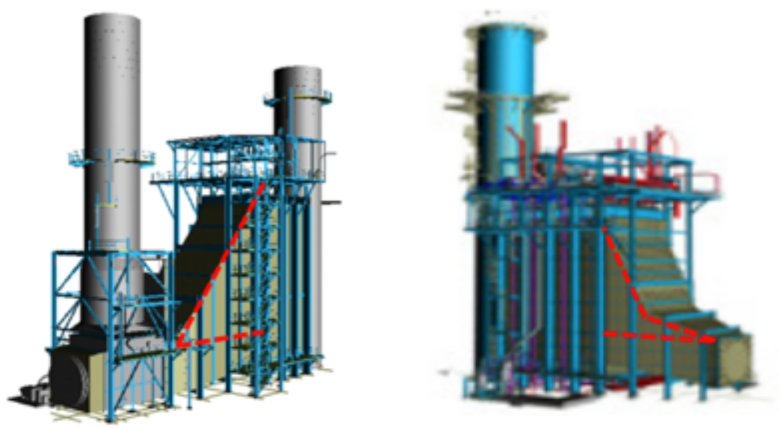

Figure 6–2 - HRSG inlet duct design types most widely used in industry: single angle inlet duct (left) and double angle inlet duct (right).

Certain manufacturers have started using alternative inlet duct designs, as can be seen in Figure 6–3. However, extensive design analyses have not been performed, as far as we know, to compare the different inlet duct designs alternatives thoroughly.

[13] In any case, if the CFD errors were systematic it would also be valid for an optimization process, because the final optimum solutions would be simulated with a much higher detail. In any case it is usually very difficult to prove that CFD errors are systematic for a particular problem.

Figure 6–3 - HRSG inlet duct alternative design types that some manufacturers are starting to use.

There are a number of works in the area of CFD modelling of an HRSG's inlet duct, but to our best knowledge, a complete shape optimization analysis of this critical element has never been addressed. The aim of these works is to analyze the flow distribution of a particular design, or the effects of elements introduced in the inlet duct to improve the flow distribution, such as Ameri and Dorcheh (2013) and Lee et al. (2002). More general works in the field of CFD analyses of complete HRSGs can be found in Aslam Bhutta et al. (2012), Daiber (2006), Galindo-García et al. (2012 and 2014), Hedge et al. (2007), Shi et al. (2009) and Sundén (2007).

The aim of applying the MOST-HDS algorithm to the design of HRSGs is to yield optimized geometries for the inlet ducts of a wide range of HRSG families. New designs or design-trends may offer better performance levels using shorter and more compact units, while having good velocity uniformity at the HRSG inlet. This is the main contribution of this Thesis, regarding this particular industrial problem.

It is worth noting that this work has been carried out for various HRSGs families of a particular manufacturer and therefore some of the results cannot be shown fully for confidentiality reasons.

The inlet duct geometry is parameterized as was explained in Chapter 4. Figure 6–4 is included here again, for the sake of clarity.

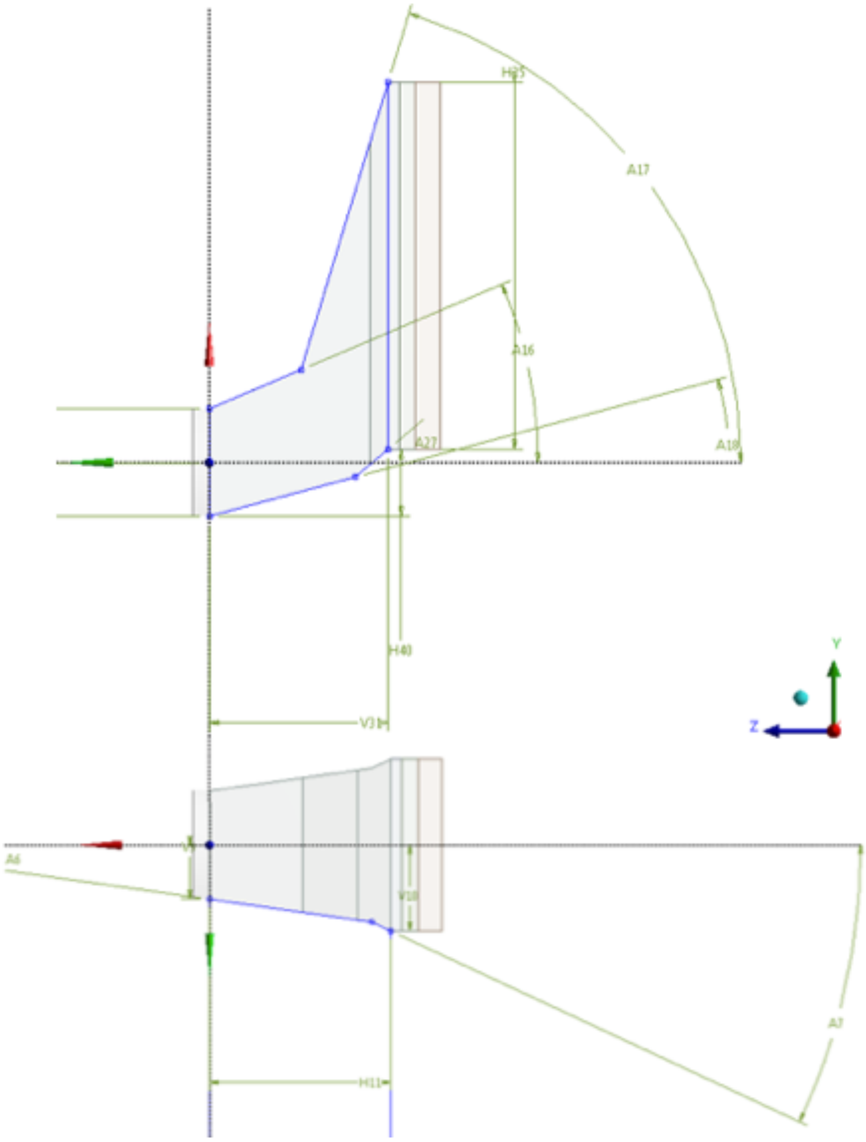

Figure 6–4 - Variables used to parameterize a general inlet duct for different HRSG families (x-axis and y-axis views).

The variables used are reminded here again: two angles for the top wall, two angles for the lateral wall (identical on both lateral walls), two more for the bottom wall and the total length of the inlet duct. These variables take into consideration the design modifications which are feasible in terms of manufacturing and assembly in real power plants. For example, curved walls or more intermediate angles are not considered of interest and they are consequently not included in this analysis.

The main concern of most HRSG manufacturers nowadays is to meet the requirements of the final client, and even improve them to be better than their competitors, while reducing the overall cost of the unit. The main requirement for a modern HRSG is keeping the pressure drop across the whole unit below a maximum allowed threshold, while recovering the maximum heat available from the gas stream. An additional and very important competitive advantage, as has been mentioned above, is being able to meet the performance requirements with smaller units (mainly reducing the total length).

The application of the MOST-HDS algorithm to this particular case of shape design optimization has produced very interesting results. In the first place, to show the performance difference of various HRSG design alternatives, so that it is clear that it is worth applying an optimization scheme, two different designs and their performance results are depicted in the following figures.

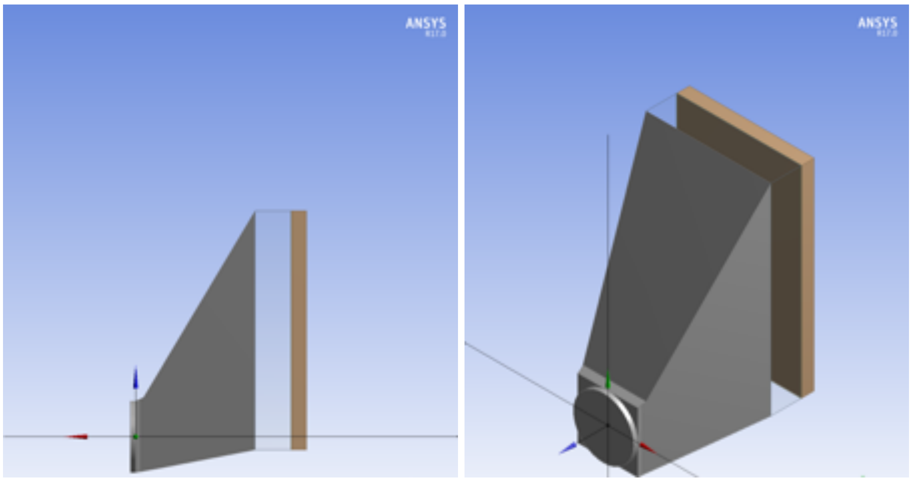

Figure 6–5 - Side and isometric views of a first example design alternative for the inlet duct of an HRSG (single angle top plane for the inlet duct). This is the real current design for this HRSG family.

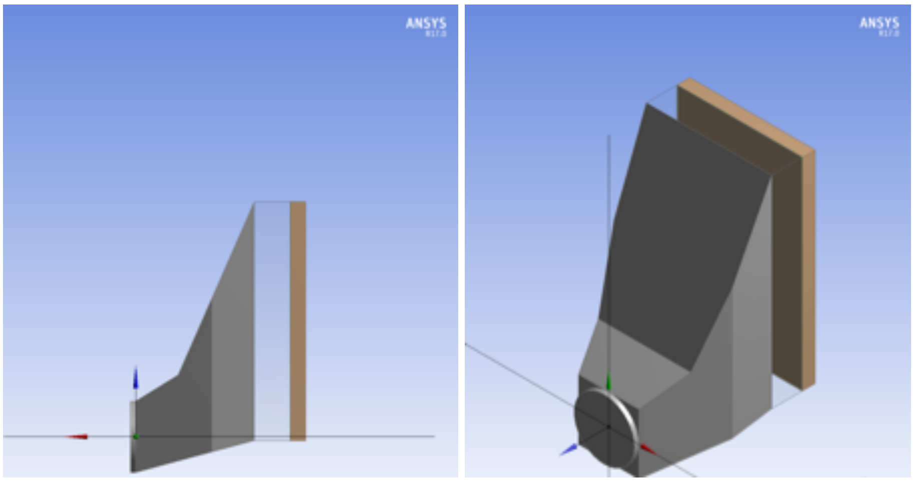

Figure 6–6 - Side and isometric views of a second example alternative design for the inlet duct of an HRSG (double angle top plane for the inlet duct). This is a common design trend line which has substituted, in many cases, the more traditional single angle version.

The first design alternative was used for the real power plant, in the particular case of one of the studied HRSG families, and it is currently in operation (single angle top plane for the inlet duct). This is a more traditional design. The second design alternative has a double angle top plane for the inlet duct, a design feature that many manufacturers introduced already years ago, because it supposedly had an improved performance over the single angle design (it is also shown in this Thesis that the double angle design is not always better than the single angle design).

The performance results are shown in Figure 6–7 for both design alternatives. Performance is expressed in terms of pressure drop and velocity uniformity, which are the two attributes selected by the manufacturer, as explained in Chapter 4.

There is a considerable improvement in terms of pressure drop with the alternative design, so it is worth exploring more design points to have a better view of where the optimum designs may be and if other more unconventional designs yield improvements in performance.

The application of MOST-HDS had a Phase 0, or design exploration phase, which in this case had 120 design points, to obtain a wide representation of the infinite space of solutions. For the purpose of this Thesis, a custom DoE scheme was used, based on the authors' experience, but Latin Hypercube Sampling (LHS) and other methods will also be tested in future work.

Of particular importance is the fact that the design points of Phase 0 need to be checked automatically to avoid absurd shapes (this is done automatically by the MOST-HDS algorithm).

Once the exploration phase has been completed, MOST-HDS carries out the optimization itself. The results of a one phase optimization for this particular HRSG family are depicted in Figure 6–7. This figure includes the comparison to the results obtained using a popular Multi-Objective Evolutionary Algorithm (MOEA), in this case NSGA-II, which is included in ANSYS optimizer as the best choice for multi-objective optimization based on direct search. The NSGA-II optimization was set up so that the number of direct evaluations would be equivalent to the one-phase optimization carried out with MOST-HDS.

The Pareto front shows the family of optimum solutions, taking into account all the attributes or objectives considered (in this case, total pressure drop across the inlet duct and velocity non-uniformity at the outlet plane of the inlet duct). All the solutions on the Pareto front are equally optimum, since the absolute optimum would be to have pressure drops and velocity non-uniformities as close to zero as possible, and therefore each of the solutions on the Pareto front are a potential optimum combination of pressure drop and velocity non-uniformity.

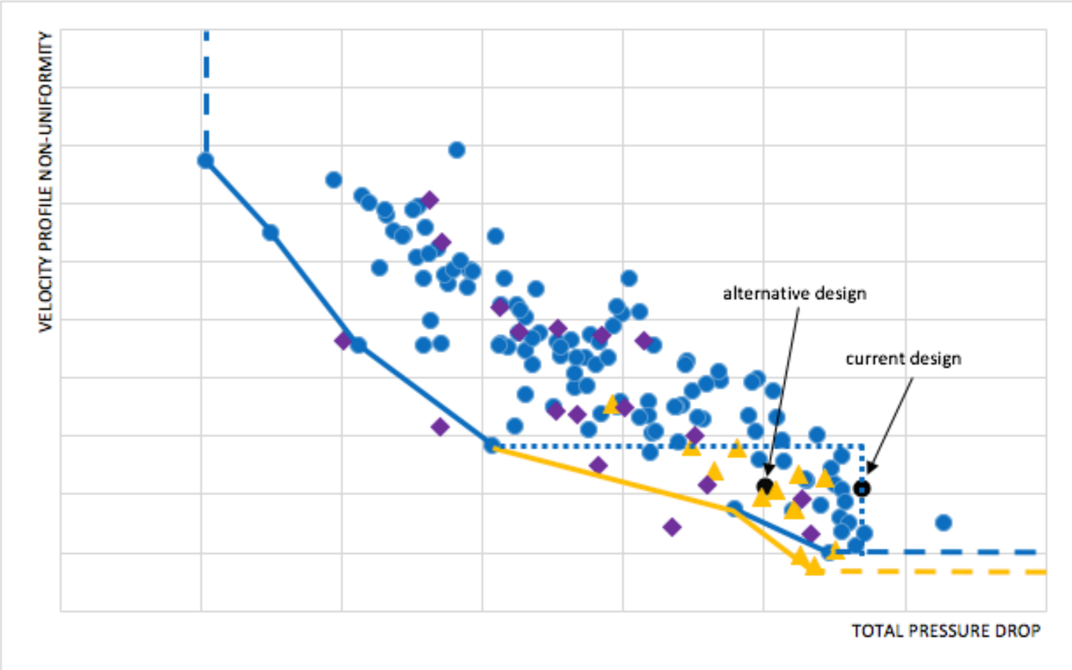

Figure 6–7 - Application of the MOST-HDS algorithm to the shape optimization of the inlet duct of a first family of HRSGs for combined cycle power plants. The results of the application of the NSGA-II evolutionary algorithm to the same optimization problem are also shown (purple diamonds).

The results of the 120 design points of Phase 0 (blue circles) are shown, alongside the results of Phase I, which has analyzed 12 points (blue triangles). The tolerance threshold (dotted line) was specified by the manufacturer. Two Pareto fronts are shown, as the lines joining the set of optimum designs after design exploration and after the one-phase optimization[14].

It can be observed how the application of the MOST-HDS algorithm has produced an improvement of the performance result of this family of HRSGs. If we compare the results of MOST-HDS and NSGA-II, this latter performs well, but yields candidate designs which are more scattered, many of which do not meet the constraint of having a velocity non-uniformity below the threshold imposed in Figure 6–7, they are globally further way from the Pareto front, and only one of the candidate designs improves the results of MOST-HDS. This particular point would very probably have been obtained by MOST-HDS if the tolerance region had been slightly expanded, to include more candidate points of Phase 0. This emphasizes the importance of choosing an appropriate tolerance region. In any case, NSGA-II is a good optimization algorithm for a wide variety of problems, but it is considered that MOST-HDS can be set-up to perform better for problems of aerodynamic shape optimization involving big geometry changes. This is the main reason why the MOST-HDS algorithm was developed in the first place.

[14] For this optimization, 132 design points were computed, in an 8-core parallel calculation, using a 32GB RAM computer. Each calculation took around 0.25-0.3 hours. The size of the meshes was between 1-2 million elements.

Regarding the specific optimization results of MOST-HDS, it is worth commenting that, although Phase 0 selects the design points following a procedure which covers the area of the search region the designer is most interested in, this phase in itself is a mere design exploration and not an optimization as such. Phase I is the first true optimization phase of the MOST-HDS algorithm.

It must be noted, in any case, that the design exploration procedure built into the model to carry out the analyses for Phase 0 is already quite good in many cases, since the design points calculated yield good performance results and cover a broad area of the space of attributes (or objectives). Hence Phase 0 is in itself valuable in the sense that manufacturers have not performed such an extensive exploration of different design points, in most cases. It can be seen that the current design trend lines (i.e. using a single angle design or, alternatively, believing a double angle design is always better) can be misleading or, at least, not optimum, and can be improved even in Phase 0 (for this particular family). Some of the types of designs found in Figure 6–7 are represented in Figure 6–8, for more clarity.

Moreover, unconventional and non-intuitive designs can prove to outperform traditional designs. As an example of this, Figure 6–9 to Figure 6–12 and Table 6–2 to Table 6–5 include the comparison between several representative design points, among all those simulated in Figure 6–7.

In these figures, it can be observed that designs which are very similar (i.e. close in the space of variables) and which would intuitively be very close also in the space of attributes (i.e. have a very similar performance), may really be far apart in their results, whereas quite different designs may perform very similarly. It is worth highlighting, in particular, that double angle designs are not necessarily better than single angle designs (for instance, design points *d* and *g* are very close in performance). This means a thorough analysis is required in each case, because traditional design trend lines may not always be the best option.

Furthermore, both Phase 0, as an exploration phase, and, most importantly, Phase I, may yield unconventional designs or designs with a non-intuitive performance (design points *i* and, especially, *j*).

All the results of Figure 6–9 to Figure 6–12 support the importance of applying an optimization methodology, be it MOST-HDS or others, to the problem of inlet duct design in HRSGs for combined cycle plants.

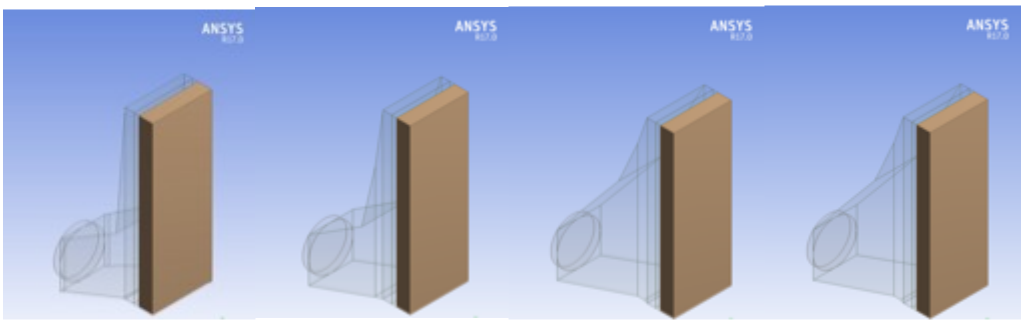

Figure 6–8 - Example designs obtained for the shape design optimization of the inlet duct of various HRSG families.

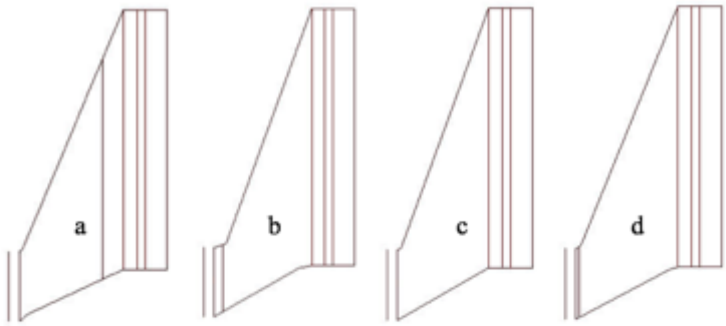

Figure 6–9 - Side view of example design points which are very close in the space of variables and also very close in the space of attributes.

Design point	Total pressure drop	Velocity non-uniformity
a	72%	146%
b	72%	145%
c	72%	145%
d	75%	139%

Table 6–2 - Comparison between different design points, to show that points which are very close in the space of variables can also be very close in the space of attributes. All results are with respect to the attribute values of the current HRSG design of Figure 6–7.

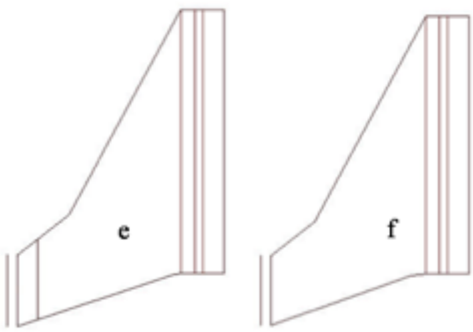

Figure 6–10 - Side view of example design points which are very close in the space of variables and quite apart in the space of attributes.

Design point	Total pressure drop	Velocity non-uniformity
e	98%	89%
f	96%	102%

Table 6–3 - Comparison between different design points, to show that points which are very close in the space of variables can also be quite apart in the space of attributes. All results are with respect to the attribute values of the current HRSG design of Figure 6–7.

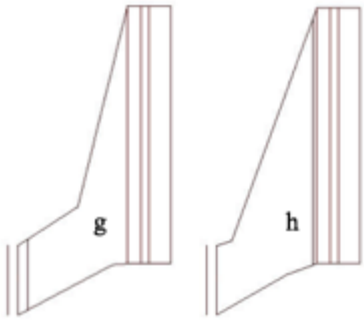

Figure 6–11 - Side view of example design points which are quite apart in the space of variables and very close in the space of attributes.

Design point	Total pressure drop	Velocity non-uniformity
g	71%	139%
h	73%	141%

Table 6–4 - Comparison between different design points, to show that points which are quite apart in the space of variables can also be very close in the space of attributes. All results are with respect to the attribute values of the current HRSG design of Figure 6–7.

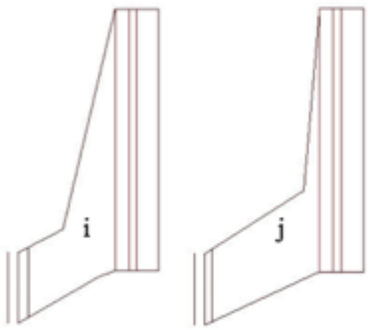

Figure 6–12 - Side view of example design points which are quite unconventional (because they are quite radical designs) and somewhat non-intuitive in their performance (especially design point j).

Design point	Total pressure drop	Velocity non-uniformity
i	64%	146%
j	60%	159%

Table 6–5 - Comparison between example design points, which are quite unconventional and somewhat non-intuitive in their performance. All results are with respect to the attribute values of the current HRSG design of Figure 6–7.

In Phase I, as can be observed, the design points improve the performance results of the design points studied in Phase 0. Additionally, it can be seen how the application of MOST-HDS improves the Pareto front obtained in Phase 0 and hence the performance results of the optimum design points. The geometries of the optimum designs obtained are, as has been shown for some solutions, quite unconventional and non-intuitive (Figure 6–12). All this has allowed the manufacturer to have a new set of design guidelines for its different HRSG families for the coming years.

Besides, the fact that the manufacturer has received Pareto fronts similar to this one shown, for each of his main HRSG families, allows for a well-based design trade-off between total pressure and velocity non-uniformity in each case. For a particular type of HRSG, design points with lower total pressure drop may be preferred, even at the expense of a higher non-uniformity (or vice versa). The exact geometries obtained for the optimum design points cannot be included in this document for confidentiality reasons.

To have a better insight into the true potential of MOST-HDS for shape design optimization involving big geometry changes, in the particular case of inlet duct design for HRSGs, the algorithm has been applied to a different HRSG family, and very interesting results can be observed in the following figure.

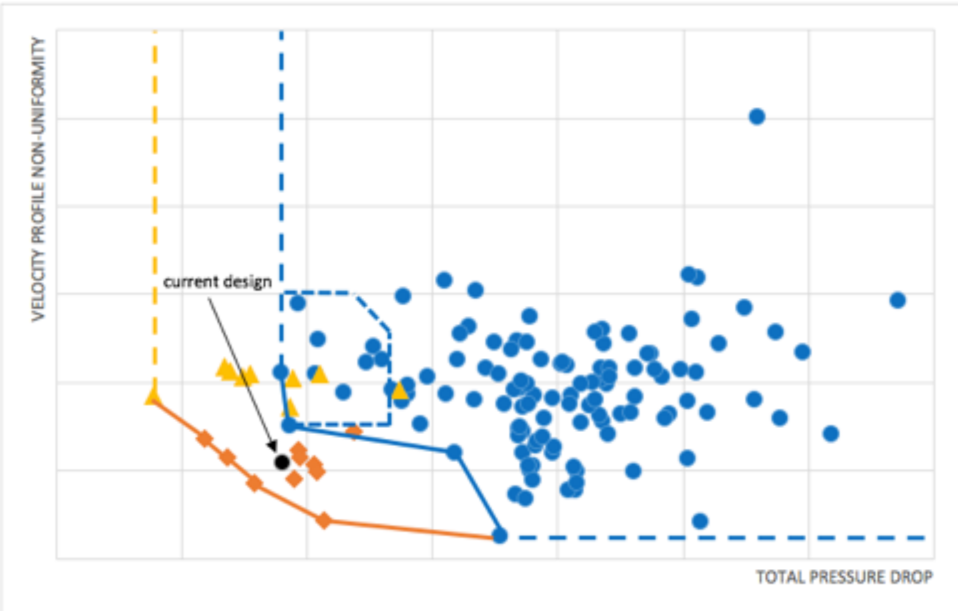

Figure 6–13 - Application of the MOST-HDS algorithm to the shape optimization of the inlet duct of a second family of HRSGs for combined cycle power plants. Increment factors (as explained in Chapter 5) below unity (candidate points marked with triangles) and above unity (candidate points marked with diamonds).

Phase 0 of MOST-HDS has analyzed 120 design points and Phase I has analyzed 10 points. The tolerance threshold (dashed line) was specified by the manufacturer, to analyze an area of design points with comparable pressure drops and velocity uniformities to the current design.

In particular, for this case, the design exploration carried out in Phase 0 (candidate points marked with circles) covers a broad area of the search region, but yet the real existing design, already built and in operation for this particular HRSG family, dominates all the other candidates, i.e. it has better values for both attributes. This means that a mere design exploration can be inadequate or not good enough in some cases. Once MOST-HDS computes the points for Phase I, the simulations show that Phase I candidate points improve considerably, not only over points in Phase 0, but, most importantly, with respect to the real current design of this HRSG.

For this second example HRSG family, an additional test has been performed. The variable increment factors used to obtain new candidate design points for Phase I from the crossover of their parents of Phase 0 are tuned. In particular, two sets of values are used. The first set (candidate points marked with triangles) has variable increment values below unity, which means that the crossover of the parent solutions lies between both parents (in the space of variables). The second set (candidate points marked with diamonds) has variable increment values above unity, which means that the crossover of the parent solutions lies beyond the parent point belonging to the Pareto front (it is always checked that the new variable values lie within that variable's value range, as defined by the designer).

For this case, the use of increment factors above unity yields better results, in general. However, the best candidate point in terms of total pressure drop is obtained with an increment factor below unity. Hence the bottom line is that both sets of values should be exploited by MOST-HDS (as explained in detail in Chapter 5) to have a higher probability of reaching optimum designs. This means performing searches within the design points already evaluated and beyond these points (in the space of variables).

CONCLUSIONS ON THE RESULTS FOR THE SHAPE OPTIMIZATION OF THE INLET DUCT OF HRSGS

This section has applied the MOST-HDS algorithm to the problem of inlet duct shape design optimization of HRSGs used in combined cycle power plants. The main conclusions drawn from this work, as well as an outline of future research lines, can be summarized in the following points:

1. The interest of applying an optimization methodology, be it MOST-HDS or any other, to the shape design optimization of the inlet duct of HRSGs, has been shown to be very valuable. The performance results of different inlet duct designs may not be intuitive in many cases and can vary considerably among different designs. Examples have been shown of design points which are very similar and yet yield different results, or different designs which have a very similar performance.

2. In particular, examples have been presented of single angle designs which are very similar in performance to double angle designs, so the current design trend line some manufacturers follow of necessarily preferring double angle designs may be misleading in some cases.

3. A design exploration phase (i.e. simulating a considerable number of design points, based on the engineer's experience, but with no real optimization behind) can already improve the results of current designs. However, this is not the case for some HRSG families, as has been shown with the results of the second HRSG family. Therefore, the best recommendation is to apply a true optimization algorithm for the shape design of inlet ducts.

4. Improvements in pressure drop of up to 40% and in velocity uniformity of up to 15% have been achieved, when applying MOST-HDS to two different HRSG families. Given that both improvements cannot be reached at the same time, optimum trade-off design points with pressure drop reductions of 20-25% and comparable velocity uniformity to the existing designs can be obtained.

5. Moreover, although pressure drop and velocity uniformity were the attributes defined by the manufacturer, the total length of the inlet duct and its lateral surface were also calculated for the different design points. These two are also important variables due to their strong impact on cost reduction, because of material cost, and the importance of having more compact (i.e. shorter) inlet duct designs. Improvements in lateral surface of up to 53% and in total inlet duct length of up to 48% have been achieved. Given that both improvements cannot be reached at the same time, optimum trade-off design points with lateral surface reductions of 38% and length reductions of 16% can be obtained, for the two HRSG families presented.

6. Taking into account the considerable performance improvements achieved, the applicability of MOST-HDS to other fields different to that presented in Prada-Nogueira et al. (2015 and 2017) has been shown. Future research will be focused on generalizing the applicability analyses of MOST-HDS as an optimization algorithm for even more fields and applications, such as those described in Paniagua (2014) or Zamorano-Rey et al. (2015).

7. Unconventional designs have been obtained, thanks to the application of MOST-HDS.

8. For future work, other Design of Experiments (DoE) techniques, such as Latin Hypercube Sampling (LHS), will be used for the design exploration phase; more HRSG families will be analyzed; and a general set of simple and practical design guidelines for each HRSG family will be developed, to improve current design trend lines.

To finish the section on the results of the application of MOST-HDS to HRSG inlet duct optimization, it is important to note that results of surrogate based optimization (using response surfaces), also for this example case, will be presented in Chapter 7. A specific chapter has been devoted to the comparison between MOST-HDS and surrogate models, given their extended use, for the particular field of aerodynamic shape optimization with big geometry changes.

6.3. Closed wind tunnel shape design optimization

The second industrial case presented in this Thesis is the aerodynamic shape optimization of closed wind tunnels. These facilities are used quite extensively for testing purposes in many different fields and also for leisure activities (indoor skydiving), as was shown in Chapter 4. It is a very general example of the optimization of complex aerodynamic bodies, to show the applicability of MOST-HDS to very different geometries.

The level of complexity is far bigger than for the HRSG case presented above, in terms of the number of variables and parameters required to represent most wind tunnel geometries (108 variables for the wind tunnel case versus 7 for the HRSG case). This makes the use of many commercial CFD optimizer packages impossible, since they are limited to 10 independent variables. Hence, for this case, an external optimizer, with the optimization algorithm selected by the user, must be plugged into the CFD solver in any case.

Due to this complexity, the case of a simplified wind-tunnel model will be presented first (so that the results are better understood), and then the optimization of a full wind tunnel model will be analyzed.

VALIDATION CASE FOR THE ANSYS CFD SOLVER FOR WIND TUNNEL SIMULATIONS

In the first place, as was also done for the HRSG case, a brief section is presented on the validation of the results of the CFD solver used (ANSYS v17.0) for the evaluation of wind tunnels.

Two validation cases will be presented; first, the pressure loss validation for a small prototype wind tunnel used for testing; and secondly, the pressure loss and velocity distribution validation for a full-size vertical wind tunnel for indoor skydiving, built in Las Rozas de Madrid (Madrid Fly, www.madridfly.com). Both tunnels were designed with a very early version of the MOST-HDS algorithm, still not fully flexible or automated.

Figure 6–14 and Figure 6–15 show the real prototype wind tunnel built and the general drawing of this horizontal closed wind tunnel.

Figure 6–14 – Prototype wind tunnel for testing purposes presented to validate the CFD solver used.

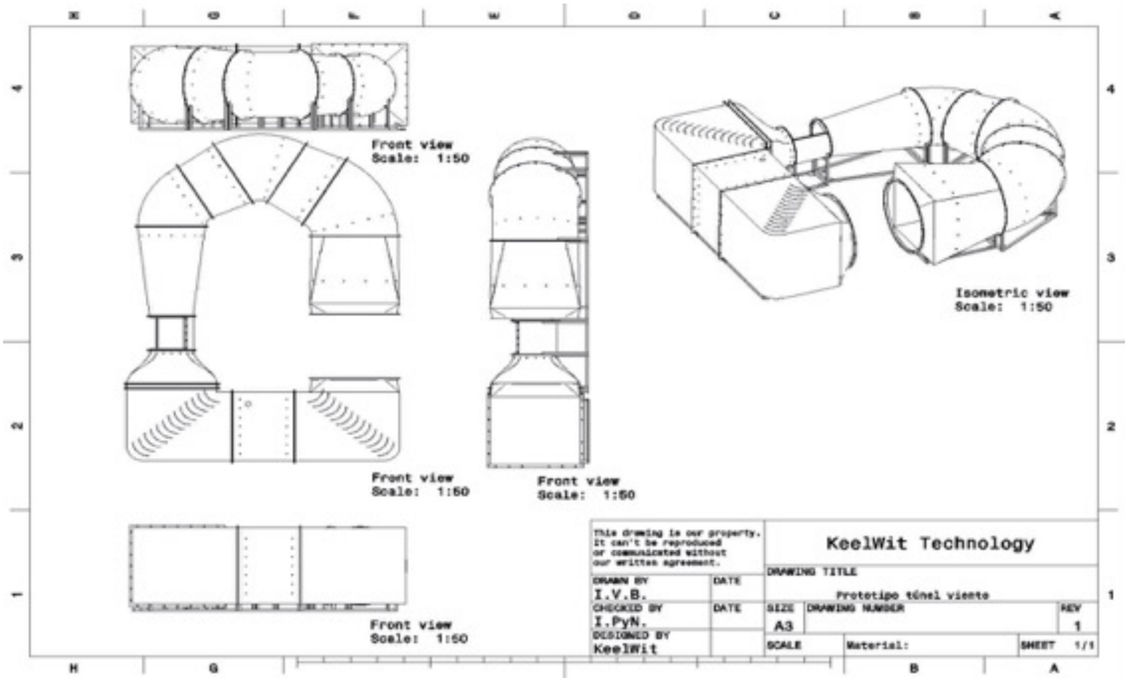

Figure 6–15 - Prototype wind tunnel for testing purposes presented to validate the CFD solver used (general drawing, not to scale).

Figure 6–16 illustrates the CFD simulation of the nominal performance point for the wind tunnel, compared to the measured performance test of the real fan in a certified test rig. The pressure and flow deviation of the CFD solver versus the measured performance values was between 5-8% for different simulation settings.

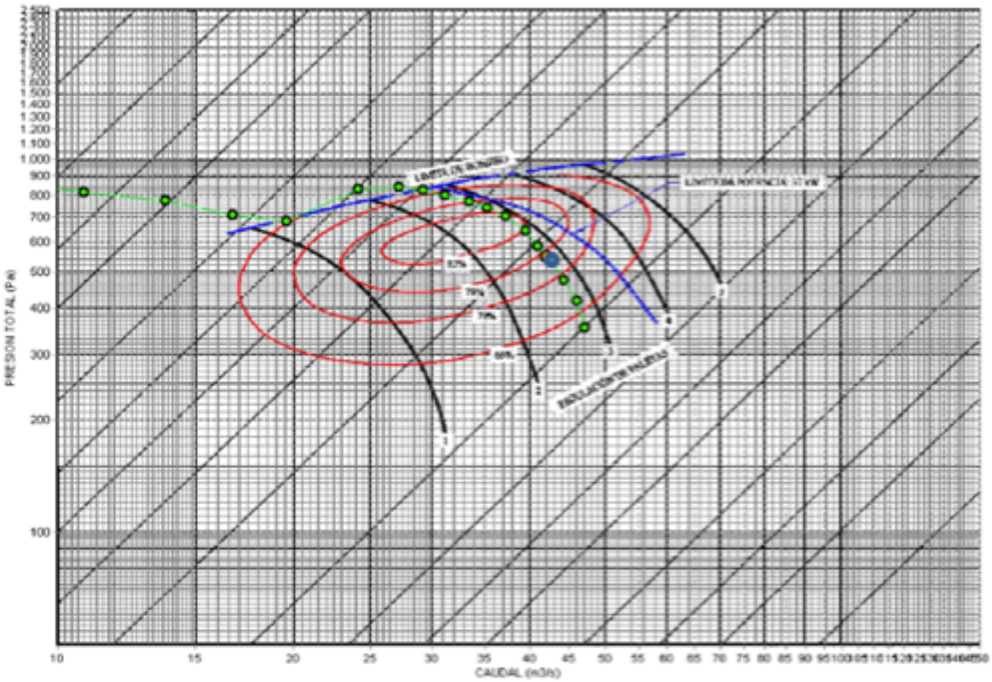

Figure 6–16 - Measured performance curve (pressure drop v. air flow) for the fan of the prototype wind tunnel, showing the measured nominal performance point (orange) and the simulated nominal performance point (blue).

Regarding the full size vertical wind tunnel built for indoor skydiving, Figure 6–17 depicts the facility and the test/flight section, alongside a picture of the typical flight of a first timer with instructor. The inlet plane to the test or flight section, which will be the reference plane for the velocity index readings shown, is also indicated in Figure 6–17 for clarity. Figure 6–18 shows the distribution of the points where the velocity sensor (Pitot tube) was placed for the measurements (corrections due to air properties during the tests were accounted for) and Table 6–6 presents the comparison of the measured versus the simulated results. Once again the accuracy of the ANSYS CFD solver is considered very high and adequate to carry out the evaluations for the optimization process.

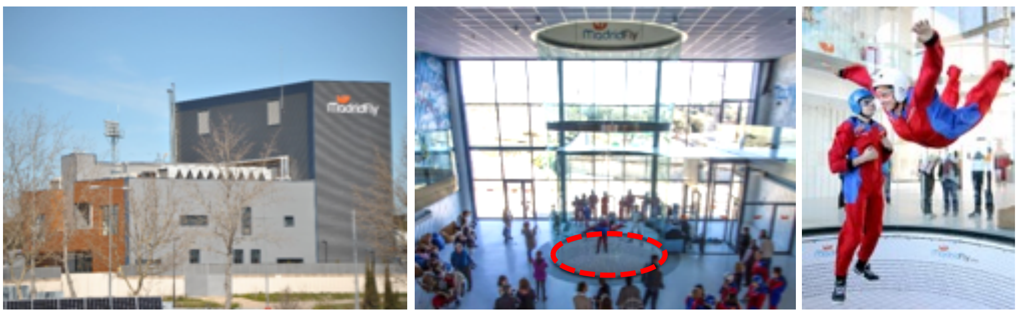

Figure 6–17 - Vertical wind tunnel for indoor skydiving (Madrid Fly, www.madridfly.com). The inlet plane to the test or flight section is shown (dashed red line).

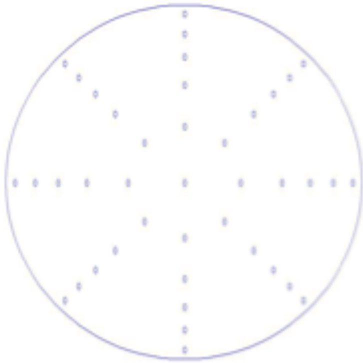

Figure 6–18 - Distribution of points for velocity measurements in the inlet plane of the wind tunnel test or flight section (measurements were carried out with a Pitot tube).

Measuring point	**Fan power [%]**	**Velocity deviation with respect to average [%] MEASURED**	**Velocity deviation with respect to average [%] SIMULATED**
#1	100%	-0,3%	-0,8%
#2	100%	-1,2%	-1,5%
#3	100%	0,2%	0,1%
#4	100%	0,4%	0,8%
#5	100%	0,4%	0,2%
#6	100%	-0,1%	0,3%
#7	100%	1,0%	1,4%
#8	100%	0,0%	0,2%
#9	100%	-0,7%	-0,5%

Table 6–6 - Velocity deviation with respect to the average for 9 relevant points (among those shown in Figure 6–18) in the inlet plane to the test or flight section of a vertical wind tunnel. Measured v. CFD simulated results.

RESULTS FOR THE SHAPE OPTIMIZATION OF CLOSED WIND TUNNELS

This section will be divided into two parts: in the first part a simplified wind tunnel model will be presented, to understand better how the MOST-HDS algorithm works and the importance of certain features of the optimization; in the second part, an example optimization for a full wind tunnel model is presented and analyzed.

Simplified wind tunnel model

The simplified wind tunnel model, already presented in Chapter 4, is represented once again in Figure 4–9.

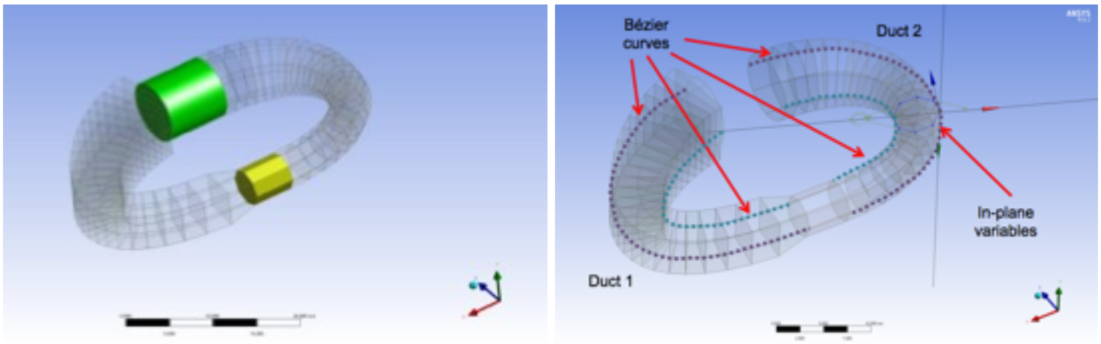

Figure 6–19 - Low detail representation of a wind tunnel design, used to illustrate better certain aspects of the optimization methodology presented in this section. Four Bézier curves are used only. Fan and test sections are both shaded in this figure (left). An example plane containing one of the transverse sections used for the tunnel geometry discretization is also shown (right).

The first step is to obtain the initial set of points for Phase 0. In this case, based on our experience, a design tree is configured with all the possible combinations of the values of a reduced number of selected variables. The rest are left constant for this simplified example. Consequently, the tree for Phase 0 will explore the extreme values of each variable's range. The tree of design points for Phase 0 is shown in Figure 6–20. It sets two values for each of the variables, taking into account their hierarchy (except for the low importance variable number of fans, which is considered constant and equal to 1, in order to limit the number of design points analysed, and because it does not add value to the explanation).

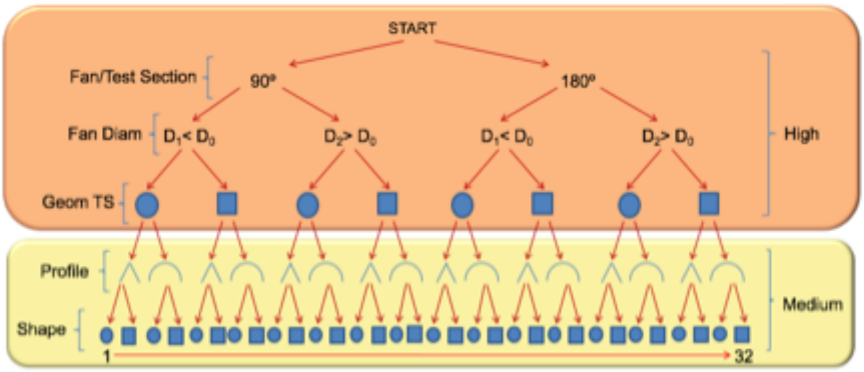

Figure 6–20 - Example tree of design point combinations for Phase 0 optimization of the simplified wind tunnel model. 32 wind tunnel designs are considered.

The variables used for the simplified case study presented are:

1. Relative position of fan and test sections
2. Fan diameter
3. Geometry of the test section
4. Profile for duct 1 (i.e. Bézier curves for duct 1)
5. Shape of sections in duct 1

A minimum and maximum value is set for the relative position of the fan and the test section and for the fan diameter. These values are derived from the user's input on the required flow, the designer's estimation for the pressure drop and the fan manufacturer's recommendation.

For the geometry of the test section there are three typical options: circular, square and rectangular. Other shapes can be analyzed with the MOST-HDS model, such as flat-oval or polygonal, as it is straightforward to add these options to the model. For this simplified example, only circular and square test sections were considered.

In terms of ducts 1 and 2, it is very important to highlight that we propose decoupling both optimizations when needed, i.e. the presented methodology will optimize ducts 1 and 2 independently and then combine the best duct 1 with the best duct 2, for those phases in which this speeds up the whole process.

This can be done because, for the flow quality required in a modern wind tunnel, the flow distribution at the inlet of the test section must be very uniform (the level of uniformity is determined by the velocity index specified by the user, but it is below 2-3% for typical commercial applications). This means that the flow at the outlet of the test section will be very similar for any duct 2 which is good enough to be considered a possible final design. Consequently, the optimization of duct 1 can be assumed independent to the optimization of duct 2. Besides, at the fan inlet the flow of any good candidate to be the final duct 1 will be reasonably comparable and, given that the fan increases the flow uniformity, at its outlet the flow will be even more similar, for most duct 1 designs. This simplifies the optimization because it breaks the wind tunnel model into two half models which can be simulated more rapidly or with finer meshes.

For this example, duct 2 is left constant and two possible Bézier curves are used for duct 1: one nearly circular and one skewed.

Finally, for the transverse shape of ducts 1 and 2, there are really only two options: circular or square/rectangular. Square and rectangular are not really two different options because the search region can be simplified forcing the algorithm to choose only one of the two to compare with a circular design, depending on the shape of the test section (if circular or square, the only transverse shapes used will be circular and square and if rectangular then the algorithm will compare circular and rectangular transverse shapes). Once again, the model allows this simplification to be eliminated if considered necessary for a particular application. In the example of this Thesis, however, only circular and square shapes are considered anyway.

The attributes selected to compare different wind tunnel designs are: a) fixed cost (which includes materials, manufacturing and assembly), and b) mass-weighted average total pressure drop from inlet to outlet of the whole wind tunnel circuit. Total pressure drop is a way of representing most of the operating cost, so the results are in essence figures of fixed cost versus operating cost.

The results of the CFD evaluation of these 32 design points is presented in Figure 6–21 and their attribute values are grouped in Figure 6–22, which also shows the Pareto front for Phase 0.

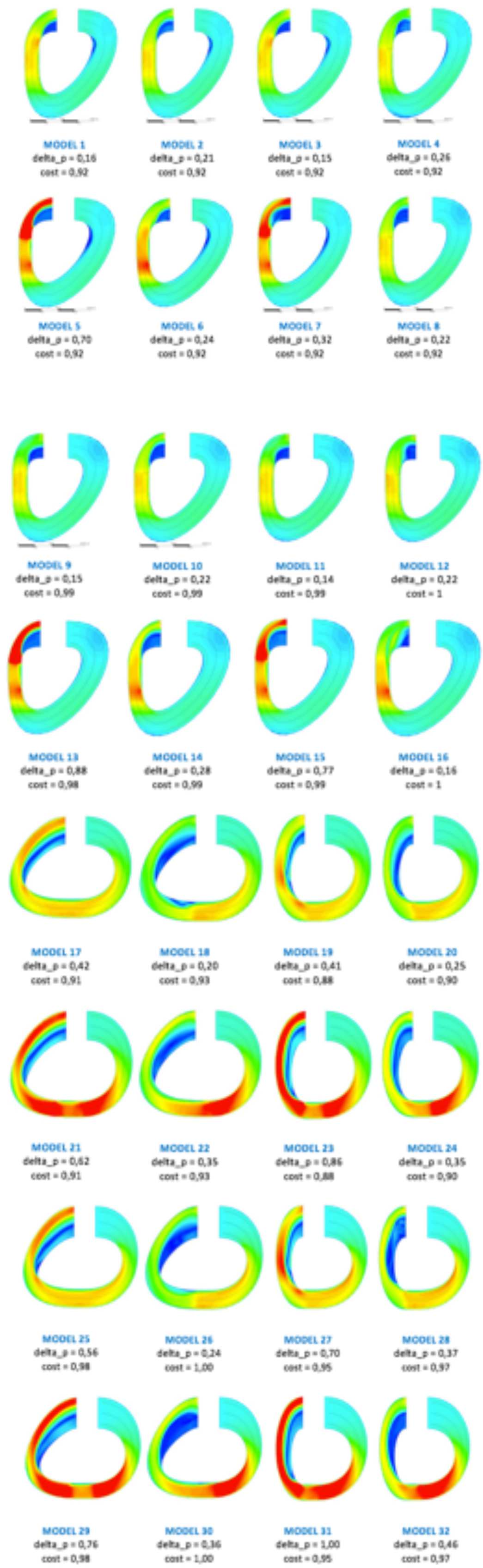

Figure 6–21 - CFD evaluation results (velocity contour plots for mid-plane, total pressure drop – delta p – and fixed cost) for each of the 32 wind tunnel design points for the simplified wind tunnel model.

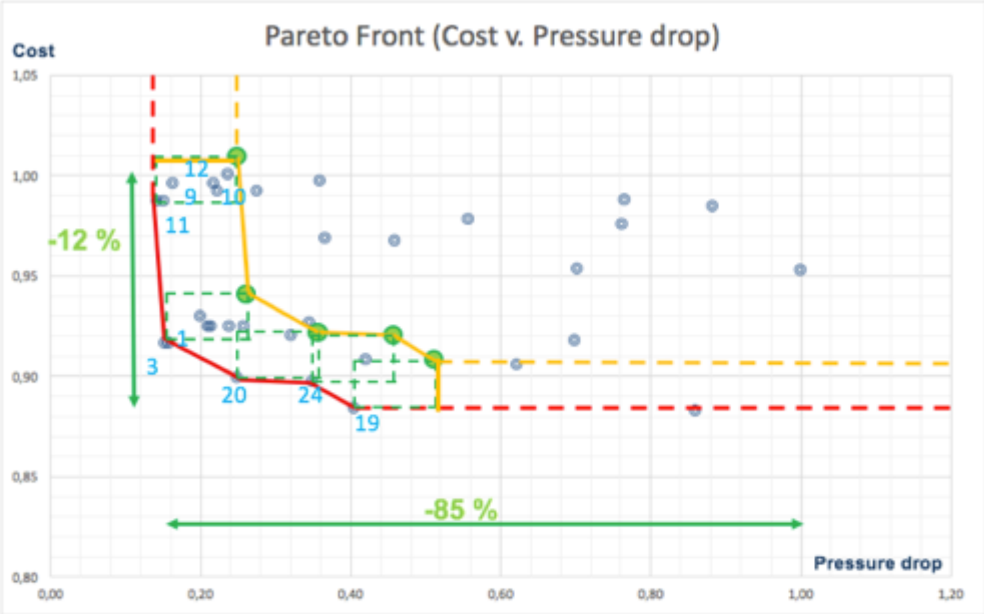

Figure 6–22 - Pareto front (red line) of fixed cost v. total pressure drop for 32 wind tunnel design points for the simplified wind tunnel model. Tolerance threshold (orange line) to select area of search region where potential candidates to optimum may lie, for subsequent optimization phases (values of both attributes are per unit). Maximum attribute ranges are shown in %.

As an example of how the algorithm performs, let us take models 3, 9, 10 and 12. They all lie within the tolerance threshold, so they would be potential candidates to be retained for Phase I. They would all move towards model 11. Model 3 is relatively close in the space of attributes (less so in cost than in pressure drop), but further away in the space of variables, so it would be kept for Phase I. Among models 9, 10 and 12, which are close both in the space of variables and attributes, a representative must be chosen. This is when clustering would be used.

For example, if we focus on model 3, and its movement towards point 11 (this movement is in fact along the Pareto front), the only difference between both design points is the fan diameter, so this is the only variable which would be changed, for this particular case. It would be changed for design point 3 taking into account that the optimization is calculating Phase I and that the fan diameter is a high importance variable.

In this example, 18 models would be retained, crossed over with their target design points on the Pareto front and CFD simulated for Phase I. The results of a complete optimization are shown for the full wind tunnel model in the next section.

Variable correlation and sensitivity analysis

At this stage, it is interesting to analyze a bit further the true independency of the selected variables and, most importantly, their impact on the results, since this is the kind of analyses that MOST-HDS performs internally. This analysis is easier to understand for the simplified wind tunnel model.

The optimization methodology presented in this Thesis performs a smarter search thanks to the selection and hierarchy of the independent variables. First, it is relevant to check if they are truly independent and cover every relevant degree of freedom. Second, independent variables with a strong impact on the attributes should be variables of higher hierarchy, whereas those with a weak impact should be in lower hierarchies. The process of mapping the variables and the various hierarchies as correctly as possible will allow for an efficient breakdown of the problem into optimization phases.

In this section independence and hierarchy will be discussed based on the example case study here presented, but indicating how the complete full optimization architecture carries out these tasks automatically.

Regarding independency, it is quite clear in this example that any of these variables can be modified without affecting the values of the others, so they are independent variables. As commented, this independency check is not as simple in complex aerodynamic problems and a more rigorous analysis is required. Commercial packages such as ANSYS offer tools to carry out complete multi-variable correlation analyses.

The important issue which is very well illustrated by the simplified example case is the sensitivity of the two attributes chosen – fixed cost and pressure drop – with respect to the variables used. Let us comment this in more detail (refer to Figure 6–21 and Figure 6–22).

Firstly, the relative position of the fan and the test section divides the 32 wind tunnel designs into two blocks of 16 models. The first 16 models have a relative position of 90°, whereas models 17-32 have a relative position of 180°. In terms of cost, both relative positions have quite a wide range of values. With 90° the span is slightly smaller, from 0.92 to 1 with respect to 0.88 to 1 for 180°. Concerning pressure drop, only 3 of the models with 90° of relative position have high pressure drops (above 0.7). All other models yield values below 0.32. In the case of 180°, the values of pressure loss are much more scattered. This shows how the behavior of the attributes, especially pressure drop, is strongly affected by the relative position of the fan and the test section. Therefore this variable is of a high importance.

Secondly, let us inspect the importance of fan diameter. Both for models with a 90° or a 180° relative position (this shows the independency of fan diameter and relative position), those models with smaller diameter have a lower fixed cost (models 1-8 and 17-24) than models with a bigger diameter (models 9-16 and 25-32). If we focus on pressure drop, one has to compare models with the same value for the rest of the variables and only different fan diameter. Thus, comparing models 1-4 with 9-12, models 5-8 with 13-16, models 17-20 with 25-28 and 21-24 with 29-32, it can be seen that, in most cases (especially for 90°), pressure drop is always lower for the smaller diameter models. This, however, is not always the case, and it is important to highlight models such as model 16. This model is surprisingly low in terms of pressure drop, even though it has a bigger diameter. However, its fixed cost is the highest. This shows how unconventional or non-expected designs, which intuitively would not be chosen, can yield optimum designs (in one or many attributes).

Fan diameter is consequently a high importance variable, due to its strong impact on the attribute values.

Regarding the next variable, the geometry of the test section, the best way to check its impact is comparing models 1 and 5, 2 and 6 and so on. Its impact is low in terms of fixed cost and, for circular test sections the pressure drop is generally smaller, except for particular cases such as, once again, model 16. For model 16, a square test section can offset circular test sections, which intuitively have lower pressure drops (and this is generally true), if the square test section is coupled with a square duct 1, as is the case in model 16. This model is effectively very close to the Pareto front (Figure 6–22) so it could be a candidate for optimum (if its design is fine-tuned in further optimization phases to reduce its cost).

Once again, the geometry of the test section has a strong impact on the final values of the attributes, mainly on the pressure drop (for instance, this can be seen comparing models 9 and 13, 27 and 31, etc.). Consequently, it is a variable of high importance.

The next two variables, profile of duct 1 and shape of the sections of duct 1, are set as medium importance variables. Let us check if this is correct, based on the results obtained for this case study. It can be seen that the profile shape affects noticeably when comparing models 5 and 7, 14 and 16, 21 and 23, 25 and 27 and 26 and 28. The shape of the sections along the profile affects substantially in most models. For models 1-16, i.e. for models with 90° relative position of the fan and the test section, those designs with circular test section and circular transverse shape in duct 1 or square test section and square transverse shape have lower pressure drops, as expected, due to the smoother transition. However, this trend is maintained for 180° models in the case of square test section and square transverse shape, but not for the case of designs with circular test section, in which the trend inverts. In models with a circular test section, the pressure drop is lower when duct 1 is a square duct. This is quite eye-catching and shows the importance of using intelligent, robust and automatic optimization tools to find optimum designs, which would probably not be found when using trial and error or manual optimization. It does not imply that there is no design with circular test section and circular transverse shape in duct 1 which can be better than designs with a square duct 1, but is does illustrate that considering non-conventional or non-intuitive designs can be very fruitful.

With respect to cost, the impact of these two last variables, profile and transverse shape, is lower, especially in the case of 90° designs.

It can be concluded that the last two variables considered, profile and transverse shape of duct 1, are variables with a minor influence on the fixed cost and mostly on the pressure drop. This influence is, in any case, not as strong as that of the previously commented variables. Therefore, these two are medium importance variables.

This section has illustrated the concept of variable hierarchy and it has shown the different impact a variable of high or medium importance has on the selected design attributes used to compare different solutions. This has been analyzed for a simplified case study, but the main conclusions are applicable to real, more complex systems, such as the one presented in the following section.

Full wind tunnel model

The full wind tunnel model, already presented in Chapter 4, is represented once again in Figure 4–9.

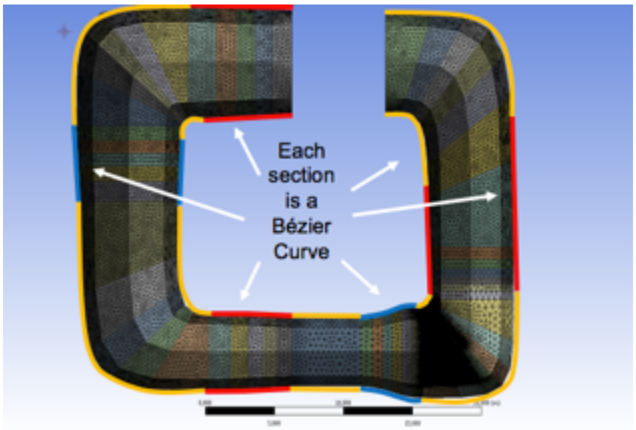

Figure 6–23 - Highly detailed representation of a generalized wind tunnel design, able to represent most tunnel geometries (18-20 Bézier curves are needed).

The design points for Phase 0 are determined following the same approach as for the simplified model (Figure 6–20).

The results of a full 2-phase optimization are shown in Figure 6–24 (the optimization is limited to 2 phases because of computation time[15]). The improvement of the Pareto front throughout the optimization process and the solutions of Phases 0, I and II can be observed. The wide variety of design types, some more conventional and some more unconventional, is quite eye-catching and is clearly seen in this figure. This is one of the relevant contributions of MOST-HDS, i.e. being able to handle big geometry changes in shape design and producing disruptive or creative design points.

[15] For this optimization, 57 design points were computed, in an 8-core parallel calculation, using a 32GB RAM computer. Each calculation took around 0.75-1 hours. The size of the meshes was between 2-5 million elements.

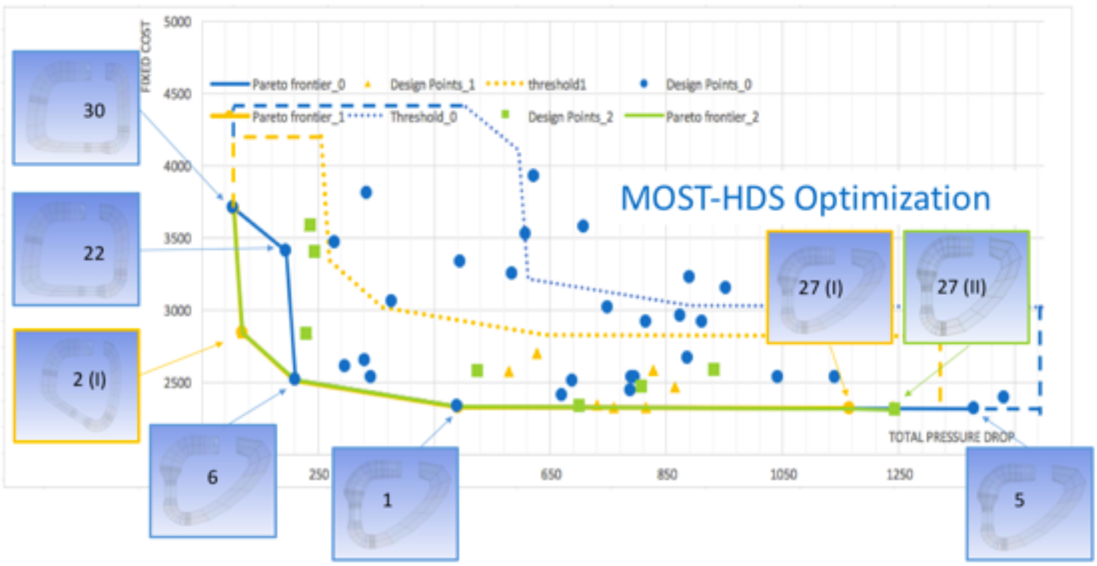

Figure 6–24 - Results obtained for a full wind tunnel 2-phase design optimization performed with the MOST-HDS algorithm. Pressure drop is in Pascals and the fixed cost is in fictitious monetary units.

As was analysed for the HRSG case, the intelligence embedded into MOST-HDS will automatically tune the optimization to proceed more efficiently, for example in terms of the increment factors. Figure 6–25 shows the impact of using increment factors below and above unity for Phase II of this optimization. MOST-HDS automatically selects the best values for the increment factors, based on the results of the different CFD evaluations.

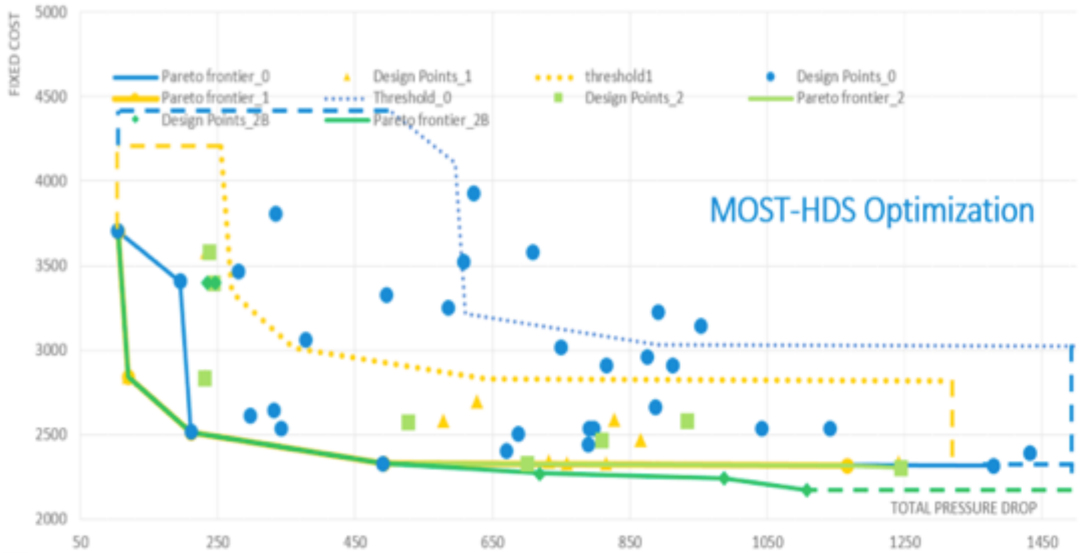

Figure 6–25 - Results obtained for a full wind tunnel 2-phase design optimization performed with the MOST-HDS algorithm, comparing the use of different increment factors for Phase II: below unity (light green squares) and above unity (dark green diamonds). Pressure drop is in Pascals and the fixed cost is in fictitious monetary units.

Let us analyze these results in more detail, to illustrate important aspects of the shape design optimization processes in cases with big geometry changes. If we take a closer look at what is happening with the different design points, from Phase 0 to Phase II, it is quite interesting to note that the search is advancing in particular areas of the search region (in the space of variables) and certain other areas of the search region are abandoned. If we analyze once more the initial tree of design points, Figure 6–26 shows the regions which gradually disappear as the search moves forward.

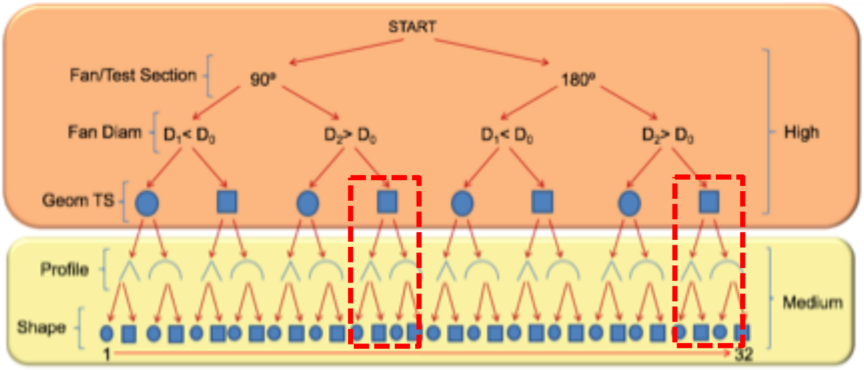

Figure 6–26 - Example tree of design point combinations for Phase 0 optimization of the full wind tunnel model. 32 wind tunnel designs are considered. The areas of the search region which disappear as the optimization proceeds are indicated.

In Phase 0 all branches of the tree are represented. In Phase I, in all 12 design points obtained, the bigger diameter has disappeared. Furthermore, for the 180° relative position of fan and test section, the circular test section disappears, whereas for 90° and for the new position value which appears in Phase I (120°), there are still circular and square test sections. Finally, for Phase II, not only the circular test sections continue to gradually disappear, but also the 90° design points. Out of the 8 models of Phase II (with increment factors below unity), only 2 keep a circular test section and only 2 are 90° design points. 5 out of the 8 models have unconventional relative positions of fan and test section (120° and 150°) so it can be said that only 3 of the models in this Phase are of a traditional type.

These are already important conclusions and being able to study them as the optimization is ongoing will allow the designer to take decisions on how to proceed for future optimizations or phases of this same optimization. The comments made are only an example of all the conclusions which can be drawn from an optimization study of this kind.

To conclude with this section, Figure 6–27 and Figure 6–28 represent the design family types present throughout the optimization, to show in a very illustrative manner how the MOST-HDS model can really handle big geometry geometry changes.

As a very important parameter to assess the quality of a wind tunnel is the velocity index in the test section (which is a measure of the velocity profile uniformity), both figures include a 2D view of the velocity contour plots at the inlet to each tunnel's test section.

The velocity index in the test section of the simulated design points (both for Figure 6–27 and Figure 6–28) ranges between 5-7%. Without any means to improve flow uniformity and reduce turbulence levels at this stage inside the tunnel (honeycombs or screens) these are reasonable velocity indexes for this phase of the optimization.

Figure 6–28 shows a very important result which puts forward the need for optimization schemes which can handle big geometry changes for many applications in the field of aerodynamic shape design. The Type III family of intermediate angles (which has either a 120° or a 150° relative position between the fan and the test section) is one of the optimum design types at the end of the final optimization and it would probably have never been tried out manually by most expert designers. Therefore MOST-HDS is capable of finding unconventional designs with better performance than other more traditional designs.

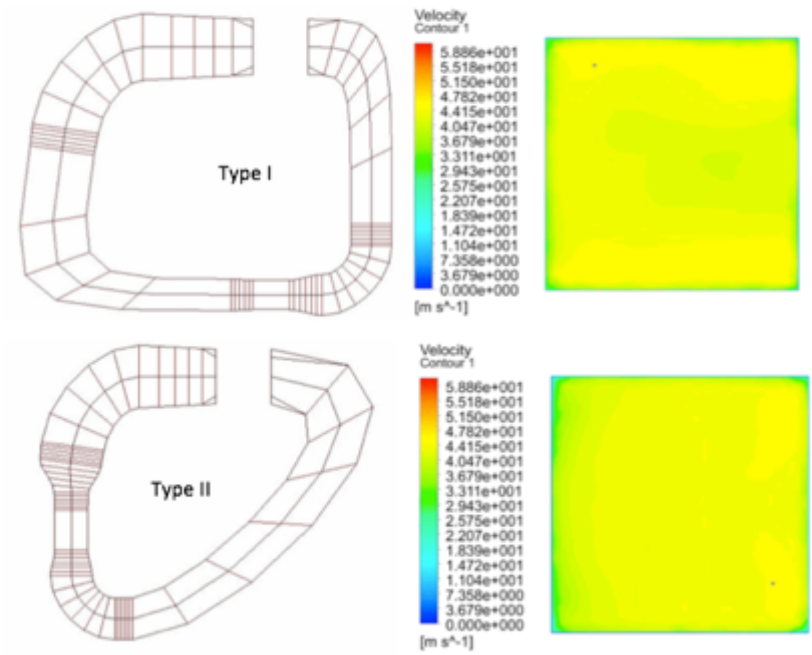

Figure 6–27 - Wind tunnel model families on the Pareto front for Phase 0 and their velocity contours in the tunnel test section (transverse plane). The Pareto front for this phase has 5 design points, 2 of type I and 3 of type II.

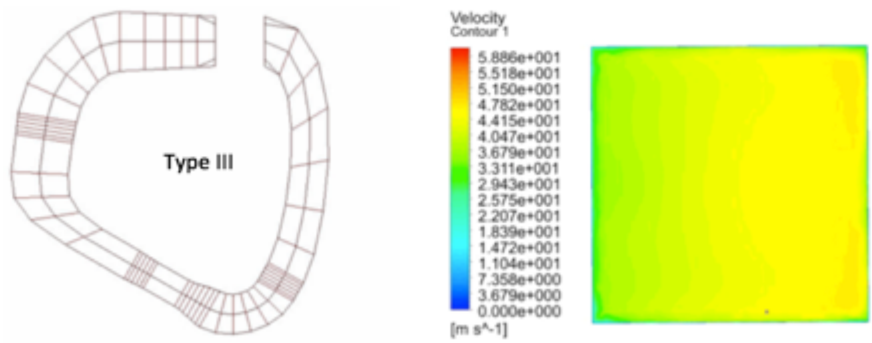

Figure 6–28 - New wind tunnel model family on the Pareto frontier for Phase I and its velocity contour in the tunnel test section. The Pareto front for this phase has 5 design points, 1 of type I, 3 of type II and 1, quite unconventional design, of type III.

CONCLUSIONS ON THE RESULTS FOR THE SHAPE OPTIMIZATION OF CLOSED WIND TUNNELS

The main conclusions drawn from this section on closed wind tunnels, along with the future research lines, are:

1. The MOST-HDS methodology is applicable to the design optimization of many kinds of complex aerodynamic bodies: vehicles, high-speed trains, aircraft, etc. This has been shown for the case of HRSGs and, in this section, for the case of closed wind tunnels.

2. The results obtained for a full wind tunnel 2-phase design optimization problem performed with the MOST-HDS algorithm have been presented as a real industrial case study. It can clearly be seen how the design points of Phase I improve the results obtained for Phase 0. Furthermore, some of the designs which yield optimum results are substantially unconventional solutions which the designer would probably never have tried by himself.

3. The importance and interest of the concepts of hierarchy of variables and optimization phases is shown. Thanks to these two concepts, many problems of aerodynamic optimization can be tackled using direct search, because the solutions computed with the CFD tool are very efficiently selected and they represent the richness of the whole search region, both in the space of variables and in the space of attributes.

4. Variable correlation and, most importantly, sensitivity analyses were presented conceptually, showing how the algorithm proceeds. This contributes to show the importance of identifying an efficient set of truly independent variables and of ranking them according to their hierarchies, to tackle the optimization in descending order of variable importance.

5. Particular interest is being given, in current research, to the acceleration of the whole procedure, to be able to evaluate even more candidate solutions. This means tackling concepts such as mesh morphing and exploiting them for the final phases of the optimization, when geometry changes are not as considerable. The method already makes extensive use of the geometry and mesh parameterization capabilities of commercial CFD software.

6. In future work, regarding wind tunnel design, fan systems using either a smaller number of fans of bigger diameter or a higher number of small fans will be analyzed and compared, because both options are found in the State of the Art, and it is very worth comparing both design trends more thoroughly. The work presented in this Thesis has only been performed on single fan wind tunnel examples.

7. Other aspects which will be covered in more detail in future research work are: mesh sensitivity analyses, and algorithm intelligence to select an efficient mesh coarseness for each optimization phase; an enhanced fine-tuning of the setup parameters in the model (tolerance threshold values, etc.) to ensure the optimization process is more robust and efficient (for example yielding similar relative error levels for every phase).

6.4. Use of the adjoint method for final fine-tuning.

The use of the adjoint method has become very popular in many fields of shape optimization. A very good example of its application to aerodynamic shape design, in particular for the nose of high-speed trains, can be found in Paniagua (2014).

The adjoint method analyzes the sensitivity of each of the attributes defined to local variations of the geometry. Commercial CFD solvers such as ANSYS include this feature and allow for the computation of these sensitivities for a given body. A general example of the geometry changes calculated for a general U-bend example is shown in Figure 6–29 to illustrate how the adjoint method works.

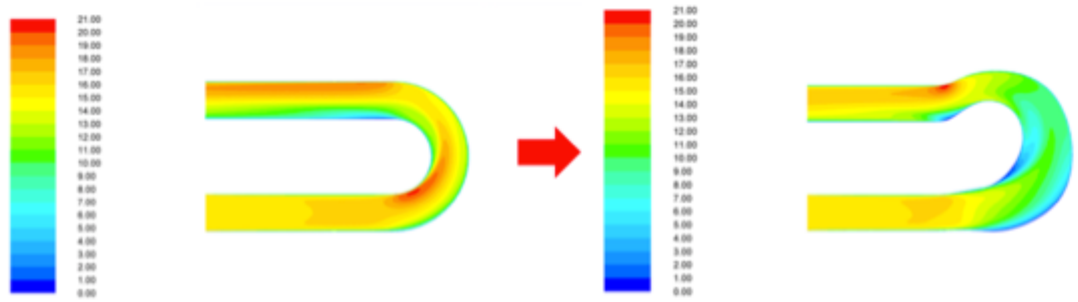

Figure 6–29 - Example application of the adjoint method for the local fine-tuning of a U-bend.

Commercial CFD solvers allow the user to set a target for the desired improvement of a particular objective (or more than one) and the adjoint method will modify the geometry (and the underlying mesh) to reach that improvement (if possible) based on the calculated sensitivities.

The adjoint method, which is a derivative-based method, is an interesting tool for the local fine-tuning of the optimum candidate points obtained in the last phase of an optimization. The MOST-HDS model makes use of the adjoint method whenever applicable to a particular case of shape design optimization. In the following figures the results of the adjoint application to optimum design points are presented, both for the HRSG inlet duct and for the closed wind tunnel cases. In both examples the target has been to reduce the pressure drop by 10%. The results once the new geometries were run in the CFD solver prove that the 10% reduction was achieved in both cases. The figures show the region selected for the fine-tuning and the results for the so-called Normal Optimal Displacement, which is the deformation the solver would introduce to the geometry to achieve the target improvement set by the user (red regions indicate maximum positive deformations and blue regions indicate maximum negative deformations).

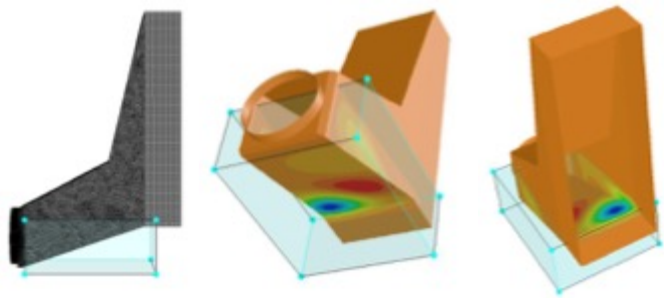

Figure 6–30 - Example application of the adjoint method for the local fine-tuning of one of the optimum design points obtained in the last phase of the optimization process for the HRSG case. The region to be optimized is shown alongside two views of the results of the Normal Optimal Displacement.

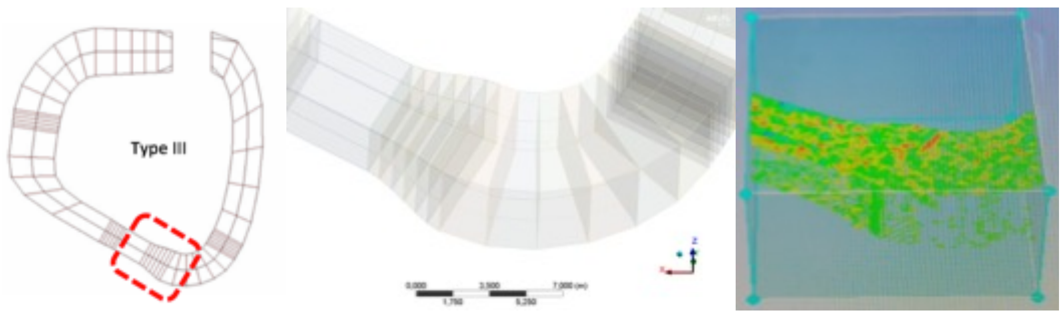

Figure 6–31 - Example application of the adjoint method for the local fine-tuning of one of the optimum design points obtained in the last phase of the optimization process for the full wind tunnel case. The region to be optimized is shown alongside a view of the results of the Normal Optimal Displacement.

The adjoint method is therefore an interesting tool for shape design optimization fine-tuning. However, given its derivative-based nature, it has a number of limitations. Firstly, it is a tool for local optimization, so it is aimed at local shape changes in the areas where the designer believes a greater impact on performance can be achieved (the adjoint can be run for different areas in separate calculations). Secondly, and particularly for the cases of aerodynamic shape optimization with big geometry changes, it must be noted that adjoints cannot be used for transient phenomena so, for instance, they are not applicable generally in areas of flow detachment (which are typical areas where the designer would like to seek for performance improvements). Finally, they may yield resulting geometries which are costly or infeasible to manufacture, so their application must be carried out wisely.

6.5. Benchmark optimization. Application of MOST-HDS to the WFG9 optimization test problem

In this section, the MOST-HDS model is applied to a completely different type of problem. Up to this point, the cases presented have been two real industrial projects of aerodynamic shape optimization. Now MOST-HDS will be applied to a well-known mathematical test problem used for benchmark optimization among different algorithms. The WFG test suite presented in Huband et al. (2006) is selected over other existing test suites for its challenging and yet comprehensive nature and because it features non-separable problems, particularly non-separable multimodal problems, which is a feature rarely found in commonly used test suites (other existing test suites used in literature are presented in the State of the Art – Chapter 3).

All WFG problems are scalable, have no extremal nor medial variables, have dissimilar variable domains and Pareto optimal trade-off magnitudes, have known Pareto optimal sets, and can be made to have a distinct many-to-one mapping from the Pareto optimal set (space of variables) to the Pareto optimal front (space of attributes) by scaling the number of position variables.

In particular, the WFG9 test problem is used. The selected WFG9 problem is a 2-objective optimization problem with the following features: non-separable objectives, multimodal and including deceptive minima, with a strong parameter dependent bias and a concave geometry of the optimal Pareto front.

The detailed description of the WFG9 can be found in Huband et al. (2006) and the summary tables describing the mathematical definition of the problem can be found in Figure 6–32 and Figure 6–33.

TABLE XIII

AN EXAMPLE TEST PROBLEM. THE NUMBER OF POSITION-RELATED PARAMETERS, k, MUST BE DIVISIBLE BY THE NUMBER OF UNDERLYING POSITION PARAMETERS, $M-1$ (THIS SIMPLIFIES $\mathbf{t}^3$). THE NUMBER OF DISTANCE-RELATED PARAMETERS, l, CAN BE SET TO ANY POSITIVE INTEGER. TO ENHANCE READABILITY, FOR ANY TRANSITION VECTOR $\mathbf{t}^i$, WE LET $\mathbf{y} = \mathbf{t}^{i-1}$. FOR $\mathbf{t}^1$, LET $\mathbf{y} = \mathbf{z}_{[0,1]} = \{z_1/2, \ldots, z_n/(2n)\}$

Type	Setting
Constants	$S_{m=1:M} = 2m$ $A_{1:M-1} = 1$ The settings for $S_{1:M}$ ensures the Pareto optimal front will have dissimilar tradeoff magnitudes, and the settings for $A_{1:M-1}$ ensures the Pareto optimal front is not degenerate.
Domains	$z_{i=1:n,\max} = 2i$ The working parameters have domains of dissimilar magnitude.
Shape	$h_{m=1:M} = \text{concave}_m$ The purely concave Pareto optimal front facilitates the use of some performance metrics, where the distance of a solution to the nearest point on the Pareto optimal front must be determined.
$\mathbf{t}^1$	$t^1_{i=1:n-1} = \text{b\_param}(y_i, \text{r\_sum}(\{y_{i+1}, \ldots, y_n\}, \{1, \ldots, 1\}), \frac{0.98}{49.98}, 0.02, 50)$ $t^1_n = y_n$ By employing the parameter dependent bias transformation, this transition vector ensures that distance- and position-related working parameters are inter-dependent and somewhat non-separable.
$\mathbf{t}^2$	$t^2_{i=1:k} = \text{s\_decept}(y_i, 0.35, 0.001, 0.05)$ $t^2_{i=k+1:n} = \text{s\_multi}(y_i, 30, 95, 0.35)$ This transition vector makes some parts of the Pareto optimal front more difficult to determine (due to the deceptive transformation), and also makes it more difficult to converge to the Pareto optimal front (due to the multi-modal transformation). The multi-modality is similar to Rastrigin's function, with many local optima ($61^l - 1$), and one global optimum, where the "hill size" between adjacent local optima is relatively small.
$\mathbf{t}^3$	$t^3_{i=1:M-1} = \text{r\_nonsep}(\{y_{(i-1)k/(M-1)}, \ldots, y_{ik/(M-1)}\}, k/(M-1))$ $t^3_M = \text{r\_nonsep}(\{y_{k+1}, \ldots, y_n\}, l)$ This transition vector ensures that all objectives are non-separable, and also reduces the number of parameters down to M, as required by the framework.

$$
\begin{array}{llcl}
\text{Given} & \mathbf{z} & = & \{z_1, \ldots, z_k, z_{k+1}, \ldots, z_n\} \\
\text{Minimise} & f_1(\mathbf{x}) & = & x_M + 2\prod_{i=1}^{M-1} \sin(x_i\pi/2) \\
 & f_{m=2:M-1}(\mathbf{x}) & = & x_M + 2m\left(\prod_{i=1}^{M-m} \sin(x_i\pi/2)\right)\cos(x_{M-m+1}\pi/2) \\
 & f_M(\mathbf{x}) & = & x_M + 2M\cos(x_1\pi/2) \\
\text{where} & x_{i=1:M-1} & = & \text{r\_nonsep}(\{y_{(i-1)k/(M-1)+1}, \ldots, y_{ik/(M-1)}\}, k/(M-1)) \\
 & x_M & = & \text{r\_nonsep}(\{y_{k+1}, \ldots, y_n\}, l) \\
 & y_{i=1:k} & = & \text{s\_decept}(y'_i, 0.35, 0.001, 0.05) \\
 & y_{i=k+1:n} & = & \text{s\_multi}(y'_i, 30, 95, 0.35) \\
 & y'_{i=1:n-1} & = & \text{b\_param}\left(z_i/(2i), \sum_{j=i+1}^{n} z_j/(2j(n-i)), 0.98/49.98, 0.02, 50\right) \\
 & y'_n & = & z_n/(2n)
\end{array}
$$

Fig. 11. The expanded form of the problem defined in Table XIII. $|\mathbf{z}| = n = k + l$, $k \in \{M-1, 2(M-1), 3(M-1), \ldots\}$, $l \in \{1, 2, \ldots\}$, and the domain of all $z_i \in \mathbf{z}$ is $[0, 2i]$.

Figure 6–32 - Mathematical definition of the WFG9 test problem used for benchmark optimization of the MOST-HDS model (taken from Huband et al. [2006]).

TABLE XI

TRANSFORMATION FUNCTIONS. THE PRIMARY PARAMETERS y AND $y_1, \ldots, y_{|\mathbf{y}|}$ ALWAYS HAVE DOMAIN [0,1]. A, B, C, α, AND β ARE CONSTANTS. FOR b_param, $\mathbf{y}'$ IS A VECTOR OF SECONDARY PARAMETERS (OF DOMAIN [0,1]), AND u IS A REDUCTION FUNCTION

Bias: Polynomial ($\alpha > 0$, $\alpha \neq 1$)

$$\text{b\_poly}(y, \alpha) = y^{\alpha}$$

When $\alpha > 1$ or when $\alpha < 1$, y is biased towards zero or towards one respectively.

Bias: Flat Region ($A, B, C \in [0, 1]$, $B < C$, $B = 0 \Rightarrow A = 0 \wedge C \neq 1$, $C = 1 \Rightarrow A = 1 \wedge B \neq 0$)

$$\text{b\_flat}(y, A, B, C) = A + \min(0, \lfloor y - B \rfloor)\frac{A(B-y)}{B} - \min(0, \lfloor C - y \rfloor)\frac{(1-A)(y-C)}{1-C}$$

Values of y between B and C (the area of the flat region) are all mapped to the value A.

Bias: Parameter Dependent ($A \in (0, 1)$, $0 < B < C$)

$$\text{b\_param}(y, \mathbf{y}', A, B, C) = y^{B+(C-B)v(u(\mathbf{y}'))}$$

$$v(u(\mathbf{y}')) = A - (1 - 2u(\mathbf{y}'))\,\big|\lfloor 0.5 - u(\mathbf{y}') \rfloor + A\big|$$

A, B, C, and the secondary parameter vector $\mathbf{y}'$ together determine the degree to which y is biased by being raised to an associated power: values of $u(\mathbf{y}') \in [0, 0.5]$ are mapped linearly onto $[B, B + (C - B)A]$, and values of $u(\mathbf{y}') \in [0.5, 1]$ are mapped linearly onto $[B + (C - B)A, C]$.

Shift: Linear ($A \in (0, 1)$)

$$\text{s\_linear}(y, A) = \frac{|y - A|}{|\lfloor A - y \rfloor + A|}$$

A is the value for which y is mapped to zero.

Shift: Deceptive ($A \in (0, 1)$, $0 < B \ll 1$, $0 < C \ll 1$, $A - B > 0$, $A + B < 1$)

$$\text{s\_decept}(y, A, B, C) = 1 + (|y - A| - B) \times \left(\frac{\lfloor y - A + B \rfloor (1 - C + \frac{A-B}{B})}{A - B} + \frac{\lfloor A + B - y \rfloor (1 - C + \frac{1-A-B}{B})}{1 - A - B} + \frac{1}{B} \right)$$

A is the value at which y is mapped to zero, and the global minimum of the transformation. B is the "aperture" size of the well/basin leading to the global minimum at A, and C is the value of the deceptive minima (there are always two deceptive minima).

Shift: Multi-modal ($A \in \{1, 2, \ldots\}$, $B \geq 0$, $(4A + 2)\pi \geq 4B$, $C \in (0, 1)$)

$$\text{s\_multi}(y, A, B, C) = \frac{1 + \cos\left[(4A+2)\pi\left(0.5 - \frac{|y-C|}{2(\lfloor C-y \rfloor + C)}\right)\right] + 4B\left(\frac{|y-C|}{2(\lfloor C-y \rfloor + C)}\right)^2}{B + 2}$$

A controls the number of minima, B controls the magnitude of the "hill sizes" of the multi-modality, and C is the value for which y is mapped to zero. When $B = 0$, $2A + 1$ values of y (one at C) are mapped to zero, and when $B \neq 0$, there are $2A$ local minima, and one global minimum at C. Larger values of A and smaller values of B create more difficult problems.

Reduction: Weighted Sum ($|\mathbf{w}| = |\mathbf{y}|$, $w_1, \ldots, w_{|\mathbf{y}|} > 0$)

$$\text{r\_sum}(\mathbf{y}, \mathbf{w}) = \left(\sum_{i=1}^{|\mathbf{y}|} w_i y_i\right) / \sum_{i=1}^{|\mathbf{y}|} w_i$$

By varying the constants of the weight vector $\mathbf{w}$, EAs can be forced to treat parameters differently.

Reduction: Non-separable ($A \in \{1, \ldots, |\mathbf{y}|\}$, $|\mathbf{y}| \bmod A = 0$)

$$\text{r\_nonsep}(\mathbf{y}, A) = \frac{\sum_{j=1}^{|\mathbf{y}|}\left(y_j + \sum_{k=0}^{A-2} |y_j - y_{1+(j+k) \bmod |\mathbf{y}|}|\right)}{\frac{|\mathbf{y}|}{A}\lceil A/2 \rceil (1 + 2A - 2\lceil A/2 \rceil)}$$

A controls the degree of non-separability (noting that $\text{r\_nonsep}(\mathbf{y}, 1) = \text{r\_sum}(\mathbf{y}, \{1, \ldots, 1\})$).

Figure 6–33 – Transformation functions used by the WFG9 test problem (taken from Huband et al. [2006]).

The MOST-HDS model is compared to a well-known Multi-Objective Evolutionary Algorithm (MOEA), NSGA-II (Deb et al. [2002]), which was the same algorithm applied to the HRSG inlet duct optimization problem in Section 6.2.

The WFG9 problem chosen is set-up with 4 position-related variables and 20 distance-related variables. NSGA-II was run in Huband et al. (2006) with real-coded parameters, a mutation probability of 1/24, a crossover probability of 0.9, a crossover distribution index of 10.0, and a mutation distribution index of 50.0.

In the case of the NSGA-II algorithm, the procedure used in the work by Huband et al. (2006) executes 35 runs of NSGA-II, with a population size of 100, for 25000 generations. The non-dominated front of the populations is saved in each case after 250, 2500, and 25000 generations. The authors state that, in the literature, a population size of 100 for 250 generations is a common choice, so 25000 generations should be more than enough to ensure convergence.

The next step is to compute the 50% attainment surface from the 35 fronts at 250, 2500 and 25000 generations. An attainment surface is the boundary in the space of attributes formed by the obtained front, which separates the region dominated by the obtained solutions from the region that is not dominated (Fonseca and Fleming [1996]). For instance, the 50% attainment surface identifies the region of the space of attributes that is dominated by half of the given attainment surfaces, whereas the 100% attainment surface identifies the region dominated by every given attainment surface. Therefore, for the 35 runs, a 50% attainment surface will be that which dominates over half of the fronts obtained and which is dominated by the other half.

To begin with, the results are shown for a random evaluation of the WFG9 problem for two different numbers of initial samples (1000 and 4600 points), to illustrate the coverage of the space of attributes for different levels of detail (Figure 6–34). This is included because MOST-HDS will select an initial set of 1000 evaluation points for Phase 0, based on a random generation scheme. Any efficient algorithm must require less function evaluations than a mere random search to find the Pareto optimal front or to get as close as possible to it[16].

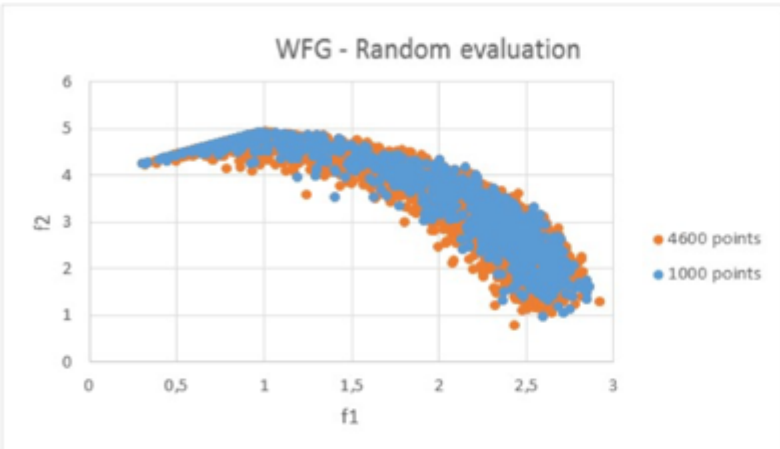

Figure 6–34 - Random evaluation of the WFG9 problem for a different number of initial samples: 1000 points and 4600 points.

[16] A non-iterative sampling method based on a quasi-random number generator is called Screening method and is occasionally used as an alternative to real optimization algorithms. Any optimization algorithm must, at least, perform better than a Screening method, for the same number of function evaluations.

Figure 6–35 shows the results presented in Huband et al. (2006) for the NSGA-II optimization of the WFG9 test problem. As can be seen, the WFG9 problem is challenging and, at 250 generations, which is the number of generations commonly used in literature, the NSGA-II algorithm shows a good coverage of the Pareto front (i.e. the whole range of the Pareto front is well represented). However, convergence is not good in all areas of the Pareto front. For 2500 and for 25000 generations the convergence is successful and the Pareto front is reached very satisfactorily.

As explained by Huband et al. (2006), WFG9 has position related variables dependent on distance related variables and, most importantly, WFG9 is also multimodal, and has a troublesome kind of non-separable reduction. This makes this optimization problem quite challenging for any optimization algorithm.

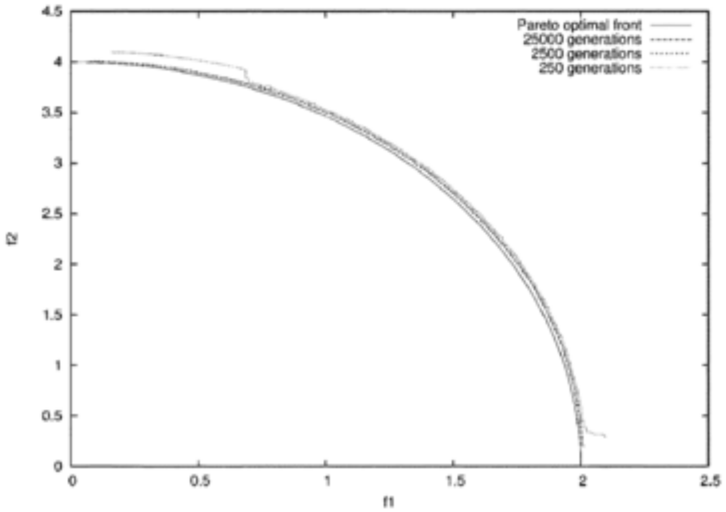

Figure 6–35 - Pareto optimal front and 50% attainment surfaces for NSGA-II after 250, 2500, and 25000 generations on the WFG9 test problem (taken from Huband et al. [2006]).

The results for MOST-HDS on this same problem are presented in Figure 6–36, for a growing number of function evaluations. Figure 6–36 (middle and bottom), in particular, shows the results after 4600 evaluations. In the first place, the results are far better than with a Screening or quasi-random method (refer to Figure 6–34). Furthermore, the number of evaluations required to produce a good coverage of the Pareto front and a good convergence is considerably reduced with respect to the 250 generation case of NSGA-II, assuming only one run and not 35 runs (1 run, for a population of 100 and for 250 generations yields 25000 function evaluations). This is not to say that NSGA-II is not a good optimization algorithm. It certainly is a very successful algorithm. It has to be understood that WFG9 is a very challenging problem. Besides, the NSGA-II could possibly be tuned to obtain even better results. Moreover, more work is in any case required on the application of MOST-HDS to other test problems.

The evolution of the optimization process of MOST-HDS is in itself quite eye-catching:

1. After 2540 evaluations the points are still scattered but the bias has been reduced and their distribution is more even and they are starting to move clearly towards the Pareto optimal front, with a better coverage of the Pareto front;

2. In phases 11 to 15 the points are clearly progressing towards the Pareto optimal front and the coverage is further improved;

3. Finally, after 4600 evaluations the coverage of the Pareto optimal front is good and it can be considered that MOST-HDS has converged successfully. Once again, it is worth noting that performing 4600 evaluations following a smart search procedure, such as that proposed by MOST-HDS, is much more efficient than the results obtained with 4600 random evaluations (Figure 6–34).

From these results it can be concluded that MOST-HDS shows a promising performance in the field of general purpose optimization. However, a more extensive study needs to be performed as part of the future work beyond this Thesis.

Figure 6–36 – Evaluation results for the MOST-HDS optimization algorithm applied to the WFG9 test problem: (top) after 10 optimization phases (2540 evaluations); (middle) after 16 phases (4600 evaluations); (bottom) a summary of the optimization results for phases 11 to 16.

6.6. Final remarks

The results of the application of MOST-HDS, the novel optimization methodology presented in this Thesis, have been presented extensively in this chapter. As detailed in Chapter 5, MOST-HDS proposes a multi-objective, structured hybrid direct search optimization approach. This approach has shown to be successful for two real industrial cases and for a benchmark optimization test problem.

In the industrial cases addressed, which are aerodynamic shape design optimizations in which big changes of the geometry are explored, the smart, robust and efficient selection of candidate solutions embedded in MOST-HDS has managed to yield solution designs with high improvements over current designs, in a reasonable time. An efficient search scheme is essential in any optimization problem and more so when the evaluations are as time-consuming as in the case of CFD problems, in which only hundreds or, at most, thousands of candidate points can be evaluated throughout the whole optimization.

The MOST-HDS methodology has been applied to wind tunnel design and HRSG inlet duct design because these are two areas in which trial and error is still widely used. The presented approach evaluates a number of candidate solutions which is 1 to 2 orders of magnitude the number of solutions frequently evaluated for similar cases if using trial and error. The automated nature of the method yields project time reductions of 5-10 times for the examples considered, as compared to the design cycle times using more traditional or manual methods.

This methodology is flexible and can be tailored for specific optimization applications. The use of this novel optimization model in many aerodynamic fields will allow for the exploration of unconventional designs which can yield considerable improvements over more traditional concepts.

Finally, a key aspect of MOST-HDS is its emphasis on a direct search or direct optimization approach, even though the evaluations are time-consuming. The use of surrogate or approximation models is not considered the most appropriate approach due to the complexity of the problems addressed. In particular, transient or advanced flow phenomena such as flow separation, vortices, etc. are not well captured by surrogate models. Besides, the high number of independent variables (and therefore the size of the search region) makes it difficult to develop surrogate models which are accurate enough. This will be analyzed in detail in Chapter 7.

List of Figures

Figure 6–19 - Low detail representation of a wind tunnel design, used to illustrate better certain aspects of the optimization methodology presented in this section. Four Bézier curves are used only. Fan and test sections are both shaded in this figure (left). An example plane containing one of the transverse sections used for the tunnel geometry discretization is also shown (right).

Figure 6–20 - Example tree of design point combinations for Phase 0 optimization of the simplified wind tunnel model. 32 wind tunnel designs are considered.

Figure 6–21 - CFD evaluation results (velocity contour plots for mid-plane, total pressure drop – delta p – and fixed cost) for each of the 32 wind tunnel design points for the simplified wind tunnel model.

Figure 6–22 - Pareto front (red line) of fixed cost v. total pressure drop for 32 wind tunnel design points for the simplified wind tunnel model. Tolerance threshold (orange line) to select area of search region where potential candidates to optimum may lie, for subsequent optimization phases (values of both attributes are per unit). Maximum attribute ranges are shown in %.

Figure 6–23 - Highly detailed representation of a generalized wind tunnel design, able to represent most tunnel geometries (18-20 Bézier curves are needed).

Figure 6–24 - Results obtained for a full wind tunnel 2-phase design optimization performed with the MOST-HDS algorithm. Pressure drop is in Pascals and the fixed cost is in fictitious monetary units.

Figure 6–25 - Results obtained for a full wind tunnel 2-phase design optimization performed with the MOST-HDS algorithm, comparing the use of different increment factors for Phase II: below unity (light green squares) and above unity (dark green diamonds). Pressure drop is in Pascals and the fixed cost is in fictitious monetary units.

Figure 6–26 - Example tree of design point combinations for Phase 0 optimization of the full wind tunnel model. 32 wind tunnel designs are considered. The areas of the search region which disappear as the optimization proceeds are indicated.

Figure 6–27 - Wind tunnel model families on the Pareto front for Phase 0 and their velocity contours in the tunnel test section (transverse plane). The Pareto front for this phase has 5 design points, 2 of type I and 3 of type II.
Figure 6–28 - New wind tunnel model family on the Pareto frontier for Phase I and its velocity contour in the tunnel test section. The Pareto front for this phase has 5 design points, 1 of type I, 3 of type II and 1, quite unconventional design, of type III.

Figure 6–29 - Example application of the adjoint method for the local fine-tuning of a U-bend.

Figure 6–30 - Example application of the adjoint method for the local fine-tuning of one of the optimum design points obtained in the last phase of the optimization process for the HRSG case. The region to be optimized is shown alongside two views of the results of the Normal Optimal Displacement.

List of Tables

7

Chapter 7 - Comparison to surrogate models

There are dark shadows on the earth, but its lights are stronger in the contrast.

Charles Dickens.

This chapter is presented as a special section of the results obtained in this Thesis with the MOST-HDS algorithm for shape design optimization with big geometry changes. The use of surrogate models to approximate the full model, in order to reduce the evaluation time of the performance of complex geometries, has become increasingly popular, so there is extensive research following this approach. Therefore, it was considered interesting to dedicate a full chapter to the discussion on the advantages and the limitations of surrogate-based optimization as compared to direct optimization. Firstly, *Section 7.1.* presents a general introduction. *Section 7.2.* includes quite eye-catching results of surrogate-based evaluations and surrogate-based optimization of the HRSG inlet duct case presented in Chapter 6. *Section 7.3.* analyzes a general summary of the main advantages and limitations of a surrogate-based methodology. In addition to this, surrogate methods are compared with direct optimization approaches, such as that followed by MOST-HDS.

7.1. Introduction

In the field of aerodynamics and fluid mechanics in general, the evaluation of the performance of a particular design is often very costly in terms of time or money. Tools available, such as CFD simulations, wind tunnel testing, or testing in the real environment, are complex and frequently too expensive, at least for the design phase of a project. Furthermore, in the case of optimization, an area in which for other applications it is common to perform thousands or millions of evaluations of the objective function, the situation for fluid mechanics problems is even more challenging. Therefore, an increasingly popular approach has been the use of different kinds of surrogate models, to approximate more complex evaluation models of the performance of the body, geometry or device of interest.

Surrogate-based evaluation, and more so surrogate-based optimization techniques, are certainly very interesting and useful tools for a wide range of applications (as shown in representative and advanced uses of these tools such as Jing et al. [2013] or Walton et al. [2013]). However, it is important to realize that, at present, there are certain limitations to the use of this approach. In these cases, direct evaluation with more complex and realistic models may be preferable, leading to direct search or direct optimization models. These complex and realistic models are also known as high-fidelity models.

As outlined in Robinson et al. (2006), surrogate models belong to one of the following categories:

1. Data fits. Typically using interpolation or regression of the high-fidelity model evaluated at one or more sample points. Among this type, response surfaces are one of the most popular and strong tools available. A good example of the application of response-surfaces and a discussion on their potential for aerodynamic and shape optimizations can be found in Krajnovic (2007).

2. Reduced Order Models (ROMs). Obtained with techniques such as modal analysis or Proper Orthogonal Decomposition (POD). The course notes by Janardhanan (2011) is a good description of modal analysis. The book by Volkwein (2013) is a very sound mathematical basis for PODs and ROMs, and the work by Walton et al. (2013) offers an interesting discussion on the applicability of POD and Radial Basis Functions (RBF).

3. Hierarchical models. They are also referred to as multi-fidelity, variable fidelity or variable complexity models. The low-fidelity surrogate may be the same as the high-fidelity model, but converged to a higher residual tolerance. For finite-element models the surrogate can make use of a lower basis function order than the high-fidelity model, or it can also be the same model on a coarser grid. The surrogate model may also be a simplified engineering model that neglects some of the physics of the real, full problem. The very interesting work by Robinson et al. (2006), which we have cited to describe the different types of surrogate models, is a very good example of the use of hierarchical models.

Already a decade ago, in Krajnovic (2007), we can find some interesting considerations on the potential of surrogate-based optimization for aerodynamic problems, in this case using response surfaces. In that work the author claims: "*Although there is a number of questions that have to be answered before the surrogate-based optimization can become a general engineering tool for the aerodynamic optimization of vehicles, there is no doubt that it represents a valuable design strategy. With increase in computer power, the steady CFD simulations will be replaced with more accurate unsteady simulations and thereby increase the accuracy of the response surface model substantially. Despite the promising computer development, the use of gradient-based search algorithms will be prohibited for many years to come (especially if time-dependent simulations are used). Using the surrogate-based optimization together with time-dependent CFD simulations for the construction of the surrogate model will certainly become an optimization tool that is capable to compete with physical optimization in wind tunnels both in terms of cost and accuracy*".

Krajnovic (2007) is already proposing the combination of highly complex CFD simulations for the evaluation of the set of points used to generate more accurate response surfaces. Today, ten years after this work, the most advanced optimization solvers offered in commercial packages (by companies such as ANSYS or Siemens CD-adapco) include hybrid approaches between surrogate-based and direct optimization, called adaptive single or multi-objective optimization.

Concerning our field of interest, aerodynamic shape design optimization, we will focus on the performance of response surfaces of various types. The results and observations made are applicable to most of the other types of surrogate techniques (ROMs or hierarchical models).

The contribution of this Thesis in this chapter is mainly to present the limitations of surrogate-based evaluation and surrogate-based optimization for cases of aerodynamic shape design in which the flow regime can change from design point to design point (for example because of the onset of flow detachment). This occurs in most cases involving big geometry changes. In these cases, the robustness and accuracy of direct optimization is shown as an alternative approach to surrogate models.

7.2. Results of a surrogate-based approach for the shape optimization of the inlet duct of HRSGs

Firstly, let us compare the results of surrogate based evaluation to the results obtained with direct evaluation. Secondly, the results of surrogate-based optimization and direct search optimization will be confronted.

For this section, the example case of the HRSG inlet duct optimization will be used. First, because it is more simple and clear to understand and will illustrate our key conclusions better. Second, because one of the limitations of surrogate models in general is that cases such as the full wind tunnel have an excessive number of variables to be analyzed with surrogate techniques. For surrogate models in general (especially of the response surface type), variables sets in excess of 10 to 15 are complex or impossible to handle (the wind tunnel case had 108 independent variables). If surrogate models are to be used for these cases, it is necessary to carry out a reduction of the number of variables or to use variable hierarchies to address only those variables with a stronger impact on the results.

SURROGATE-BASED EVALUATION

In the first place, the results of surrogate based evaluation will be compared to those obtained by direct CFD evaluation. Various response-surface models can be used. To analyze the accuracy and applicability of some of the most relevant, the CFD results will be compared to the results obtained with the following types of response surfaces: Neural Network, Genetic, Non-Parametric Regression and Kriging (with auto-refinement).

Sparse Grid is another interesting type of response surface, which could not be used because it does not allow the sample points to be introduced by the user and it generates them automatically[17]. For the particular case of the HRSG inlet duct, given that a further limitation of response surface modules in commercial packages is that the user cannot introduce any kind of constraints on the variables, the automatic sampling generates absurd geometries and this makes the use of the Sparse Grid response surface impossible. For the other four types of response surface used, the points were generated automatically by the program used (ANSYS in this case), but the absurd points could be corrected manually before each response surface was computed.

Table 7–1 presents the results for the relative errors of the values calculated using the different response surfaces with respect to the values calculated using CFD. 14 representative design points (i.e. quite spread out in the space of variables) have been used for the comparison. Figure 7–1 shows these results graphically, so that the performance of each response surface is more clear.

It is important to note that the prediction of the results for a particular design point, once the response surface has been computed, is quasi instantaneous, and the calculation of the response surface in the first place takes a negligible amount of time (a few seconds in an i7, 8-core, 32GB RAM computer).

[17] Both Kriging (with auto-refinement) and Sparse Grid are the two response surface types recommended by ANSYS and other commercial packages for a higher accuracy. As is shown in this chapter, Kriging is not always the best choice in terms of accuracy of the predictions (Sparse Grid could not be used, as explained). However knowing beforehand which type of response surface is best suited for a particular problem is quite frequently complex or infeasible.

RESPONSE SURFACE TYPE	NEURAL		GENETIC		NON-PARAMETRIC REGRESSION		KRIGING + auto-refinement	
Design point	**Error in total pressure drop**	**Error in velocity non-uniformity**	**Error in total pressure drop**	**Error in velocity non-uniformity**	**Error in total pressure drop**	**Error in velocity non-uniformity**	**Error in total pressure drop**	**Error in velocity non-uniformity**
#1	-2%	17%	-2%	6%	-7%	15%	-2%	2%
#2	26%	-23%	22%	-17%	27%	-19%	0%	-17%
#3	-35%	-9%	-33%	-1%	-27%	2%	-43%	2%
#4	7%	-19%	9%	-9%	12%	-1%	-11%	-9%
#5	21%	-17%	21%	-7%	22%	4%	-1%	-8%
#6	24%	-22%	18%	-16%	27%	-17%	-3%	-17%
#7	-6%	-14%	-4%	-11%	9%	-7%	-22%	-22%
#8	-6%	-16%	-6%	-11%	8%	-8%	-27%	-21%
#9	-8%	19%	-1%	12%	-7%	16%	-2%	14%
#10	3%	-11%	24%	-1%	40%	-2%	-12%	-29%
#11	-5%	12%	-3%	5%	-8%	9%	-3%	16%
#12	-2%	11%	-2%	3%	-2%	-3%	-3%	15%
#13	-1%	9%	-2%	2%	5%	-18%	-3%	11%
#14	7%	-6%	4%	-12%	13%	-29%	5%	-9%

Table 7–1 - Relative errors with respect to the CFD values for four different types of response surface and for a number of representative design points.

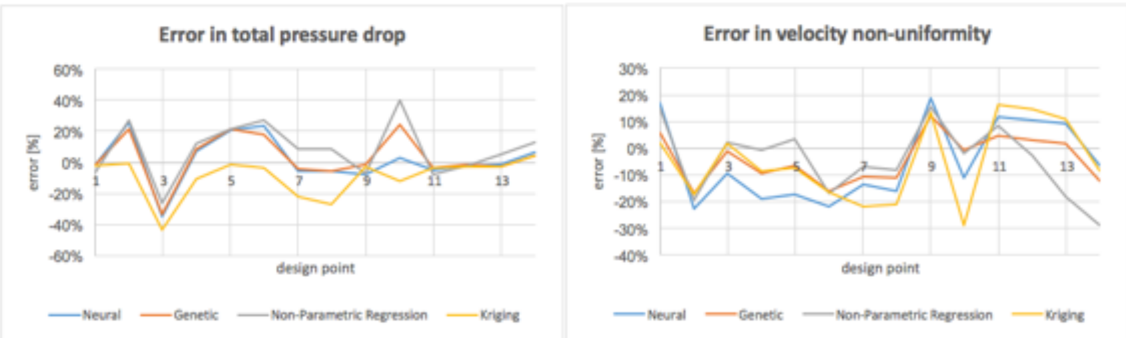

Figure 7–1 - Relative errors with respect to the CFD values for four different types of response surface and for a number of representative design points.

For this particular case, the genetic type behaves better for both attributes, but this will be different for other examples. The important observations to make here are that the relative errors can reach values of up to 20% or higher and, furthermore, that the error is not always systematic or predictable. Besides, for many points, different response surfaces yield quite different errors, and not always in the same relative direction. This means that response surface approximations have to be used sensibly and the user should bear these considerations in mind.

A method used to check the accuracy of the data fit carried out to generate each response surface is the Goodness of Fit (GoF). The GoF is showed in Figure 7–2 for all four response-surfaces. As is common, Neural and Genetic are not that close to the values of the points used to compute the response surface. The Non-Parametric Regression tries to force all points to be within a +/-ε distance of the response surface (this cannot be observed clearly in the graph for this case). The Kriging response surface matches the exact values of all sample points (including auto-refinement, which means that additional sample points are generated automatically to improve the first version of the surface). Despite the GoF figures for each response surface, Kriging and Non-Parametric Regression are not necessarily the most accurate surfaces, as seen in Table 7–1 and Figure 7–1.

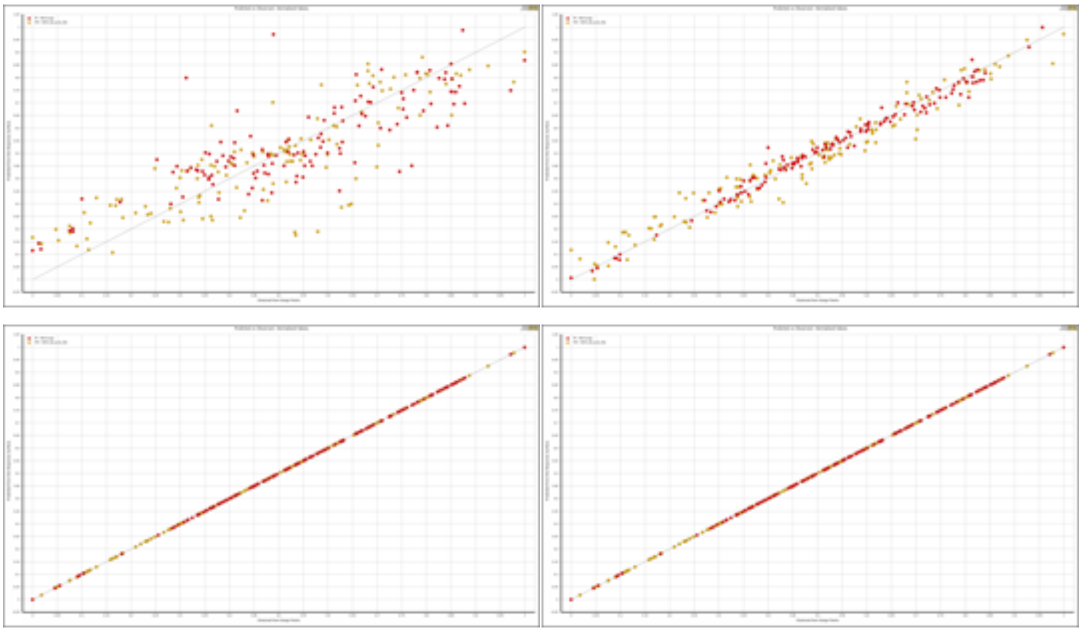

Figure 7–2 - Goodness of Fit (GoF) for the different response surfaces. Predicted versus CFD computed results for the four response surface types: Neural (top left), Genetic (top right), Non-Parametric Regression (bottom left) and Kriging with auto-refinement (bottom right) (all values are normalized). Red dots are for pressure drop and yellow dots are for velocity non-uniformity.

Let us go a bit further to understand the causes of these errors. In order to do so, we will use the example design points of Figure 7–3. These design points have been selected, out of all of the points in Table 7–1, because the flow regime changes abruptly between them. Only the values of the two angles of the bottom plane of the HRSG inlet duct are modified, keeping the rest of the variables constant. The flow for points 4 and 5 is still attached to the floor of the inlet duct, although it starts to have a minor detachment towards the end of the floor for design point 4. Design point 3, which has a much steeper first angle for the floor plane (i.e. a big geometry change with respect to points 4 and 5), has a clear flow detachment and hence a qualitatively different flow regime. This matches nicely with what is expected to happen as the floor angle increases and the result can be seen in the CFD evaluation values of Table 7–2. It is interesting to point out that, while the pressure drop is the highest for point 3 and reduces gradually, the non-uniformity is the lowest (i.e. the velocity at the outlet of the inlet duct is more uniform) because the flow detachment generates a better flow distribution. This is reasonable and it is very well captured by a direct evaluation of each design point.

However, if we analyze the data of Table 7–1 closely, it is plain to see three sources of error. First, the different response surfaces do not manage to reproduce the gradual reduction in the pressure drop from point 3 to point 5 at the same time as the change in velocity non-uniformities. Second, the relative error values are quite considerable, especially for design point 3, where flow detachment occurs. Third, the error values among the different response surfaces are quite different in some cases; while some of them underestimate the results, others overestimate them, and this is not always consistent or predictable. As will be concluded in the final section of this chapter, it has been shown that response surfaces, and this can be extended to most surrogate models, are not accurate enough to predict the results of complex fluid problems with big geometry changes and phenomena such as flow detachment. The results of the response surfaces will only be acceptable if the number of sample points increases in the region of design points where these phenomena occur. This, in any case, means that more CFD evaluations are required to compute an accurate response surface, so surrogate models are not so time-competitive. For these cases, direct CFD evaluation can yield better results with less evaluations and thus with a reduced computation time. This should be the approach used for these situations, very especially if an optimization is to be performed.

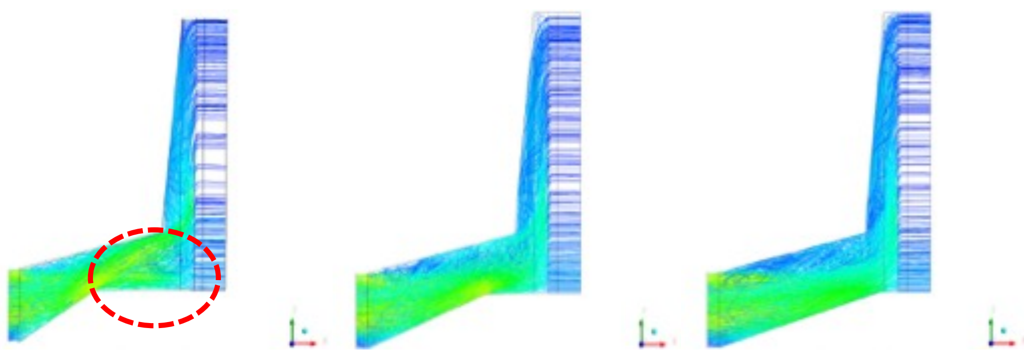

Figure 7–3 - Side-view of the velocity contours for design points #3, #4 and #5 of Table 7–1.

Design point	Total pressure drop	Velocity non-uniformity
#3	100%	100%
#4	63%	109%
#5	57%	105%

Table 7–2 - CFD evaluation results for design points #3, #4 and #5 of Table 7–1.

SURROGATE-BASED OPTIMIZATION

Once the results of surrogate-based evaluation with different response surfaces has been analyzed, this section presents the results obtained when a surrogate-based approach is followed for the optimization of a complex fluid problem, frequently involving big changes of the body geometry.

The four response surface types of the previous section have been used for the shape optimization of the HRSG inlet duct presented in Chapter 6. In particular surrogate-based optimization has been applied to the first HRSG family presented. The results obtained for the optimization carried out with MOST-HDS are included again here for easier reference (Figure 6–7).

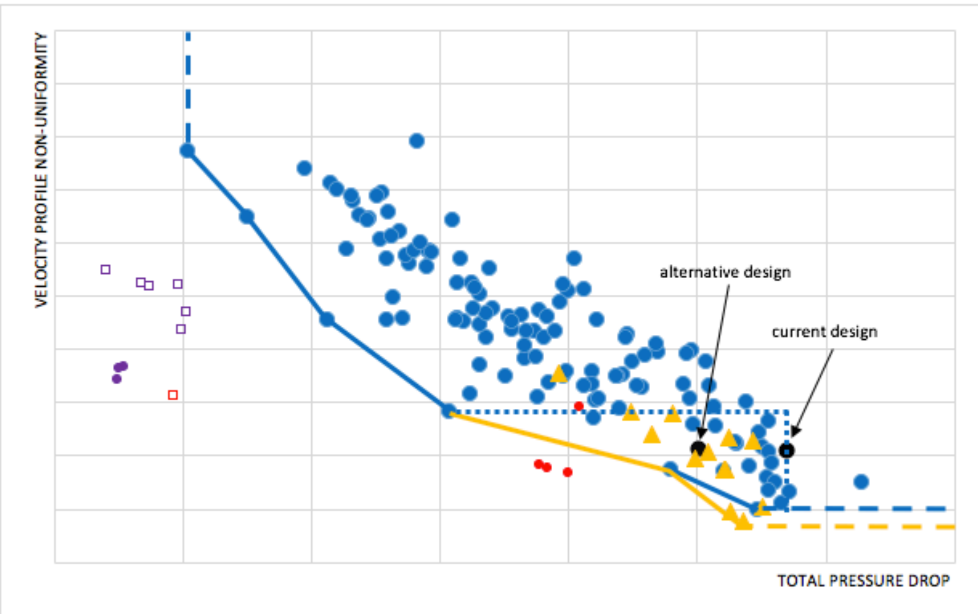

Figure 7–4 - Application of the MOST-HDS algorithm to the shape optimization of the inlet duct of a first family of HRSGs for combined cycle power plants. Surrogate-based optimization results: i) Unconstrained optimization: surrogate predictions (purple circles) v. CFD evaluations (purple squares); ii) Constrained optimization (velocity non-uniformity below a certain value): surrogate predictions (red circles) v. CFD evaluations (red square).

As can be seen in Figure 6–7, the Phase 0 evaluation already improved the performance of the current design quite considerably and Phase I was only able to improve that slightly further so, at least based on the results obtained with MOST-HDS, one could presume that continuing with the optimization may not produce considerable improvements.

Four response surfaces have been generated with the 120 sample points of Phase 0, the same points used for the MOST-HDS optimization. An unconstrained optimization was launched in the first place. In this case, as can be seen in Figure 6–7, the response surface predicted a considerable improvement over the Pareto front of Phase 0. The CFD evaluation for the predicted optimum points is also included. There are differences in the results, as commented in the section on surrogate-based evaluation, but still the use of surrogates for the optimization gives a clear indication of an interesting area of the search region where optimum designs may lie.

However, to compare the results of a surrogate-based optimization to MOST-HDS, a constrained optimization must be launched. In this case, based on the results shown in Figure 6–7, some key observations can be made:

1. The surrogate-based optimization yields design points that may have an absurd geometry. This is because, at least in commercial packages, no constraints can be imposed on the variable values when generating a response surface. Therefore, the optimum points predicted by a response surface have often to be corrected if the problem has these constraints.

2. Only the Neural response surface was able to calculate predicted optimum points. The other response surfaces types indicated that no candidate could be found.

3. Most of the predicted optimum points appear to meet all constraints and they appear to improve the Pareto front of Phase 0. However, once these points are checked for absurdity only one real candidate design point is left and, after a CFD evaluation, it can be seen that it lies above the velocity non-uniformity level imposed for the MOST-HDS search.

Consequently, the results of the use of a surrogate-based approach for optimization can be useful and give strong indications of where the optimum designs may lie, and in some cases their results may be accurate enough. However, they have a number of limitations for complex problems, such as many found in fluid mechanics. Surrogate models are not fit for big geometry changes, and they frequently miss flow-detachment critical points. These features are precisely what the designer wants to focus on, in many cases.

7.3. Discussion on the advantages and limitations of a surrogate-based approach

This chapter has focused on the use of surrogate models both for evaluation and for optimization of complex problems in fluid mechanics, particularly aerodynamic shape design optimization with big geometry changes. Among all the types of surrogate models, this chapter has focused on the performance of response surfaces of various types. The results and observations made are applicable to most of the other types of surrogate techniques (ROMs or hierarchical models), although a more extensive work for each surrogate model would be necessary to prove it satisfactorily.

In the first place, it must be stated that surrogate models are a very useful tool and allow for faster and more accurate evaluation and optimization of many complex problems. However, a number of limitations and considerations must be kept in mind to exploit the potential of surrogate models more adequately:

1. Surrogate models in general have a limitation on the number of input or independent variables they can handle. This limit is typically around 10-15 variables, especially for response surfaces. Besides, for some techniques used in the field of surrogate models, such as Radial Basis Function (RBF) interpolation, more than 100 points for the initial sample set are too time-consuming to process (Walton et al. [2013] and Franke [1982]). If surrogate models are to be used for these cases, it is either necessary to carry out a reduction of the number of variables, or to use hierarchies of variables to address only those variables with a stronger impact on the results, or to use low fidelity models which are simpler to handle.

2. Some surrogate models, such as response surfaces, cannot incorporate constraints on variables to ensure the design points are not absurd geometries. This means that some of the candidate designs they predict as potential optima are not even feasible. If response surfaces are to be used, checks for absurd geometries should be included. In the particular case of the very interesting type of response surface referred to as Sparse Grid, this means that it may not be possible to use because it does not allow the sample points to be introduced by the user and it generates them automatically. For the particular case of the HRSG inlet duct, given that the user cannot introduce any kind of constraints on the variables, the automatic generation of sample points generates absurd geometries and this makes the use of the Sparse Grid response surface impossible.

3. Moreover, certain surrogate models, such as most response surfaces, are not supported for discrete variables.

4. The accuracy of surrogate evaluation, even for complex fluid problems such as unsteady cases, can be adequate. However, it must be ensured that there is no change of flow-regime within the search region (i.e. points with or without flow detachment, for example). This is frequently difficult to ensure for shape optimizations involving big geometry changes. This limitation means that approximate models may yield results that cannot be trusted. Furthermore, the designer is quite commonly interested precisely in studying when a particular flow-regime changes. Some examples are the analysis of flow separation initiation, the change of turbulence regime, or the onset of fluid induced vibrations.

5. Since many surrogate models rely on some sort of data fit or interpolation scheme, prediction errors are rarely systematic, and can therefore be in any direction with respect to the real value. This means that error-correction is difficult or too complex to perform.

6. In order to increase the accuracy of the surrogate models, most require more sample points (also referred to as snapshots) to derive a better approximate model. This may require the evaluation of points in areas of the search region where the attribute values may have strong variations (hence the need for more points), but where the optimum points may not lie, so time-consuming CFD evaluations are wasted anyway. More efficient direct search schemes, such as that developed for the MOST-HDS model, may yield better results with less CFD evaluations.

7. Given that there are multiple surrogate models available, it is not always easy, or even possible, to decide which will be more appropriate or accurate for a particular problem. Regarding response surfaces, both Kriging (with auto-refinement) and Sparse Grid are the two response surface types recommended by ANSYS and other commercial packages for a higher accuracy. As is shown in this chapter, Kriging is not always the best choice in terms of accuracy of the predictions (Sparse Grid could not be used, as explained). However, knowing beforehand which type of response surface is best suited for a particular problem is quite frequently complex or infeasible.

8. The application of surrogate models for optimization of fluid-related problems always requires a final CFD evaluation of the optimum candidates to ensure that the predicted results are correct. This means an additional calculation time, which must be accounted for when comparing a direct versus a surrogate-based optimization.

9. For cases in which the CPU time of a full-order evaluation is very high and the variable space is not too large, surrogate models can prove interesting. For cases such as those addressed by this Thesis (which are very common in industry and in research), direct search can be more adequate than surrogate models. This is because the full-order evaluation, although complex and requiring CFD, is not extremely time-consuming[18], and because the variable space can be large (more than 10-15 variables),

Taking all these limitations into account, it is considered that the work presented in this Thesis is an improvement over many other techniques for aerodynamic optimization of complex components (wings, high-speed train noses, automotive designs, etc.), which rely on surrogate-based optimization. Those surrogate-based models include data fits, response surfaces, by reduced order models, and hierarchical or multi-fidelity models, as explained in Robinson et al. [2006].

The main terms to compare the approach of this Thesis to other alternatives are accuracy, flexibility and applicability to big geometry changes. Surrogate models are not good in estimating strongly non-linear objective functions, including phenomena such as flow separation. They are also poor in combining variables of many different types (discrete, continuous, etc.). This is very much the case when big variable variations are allowed in aerodynamic optimization problems and when a whole body (wind tunnel, for instance) is optimized, and not only certain parts or components of it.

List of Figures

[18] The optimizations carried out for this Thesis (closed wind tunnel and industrial boilers - HRSGs) were performed in an 8-core parallel calculation, using a 32GB RAM computer. Each calculation took around 0.25-0.3 hours for the HRSG case and 0.75-1 hours for the full wind tunnel case. The size of the meshes was between 1-2 million elements for the HRSG case and 2-5 million elements for the full wind tunnel case.

List of Tables

8

Chapter 8 - Conclusions

It’s more fun to arrive at a conclusion than to justify it.

Malcolm Forbes.

This chapter summarizes the main conclusions and Thesis contributions, the results obtained, the advantages and limitations for the application of the MOST-HDS model developed and the future work to be carried out, based on the results of this research. *Section 8.1* presents and discusses the general and most relevant conclusions and contributions. *Section 8.2* presents the future research work to be carried out beyond this Thesis.

8.1. Conclusions and Thesis contributions

The problem this Thesis has dealt with has been the multi-attribute or multi-objective aerodynamic shape optimization of real geometries of different fields of application, subject to a set of constraints, and taking into account both small and big changes of the geometry of interest.

The approach proposed for the problem described above has been the development of a general method based on a **M**ulti-**O**bjective **St**ructured **H**ybrid **D**irect **S**earch optimization algorithm (referred to as **MOST-HDS**).

The main conclusions that can be drawn from this Thesis, alongside its key contributions, are now presented, grouped into a set of categories for better clarity:

OPTIMIZATION APPROACH AND COMPARISON TO SURROGATE-BASED OPTIMIZATION

1. This research work has addressed optimization problems involving time-consuming objective function evaluation, in particular requiring CFD evaluation. For this kind of optimization problems, there are two general ways of approaching the search process in a smart way. One is using techniques that allow for a faster evaluation (surrogate models), because the full-order function is somehow simplified. The other is developing smarter search schemes that reach the optimum solutions reducing the number of evaluations, but which introduce little or no simplification to the full-order model. This latter approach, called direct search or direct optimization, has been the technique selected for this Thesis;

2. It has been shown that surrogate models (mainly response surfaces have been analyzed in this Thesis) are useful tools for faster evaluation and optimization, but they have a number of limitations. The most important ones, applicable to most types of surrogate models, are:

    a. the number of input or independent variables should not exceed 10-15;

    b. some surrogate models cannot incorporate constraints on variables, for example to ensure the design points are not absurd geometries;

    c. a number of surrogate models are not supported for discrete variables;

    d. their accuracy is compromised when there is a change of flow regime between different design points (such as the onset of flow detachment), which are frequently cases of special interest for the designer;

    e. errors are not systematic and are difficult or too complex to correct;

    f. finally, it may well happen that the number of CFD evaluations required to compute an accurate surrogate model exceeds the number of evaluations needed by a smart direct search process.

3. Surrogate models can prove interesting for cases in which the CPU time of a full-order evaluation is very high and the space of variables is not too large. However, direct search can be more adequate than surrogate models for cases such as those addressed by this Thesis (which are very common in industry and in research). This is because the full-order evaluation, although complex and requiring CFD, is not extremely time-consuming, and because the space of variables can be large (more than 10-15 variables).

4. Taking all these limitations into account, it is considered that the work presented in this Thesis contributes to the State of the Art because it is an improvement over the use of surrogate-based models for aerodynamic optimization of complex components (wings, high-speed train noses, automotive designs, etc.). This is especially the case in terms of accuracy, flexibility, applicability to big geometry changes, and changes of flow regime. The errors of surrogate-based evaluation can be non-systematic and can reach average values of 10-20% for real industrial cases, such as those analyzed in this Thesis (refer to Chapter 7 for more details). In the specific case of a change of flow regime within the search region, the errors can be much higher.

5. Direct search is an alternative to surrogate models to tackle optimization problems that require time-consuming evaluations. Instead of approximating the evaluation model, direct search use algorithms with embedded intelligence to carry out an intelligent and efficient search, minimizing the number of evaluations. In order to justify the development of the novel algorithm, MOST-HDS, it is compared to one of the most popular Multi-Objective Evolutionary Algorithms (MOEAs), the NSGA-II, for the shape optimization of an HRSG inlet duct. Although the results obtained with NSGA-II are good, clear improvements are shown with MOST-HDS. This is an important contribution of this Thesis, since NSGA-II is already a very good and well-known optimization algorithm. Using MOST-HDS, the candidate solutions of the optimization phases are more concentrated on the area of interest in the space of attributes, and there is a higher rate of improvement from phase to phase. Therefore, the optimized Pareto front after an equivalent number of evaluations (i.e. equivalent computing time, because the evaluations are the most time consuming part of the process) is better. However, much fine-tuning and upgrading work needs carrying out on the MOST-HDS algorithm, since there is still substantial room for improvement.

GENERAL APPLICABILITY OF MOST-HDS: REAL INDUSTRIAL CASES

6. MOST-HDS has been applied successfully to two real industrial case studies of shape design optimization: the inlet duct of HRSGs for combined cycle power plants, and closed wind tunnels. It has been shown that the optimization results yield important improvements over current existing designs. This is a key contribution of this Thesis, not only because performance results are improved for the optimum designs obtained, but also because some of these designs are very unconventional. Consequently, this Thesis has allowed to develop a new set of design guidelines, very specifically in the case of the optimization of the industrial boiler (HRSG) inlet duct. In this particular case, for instance, it is shown in this Thesis that the double angle design of HRSG inlet ducts, which is the current design trend, is not always better than the single angle design, which was the traditional guideline followed.

7. The results obtained for the two HRSG families presented show that there are optimum trade-off designs with simultaneous reductions in pressure drop of up to 20-25%, in lateral surface of up to 38%, and in length of up 16%, while having comparable velocity uniformities to the existing designs. Some of these results are obtained with noticeably unconventional designs. The length reduction obtained results in average savings in costs of around 95k€ per inlet duct.

8. Regarding the full wind tunnel case, the pressure drop can be improved by 30-40% and the cost can be reduced by 15-20% (with respect to designs with already a good performance). Again, some of these results are obtained by clearly disruptive or creative designs.

9. Given that MOST-HDS is capable of addressing problems involving big geometry changes, it can move efficiently throughout areas of the search region which produce unconventional or non-intuitive designs, which would probably never have been tried by the designer. This is a particularly important contribution of this Thesis, since there are very few references in the State of the Art addressing big geometry changes in shape optimization problems and very important performance improvements can be achieved. Most researchers focus on small geometry changes or, even more, on fine-tuning of the geometry of interest.

10. The MOST-HDS methodology has been applied to wind tunnel design and HRSG inlet duct design because these are two areas in which trial and error is still widely used. The presented approach evaluates a number of candidate solutions that is 1 to 2 orders of magnitude higher than the number of solutions frequently evaluated in manual trial and error designs. The automated nature of the method yields project time reductions of 5-10 times for the examples considered, as compared to the design cycle times using more traditional or manual methods. This is also a contribution which is very much worth highlighting.

GENERAL APPLICABILITY OF MOST-HDS: MATHEMATICAL TEST FUNCTION OPTIMIZATION

11. MOST-HDS has also been applied to a very different problem: the WFG9 problem of the WFG test suite, a challenging test function used in literature for benchmark optimization among different algorithms. Once again, the popular NSGA-II algorithm is used as benchmark. For a smaller number of function evaluations, MOST-HDS shows good coverage of the whole span of the Pareto front, as well as a good convergence. Based only on the results of this test problem, the performance of MOST-HDS is, at least, as good as that of NSGA-II. More extensive work will be performed in further benchmark testing in the future. Consequently, this Thesis contributes to general purpose optimization and, more specifically, to mathematical test function optimization, because it can beat NSGA-II quite clearly for WFG9. However, more research is required to compare it to more algorithms and for more test problems.

GENERAL APPLICABILITY OF MOST-HDS: GENERAL-PURPOSE OPTIMIZATION

12. Therefore, based on the results obtained in this Thesis, it can be claimed that MOST-HDS has shown to perform well in many different problems, matching or improving currently existing techniques. The key aspects of MOST-HDS are a structured optimization architecture (exploiting the concepts of hierarchy of variables and optimization phases) and the hybrid direct-search approach.

13. The use of a structured optimization scheme is novel in the field of aerodynamic shape optimization, as far as we have found in the State of the Art reviewed. Hence this Thesis contributes to the research work in this field, since the results obtained show either clear improvements in performance or cost reductions.

14. In every iteration, MOST-HDS features the combination of non-gradient-based and gradient-based techniques (i.e. genetic, gradient and swarm search intelligence). Other hybrid direct-search algorithms found in literature use a different combination of techniques but, most importantly, they do not combine them all in every iteration, using each of them for different stages of the optimization process. Once again, the approach followed by MOST-HDS has proved successful, for the cases analyzed in this Thesis.

15. The concepts of space of variables and space of attributes (also referred to in literature as search space and fitness space) are clarified, so that it can be fully understood how the search process takes into account the position of each design point in both spaces. The fact that the optimization process within MOST-HDS takes into account the distance of candidate solutions in both spaces, and not only in the space of attributes, as is more frequent in literature, is also a key contribution of this tool. The results obtained (Chapters 6 and 7) show the potential and advantages of this approach.

16. Regarding optimization of fluid mechanics problems, the MOST-HDS model architecture contributes to the State of the Art because it carries out a full implementation of an automatic workflow simulation environment for optimization of CFD problems, based on direct search, for a wide range of fields. A key challenging feature of the architecture, which justifies its novelty, is that the optimizer tool is external to the CFD solver and takes full control of the optimization process. An optimization architecture as general and flexible as the MOST-HDS model has not been found in literature. As has been mentioned above, this architecture has shown important project time reductions and an increase of the number of design candidates evaluated.

17. The model developed is thus a fully automatic, robust and highly flexible optimization tool which, once set-up by an expert engineer, can be used by any non-expert person.

18. In order to justify the novelty of the research work carried out for this Thesis, and to serve as a basis for reference for future authors working in this field, a review of the State of the Art has been presented, for the various areas applicable to this work. This is considered an additional contribution, as it offers an exhaustive survey of the research in this area, and such a survey has not been found elsewhere.

19. To conclude, it is considered that the whole set of objectives described at the beginning of this Thesis have been met quite successfully. Moreover, it is believed that this Thesis has contributed to the State of the Art in many aspects. All of these contributions, which were explained in Chapter 1, have been analyzed in depth throughout the whole document and again, as a summary, in this Conclusions section.

8.2. Future research work beyond this Thesis

Apart from the more detailed future lines indicated throughout the document, the most relevant future research lines are outlined below:

1. A more extensive research on the effect of other initial evaluation sets (i.e. the points for Phase 0) on the type of problems we analyze will be carried out. In the case of this Thesis, a custom DoE scheme was used, based on the author’s experience, but Latin Hypercube Sampling (LHS) and other methods will also be tested in future work.

2. Further developments will be carried out concerning: tolerance threshold dynamic calculation (other schemes will be tested); effect of more than one search directions per point; increment factor dynamic calculation (other schemes will be tested); use of other concepts to assess success of a particular phase of the search; evaluation of the potential of mesh morphing for the MOST-HDS general model.

3. A more exhaustive comparison to other optimization algorithms for the types of industrial problems presented in this Thesis. Based on the results obtained throughout this research work, other optimization tools are suspected to have limitations when dealing with aerodynamic shape optimization and involving big geometry changes. In particular, some challenges to be checked for are the requirement of large initial set of sample points, the poor coverage of the whole Pareto front span, or slow convergence, requiring more function evaluations than MOST-HDS.

4. The results and observations made concerning surrogate models are especially focused on response surfaces. The conclusions on their limitations are applicable to most of the other types of surrogate techniques (ROMs or hierarchical models), although a more extensive work for each surrogate model would be necessary to prove it completely.

5. MOST-HDS will be applied to other areas of aerodynamic shape design optimization. Potential areas considered for application are those described in Paniagua (2014) (high-speed train nose design) or Zamorano et al. (2015) (vortex generator design).

6. Finally, as regards to the results of the benchmark test of MOST-HDS when applied to a commonly-used mathematic problem, it can be concluded that this algorithm shows a promising performance in the field of general purpose optimization. However, a more extensive study needs to be performed as part of the future work beyond this Thesis.

9

Chapter 9 - References

No one can read with profit that which he does not learn to read with pleasure.

Thomas Hardy.

References

1. Abbaspour, M., and M.N. Shojaee. 2009. "Innovative Approach to Design a New National Low Speed Wind Tunnel", International Journal of Environmental Science and Technology 6 (1): 23–34.

2. Allen, C.B., D.J. Poole, and T. Rendall. 2016. "Efficient Modal Design Variables Applied to Aerodynamic Optimization of a Modern Transport Wing". Paper presented at the 17^{th} AIAA/ISSMO Multidisciplinary Analysis and Optimization Conference.

3. Ameri, M., and F.J. Dorcheh. 2013. "The CFD Modelling of Heat Recovery Steam Generator Inlet Duct". International Journal of Energy Engineering 3 (3): 74-79. doi: 10.5963/IJEE0303003.

4. Ardekani, M. A. 2013. "Optimization of a vertical wind tunnel nozzle length using numerical and experimental methods". Journal of Solid and Fluid Mechanics 3 (3): 137-147 (in Persian).

5. Aslam Bhutta, M.M., N. Hayat, M.H. Bashir, A.R. Khan, K.N. Ahmad, and S. Khan. 2012. "CFD Applications in Various Heat Exchangers Design: A Review". Applied Thermal Engineering 32: 1-12.

6. Arreckx, S., A. Lambe, J.R.R.A. Martins, and D. Orban. 2016. "A matrix-free augmented lagrangian algorithm with application to large-scale structural design optimization". Optimization and Engineering 17 (2): 359-384.

7. Auger, A., J. Bader, D. Brokhoff, and E. Ziztler. 2012. "Hypervolume-based multiobjective optimization: Theoretical foundations and practical implications". Theoretical Computer Science 425: 75-103. http://dx.doi.org/10.1016/j.tcs.2011.03.012.

8.Azevedo, C.R.B., and A.F.R. Araújo. 2011. “Correlation between diversity and hypervolume in evolutionary multiobjective optimization”. Paper presented at the IEEE Congress on Evolutionary Computation (CEC). doi: 10.1109/CEC.2011.5949962.

9. Babu, A. 2014. “Power Optimisation Techniques at Circuit and Device Level in Digital CMOS VLSI – A Review”. International Journal of Engineering Research and Technology 3 (11): 375-379.

10. Bader, J. 2009. “Hypervolume-Based Search for Multiobjective Optimization: Theory and Methods”. PhD diss. ETH Zurich.

11. Bader, J., and E. Zitzler. 2011. “HypE: An algorithm for fast hypervolume-based many-objective optimization”. Journal of Evolutionary Computation 19 (1): 45-76. doi: 10.1162/EVCO_a_00009.

12. Bell, J.H., and R.D. Mehta. 1988. “Boundary–layer Predictions for Small Low–speed Contractions”, AIAA Journal (ISSN 0001–1452) 27 (3): 372–374.

13. Borger, G.G. 1976. “The Optimisation of Wind Tunnel Contractions for the Subsonic Range”. NASA Technical Translation / F–16899, NASA Washington.

14. Bradstreet, L., L. Barone, L. While, S. Huband, and P.F. Hingston. 2007. “Use of the WFG Toolkit and PISA for Comparison of MOEAs”. Proceedings of the IEEE Symposium on Computational Intelligence in Multi-Criteria Decision-Making (pp. 382-389), Honolulu, Hawaii, USA.

15. Bradstreet, L. 2011. “The hypervolume indicator for multi-objective optimization: calculation and use”. PhD diss. University of Western Australia.

16. Branke, J., S. Nguyen, C.W. Pickardt, and M. Zhang. 2016. “Automated Design of Production Scheduling Heuristics: A Review”. IEEE Transactions on Evolutionary Computation 20 (1): 110-124. doi: 10.1109/TEVC.2015.2429314.

17. Burke, E., M. Gendreau, M. Hyde, G. Kendall, G. Ochoa., E. Özcan, and R. Qu. 2013. “Hyper-heuristics: a survey of the state of the art”. Journal of the Operational Research Society 64 (12): 1695-1724. doi: 10.1057/jors.2013.71.

18. Calautit, J.K., H.N. Chaudhry, B.R. Hughes, and L.F. Sim. 2014. “A validated design methodology for a closed-loop subsonic wind tunnel”. Journal of Wind Engineering and Industrial Aerodynamics 125: 180-194. doi: http://dx.doi.org/10.1016/j.jweia.2013.12.010.

19. Chao, T., N. Li., G. Gong., and Z. Su. 2013. “A Parameterized Geometry Design Method for Inward Turning Inlet Compatible Waverider”. Chinese Journal of Aeronautics 26 (5): 1135–1146.

doi:10.1016/j.cja.2013.07.003

20. Courty, F., and A. Dervieux. 2006. “Multilevel Functional Preconditioning for Shape Optimisation”. International Journal of Computational Fluid Dynamics 20 (7): 481–490. doi: 10.1080 / 10618560600839415.

21. Daiber, J. 2006. “Fluid Dynamics of the HRSG Gas Side”. Power Magazine, (http://www.powermag.com/gas/534.html).

22. de Cuadra, F. 1990. “El problema general de la optimización de diseño por ordenador: aplicación de técnicas de ingeniería del conocimiento [The General Problem of Computer-based Design Optimisation: Application of Knowledge Engineering Techniques]”. PhD diss., Pontificia COMILLAS–ICAI University.

23. Deb, K., L. Thiele, M. Laumanns, and E. Zitzler. 2001. “Scalable Test Problems for Evolutionary Multi-Objective Optimization”. Kanpur, India: Kanpur Genetic Algorithms Lab. (KanGAL), Indian Inst. Technol. KanGAL Report 2 001 001.

24. Doolan, C.J., and R.C. Morgans. 2007. “Numerical Evaluation and Optimisation of Low Speed Wind Tunnel Contractions”. Paper presented at the 18th AIAA Computational Fluid Dynamics Conference, Miami, FL, July 25–28.

25. Downie, J.H., R. Jordinson, and F.H. Barnes. 1984. “On the Design of Three–dimensional Wind Tunnel Contractions”. Aeronautical Journal 88: 287–295.

26. Drela, M., and H. Youngren. 1995. A Users Guide to MISES 2.1. MIT Computational Aerospace Sciences Laboratory.

27. Du, X., and W. Chen. 2004. “Sequential Optimisation and Reliability Assessment Method for Efficient Probabilistic Design”. Journal of Mechanical Design 126: 225-233.

doi: 10.1115/1.1649968.

28. Eça, L., and M. Hoekstra. 2014. “A procedure for the estimation of the numerical uncertainty of CFD calculations based on grid refinement studies”. Journal of Computational Physics 262 (1): 104-130. doi: http://doi.org/10.1016/j.jcp.2014.01.006.

29. Eckert, W.T., K.W. Mort, and J. Jope. 1976. “Aerodynamic Design Guidelines and Computer Program for Estimation of Subsonic Wind Tunnel Performance”. NASA Technical Note / D–8243, NASA Washington.

30. Eckert, W.T., B.M. Wettlaufer, and K.W. Mort. 1982. “The Aerodynamic Performance of Several Flow Control Devices for Internal Flow Systems”. NASA Technical Paper 1972, AVRADCOM Technical Report 82–A–2.

31. Edelkamp, S., and S. Schroedl. 2011. Heuristic Search: Theory and Applications. Edited by Morgan Kaufmann.

Print Book ISBN: 9780123725127.

eBook ISBN: 9780080919737.

32. Eldred, M., S. Giunta, and S. Collis. 2004. “Second-order corrections for surrogate-based optimisation with model hierarchies”. Proceedings of the 10th AIAA/ISSMO Multidisciplinary Analysis and Optimisation Conference, AIAA, Albany, New York, August 30-September 4.

33. Eres, M.H., M. Bertoni, M. Kossmann, and J. Scanlan, 2014. “Mapping Customer Needs to Engineering Characteristics: An Aerospace Perspective for Conceptual Design”. Journal of Engineering Design 25 (1–3): 64-87. doi: 10.1080/09544828.2014.903387.

34. Eschenauer, H., J. Koski, and A. Osyczka. 2012. Multicriteria design optimization. Procedures and applications. Edited by Springer Verlag.

Print Book ISBN: 978-3-642-48699-9.

eBook ISBN: 978-3-642-48697-5.

35. Fabiano, E., A. Mishra, D.J. Mavriplis, and K. Mani. 2016. “Time-dependent Aero-acoustic Adjoint-based Shape Optimization of Helicopter Rotors in Forward Flight”. Paper presented at the 57th AIAA/ASCE/AHS/ASC Structures, Structural Dynamics, and Materials Conference, San Diego, California, USA, 4-8 January.

36. Forti, D., and G. Rozza. 2014. “Efficient Geometrical Parameterization Techniques of Interfaces for Reduced–order Modelling: Application to Fluid–structure Interaction Coupling Problems”. International Journal of Computational Fluid Dynamics 28 (3–4): 158–169. doi: 10.1080/10618562.2014.932352.

37. Franke, R. 1982. “Scattered data interpolation: tests of some methods”. Mathematics of Computation 38: 181-200. doi: https://doi.org/10.1090/S0025-5718-1982-0637296-4.

38. Friedman, D., and W.R. Westphal. 1952. “Experimental Investigation of a 90^{o} Cascade Diffusing Bend with an Area Ratio of 1.45:1 and with Several Inlet Boundary Layers”. NACA Technical Note 2668.

39. Fürnkranz, J., and M. Kubat. 2001. “Machine Learning in Games: A Survey” In Machines that Learn to Play Games, edited by Nova Scientific Publishers, Huntington, NY, Chapter 2: 11-59.

40. Galindo-García, I.F., A.K. Vázquez-Barragán, and M. Rossano-Román. 2012. “CFD Simulations of a Heat Recovery Steam Generator for the Aid of Power Plant Personnel”. Proceedings of the 20th International Conference on Nuclear Engineering and ASME 2012 Power Conference, Anaheim, California, USA, July 30-August 3.

41. Galindo-García, I.F., A.K. Vázquez-Barragán, and M. Rossano-Román. 2014. “CFD Simulations of Heat Recovery Steam Generators Including Tube Banks”. Proceedings of the ASME 2014 Power Conference POWER2014, Baltimore, Maryland, USA, July 28-31.

42. Giles, M.B., and M. Drela. 1987. “Two–Dimensional Transonic Aerodynamic Design Method”. AIAA Journal 25: 1199–1206.

43. Giles, M.B., and N.A. Pierce. 2000. “An Introduction to the Adjoint Approach to Design”. Flow, Turbulence and Combustion 65: 393-415.

44. González, M.A., A.I. Moreno, A.A. Jarzabek, J.M. Perales, Y. Wu, and S. Xiaoxiao. 2013. “Design Methodology for a Quick and Low–Cost Wind Tunnel” In Wind Tunnel Designs and Their Diverse Engineering Applications, edited by Dr. Noor Ahmed, ISBN: 978–953–51–1047–7. doi: 10.5772/54169.

45. Guliashki, V. 2008. “A Hybrid Direct Search – Quasi-Newton Method for the Inverse EIT Problem”. Bulgarian Academy of Sciences. Cybernetics and Information Technology 8 (2).

46. Hartigan, J.A. 1975. Clustering Algorithms. John Wiley & Sons, New York.

47. Hegazi, H.A., A.O. Nassef, and S. Metwalli. 2002. “Shape Optimization of NURBS Modeled 3D C-Frames Using Hybrid Genetic Algorithm”. Proceedings of the ASME 2002 International Design Engineering Technical Conferences and Computers and Information in Engineering Conference. doi: http://dx.doi.org/10.6036/NT7357.

48. Hegde, N., I. Han, T.W. Lee, and R.P. Roy. 2007. “Flow and Heat Transfer in Heat Recovery Steam Generators”. Journal of Energy Resources Technology 129: 232-242.

49. Held, S., B. Korte, D. Rautenbach, and J. Vygen. 2006. “Combinatorial Optimisation in VLSI design”. Paper presented at the 45th Session of the Séminaire de Mathématiques Supérieures, Montréal, June 19-30.

50. Hicken, J.E., and D.W. Zingg. 2010. “Aerodynamic Optimisation Algorithm with Integrated Geometry Parameterization and Mesh Movement”, AIAA Journal 48 (2): February.

51. Hoffenson, S., A. Dagman, and R. Söderberg. 2015. “Tolerance Optimisation Considering Economic and Environmental Sustainability”. Journal of Engineering Design 25 (10–12): 367–390.

doi: 10.1080/09544828.2014.994481.

52. Hoghooghi, H., M.N. Ahmadabadi, and M.D. Manshadi. 2016. “Optimization of a subsonic wind tunnel nozzle with low contraction ratio via ball-spine inverse design method”. Journal of Mechanical Science and Technology 30: 2059. doi:10.1007/s12206-016-0412-2.

53. Hooke, R., and T.A. Jeeves. 1961. ““Direct Search” solutions of numerical and statistical problems”. Journal of the ACM 8 (2): 212-229. doi: 10.1145/321062.321069.

54. Hsiao, C.T., Chahine, G., and Gumerov, N. 2001. “Application of a Hybrid Genetic/Powell Algorithm and a Boundary Element Method to Electrical Impedance Tomography”. Journal of Computational Physics 173: 433-454. doi:10.1006/jcph.2001.6866.

55. Huband, S., P. Hingston, L. Barone, and L. While. 2006. “A Review of Multi-objective Test Problems and a Scalable Test Problem Toolkit”. IEEE Transactions on Evolutionary Computation 10 (5): 477-506.

56. Idel’Cik, I.E. 1969. Memento des pertes de charge: Coefficients de pertes de charge singulières et de pertes de charge par frottement [Hydraulic Handbook on Pressure Losses: Shape and Friction Pressure Loss Coefficients]. Eyrolles Editeur, Paris.

57. Janardhanan, S. 2011. Model Order Reduction and Controller Design Techniques. Course notes. IIT Delhi, India.

58. Jeong, S., M. Murayama, and K. Yamamoto. 2005. “Efficient Optimisation Design Method Using Kriging Model”. Journal of Aircraft 42 (2): March-April.

59. Jing, L., G. Zhenghong, H. Jiangtao, and Z. Ke. 2013. “Aerodynamic design optimization of nacelle/pylon position on an aircraft”. Chinese Journal of Aeronautics 26 (4): 850-857.

60. Jordinson, R., and D.I.C. 1961. “Design of Wind Tunnel Contractions: A Method Based on the Use of the Schwarz-Cristoffel Transformation for Incompressible Inviscid Flow”. Aircraft Engineering and Aerospace Technology 33 (10): 294–297.

61. Katz, J. 2006. New Directions in Race Car Aerodynamics. Designing for Speed. Edited by Bentley Publishers.

ISBN-10: 0837601428.

ISBN-13: 978-0837601427.

62. Kelly, J.C., P. Maheut, J.F. Petiot, and P.Y. Papalambros. 2010. “Incorporating User Shape Preference in Engineering Design Optimisation”. Journal of Engineering Design 22 (9): 627–650.

doi: 10.1080/09544821003662601.

63. Kenway, G.K., A. Mishra, N.R. Secco, K. Duraisamy, and J. Martins. 2017. “An Efficient Parallel Overset Method for Aerodynamic Shape Optimization”. Paper presented at the 58th AIAA/ASCE/AHS/ASC Structures, Structural Dynamics, and Materials Conference, Grapevine, Texas, USA, January 9-13.

64. Koziel, S., and X-S. Yang. 2011. Computational Optimisation, Methods and Algorithms. Springer-Verlag Berlin Heidelberg. doi: 10.1007/978-3-642-20859-1.

65. Krajnovic, S. 2007. “Aerodynamic Optimisation of Vehicles Using Computational Fluid Dynamics and Response Surface Methodology”. Paper presented at the 21st International JUMV Automotive Conference SCIENCE & MOTOR VEHICLES (Paper NMV0724), Beograd.

66. Lee, B.E., S.B. Kwon, and C.S. Lee. 2002. “On the Effect of Swirl Flow of Gas Turbine Exhaust Gas in an Inlet Duct of Heat Recovery Steam Generator”. ASME Journal of Engineering for Gas Turbines and Power 124: 496-502.

67. Lee, C., D. Koo, and D.W. Zingg. 2017. “Comparison of B-Spline Surface and Free-Form Deformation Geometry Control for Aerodynamic Optimization”. AIAA Journal 55 (1): 228-240.

68. Li, H., and Q. Zhang. 2009. “Multiobjective Optimization Problems with Complicated Pareto Sets, MOEA/D and NSGA-II”. IEEE Trans. on Evolutionary Computation 12 (2): 284-302.

69. Liem, R.P., J.R.R.A. Martins, and G.K.W. Kenway. 2017. “Expected drag minimization for aerodynamic design optimization based on aircraft operational data”. Aerospace Science and Technology 63: 344-362.

70. Lindgren, B., J. Österlund, and A.V. Johansson. 1998. "Measurement and Calculation of Guide–vane Performance in Expanding Bends for Wind–Tunnels". Experiments in Fluids 24: 265–272.

71. Liu, X., and Z. Zhang. 2014. "A Hybrid Reliability Approach for Structure Optimisation Based on Probability and Ellipsoidal Convex Models". Journal of Engineering Design 25 (4–6): 238–258.

doi: 10.1080/09544828.2014.961060.

72. Lund, E., H. Møller, and L. Jakobsen. 2003. "Shape design optimization of stationary fluid-structure interaction problems with large displacements and turbulence". Structural and Multidisciplinary Optimization 25 (5): 383-392. doi:10.1007/s00158-003-0288-5.

73. Lyu, Z., G.K.W. Kenway, and J.R.R.A. Martins. 2014. "Aerodynamic Shape Optimization Investigations of the Common Research Model Wing Benchmark". AIAA Journal 53 (4): 968-985. doi: 10.2514/1.J053318.

74. Mani, K., and D.J. Mavripilis. 2009. "Adjoint-Based Sensitivity Formulation for Fully Coupled Unsteady Aeroelasticity Problems". AIAA Journal 47 (8): 1902-1915. doi: 10.2514/1.40582.

75. Marduel, X., C. Tribes, and J-Y. Trépanier. 2006. "Variable-fidelity Optimisation: Efficiency and Robustness". Optimisation and Engineering 7 (4): 479-500.

doi: 10.1007/s11081-006-0351-3.

76. Mavripilis, D.J. 2007. "A Discrete Adjoint-Based Approach for Optimization Problems on Three-Dimensional Unstructured Meshes". AIAA Journal 45 (4):740-750. doi: 10.2514/1.22743.

77. Mengistu, T., and W. Ghaly. 2008. "Aerodynamic Optimisation of Turbomachinery Blades Using Evolutionary Methods and ANN–based Surrogate Models". Optimisation and Engineering 9: 239-255.

78. Mikhail, M.N. 1979. "Optimum Design of Wind Tunnel Contractions". AIAA Journal 17 (5): article no. 78–819.

79. Minella, G., R. Ruiz, and M. Ciavotta. 2008. "A Review and Evaluation of Multiobjective Algorithms for the Flowshop Scheduling Problem". INFORMS Journal on Computing 20 (3): 451-471. doi: 10.1287/ijoc.1070.0258.

80. Morel, T. 1975. "Comprehensive Design of Axisymmetric Wind Tunnel Contractions" ASME Journal of Fluids Engineering 97: 225–233.

81. Morel, T. 1977. "Design of Two–dimensional Wind Tunnel Contractions". ASME Journal of Fluids Engineering 99: 371–378.

82. Nelder, J.A., and R. Mead. 1965. "A Simplex Method for Function Minimization". The Computer Journal 7 (4): 308-313. doi: https://doi.org/10.1093/comjnl/7.4.308.

83. Nielsen, E.J., E.M. Lee-Rausch, and W.T. Jones. 2010 (a). “Adjoint-Based Design of Rotors Using the Navier-Stokes Equations in a Non-inertial Reference Frame”. Journal of Aircraft 47 (2). doi: 10.2514/1.46044.

84. Nielsen, E.J., B. Diskin, and N. Yamleev. 2010 (b). “Discrete Adjoint-Based Design Optimization of Unsteady Turbulent Flows on Dynamic Unstructured Grids”. AIAA Journal 48 (6): 1195-1206. doi: 10.2514/1.J050035.

85. Nunez, M., V.C. Datta, A. Molina-Cristobal, M. Guenov, and A. Riaz. 2012. “Enabling Exploration in the Conceptual Design and Optimisation of Complex Systems”. Journal of Engineering Design 23 (10–11): 852–875.

doi: 10.1080/09544828.2012.706800.

86. Okumura, H., Y. Hikino, and M. Kawahara. 2013. “A Shape Optimisation Method of a Body Located in Adiabatic Flows”. International Journal of Computational Fluid Dynamics 27 (6–7): 297–306.

doi:10.1080/10618562.2013.828049.

87. Paniagua, J. 2014. “Aerodynamic Optimisation of the Nose Shape of a High–Speed Train”. PhD diss., Technical University of Madrid.

88. Pillay, N. 2016. “A review of hyper-heuristics for educational timetabling”. Annals of Operations Research 239 (1): 3-38. doi:10.1007/s10479-014-1688-1.

89. Poole, D.J., C.B. Allen, and T.C.S. Rendall. 2017. “High-fidelity aerodynamic shape optimization using efficient orthogonal modal design variables with a constrained global optimizer”. Computers and Fluids 143: 1-15.

90. Prada-Nogueira, I., F. de Cuadra, and A. Sánchez-Miralles. 2015. “Towards a general model for automatic and flexible design of closed wind tunnels”. Internal publication. Institute for Research in Technology IIT-15-154A.

http://www.iit.upcomillas.es/publicaciones/mostrar_publicacion_working_paper.php.en?id=259.

91. Prada-Nogueira, I., F. De Cuadra, and A. Sánchez-Miralles. 2017 (a). “General Model for Automatic Design Optimisation of Aerodynamic Components. Wind Tunnel Case Study”. DYNA. DYNA-ACELERADO. (0): 0. doi: http://dx.doi.org/10.6036/8144.

92. Prada-Nogueira, I., F.J. Álvarez, F. De Cuadra, and A. Sánchez-Miralles. 2017 (b). “Boiler Inlet Duct Shape Design Optimization for Combined Cycle Power Plants”. DYNA (approved for publication).

93. Roache, P.J. 1994. “Perspective: A Method for Uniform Reporting of Grid Refinement Studies”. Journal of Fluids Engineering 116 (3): 405-413. doi: 10.1115/1.2910291.

94. Robinson, T.D., MS. Eldred, K.E. Willcox, and R. Haimes. 2006. “Strategies for Multifidelity Optimisation with Variable Dimensional Hierarchical Models”. Paper presented at the 47th AIAA/ASME/ASCE/AHS/ASC Structures, Structural Dynamics, and Materials Conference, Newport, Rhode Island, May 1-4.

95. Rumpfkeil, M.P., and D.W. Zingg. 2010. “The optimal control of unsteady flows with a discrete adjoint method”. Optimization and Engineering 11 (1): 5-22. doi:10.1007/s11081-008-9035-5.

96. Schaumont, P., and I. Verbauwhede. 2004. “Interactive Cosimulation with Partial Evaluation”. Paper presented at the 7th Design, Automation on Test in Europe Conference (DATE’04), Paris, France.

97. Schweppe, F.C., and H.M. Merril. 1986. “Multiple Attribute Trade-Off Analysis”. EPRI RP 2537, April.

98. Shi, Y., and R. Eberhart. 1998. “A Modified Particle Swarm Optimizer”. IEEE: 69-73.

0-7803-4869-9198.

99. Shi, X., W. Chriswindarto, and D. Boyce. 2009. “Application of CFD Modelling in HRSG Evase Design”. Proceedings of the 2009 Power Conference, ASME, Albuquerque, New Mexico, USA, July 21-23.

100. Simpson, T. W., J. D. Peplinski, P. N. Koch, and J. K. Allen. 2001. “Metamodels for computer-based engineering design: Survey and recommendations”. Engineering with Computers 17: 129-150.

101. Su, W., S.S-M. Swei, and G.G. Zhu. 2016. "Optimum Wing Shape of Highly Flexible Morphing Aircraft for Improved Flight Performance". Journal of Aircraft 53 (5): 1305-1316. doi: http://dx.doi.org/10.2514/1.C033490.

102. Sundén, B. 2007. “Computational Fluid Dynamics in Research and Design of Heat Exchangers”. Heat Transfer Engineering 28 (11): 898-910.

103. Takagi, H. 2001. “Interactive Evolutionary Computation: Fusion of the Capacities of EC Optimisation and Human Evaluation”. Proceedings of the IEEE 89 (9): 1275–1296.

104. Vieira, E.D.R., and J.B. Aparecido. 1999. “Design and Construction of Small Axisymmetric Contractions”. In 5ª Reunión do Grupo De Trabajo Sobre Hidromecánica publication, 103–116.

105. Volkwein, S. 2013. Proper Orthogonal Decomposition: Theory and Reduced Order Modelling. Lecture notes. University of Konstanz.

106. Walton, S., O. Hassan, and K. Morgan. 2013. “Reduced order modelling for unsteady fluid flow using proper orthogonal decomposition and radial basis functions”. Applied Mathematical Modelling 30 (20-21): 8930-8945. doi: http://dx.doi.org/10.1016/j.apm.2013.04.025.

107. Washabaugh, K., D. Amsallem, M. Zahr, and C. Farhat. 2012. “Nonlinear Model Reduction for CFD Problems Using Local Reduced Order Bases”. Paper presented at the 42nd AIAA Fluid Dynamics Conference and Exhibit, New Orleans, LA, June 25-28.

108. Wild, J. 2008. “Multi–objective Constrained Optimisation in Aerodynamic Design of High–lift Systems”. International Journal of Computational Fluid Dynamics 22 (3): 153–168.

doi: 10.1080/10618560701868420.

109. Xiao, M., L. Gao, X. Shao, H. Qiu, P. Jiang. 2012. “A Generalised Collaborative Optimisation Method and its Combination with Kriging Metamodels for Engineering Design”. Journal of Engineering Design 23 (5): 379–399.

doi: 10.1080/09544828.2011.595706.

110. Yoshimura, M., M. Hasuike, T. Miyashita, and H. Yamakawa. 2013.“Evaluation of Industrial Machine Design Improvement Ideas Using Characteristic-based Hierarchical Optimisation Strategies”. Journal of Engineering Design 24 (11): 794–813.

doi: 10.1080/09544828.2013.862226.

111. Youngren, H., and M. Drela. 1991. “Viscous/Inviscid Method for Preliminary Design of Transonic Cascades”. Paper presented at the 27th AIAA, SAE, ASME, and ASEE Joint Propulsion Conference.

112. Zamorano-Rey, G., B. Garro, U. Fernández-Gámiz, and E. Zulueta. 2015. “A Computationl Study of the Variation of the Incidence Angle in a Vortex Generator”. DYNA New Technologies 2 (1): 1-13. doi: http://dx.doi.org/10.6036/NT7357.

113. Zhao, L. 2007. “Performance of multi-objective algorithms on varying test problem features using the WFG toolkit”. Thesis. The University of Western Australia.

114. Zhou, Q., X. Shao, P. Jiang, H. Zhou, L. Cao, and L. Zhang. 2015. “A Deterministic Robust Optimisation Method Under Interval Uncertainty Based on the Reverse Model”. Journal of Engineering Design 26 (10-12): 416-444. doi: 10.1080/09544828.2015.1072763.

115. Zitzler, E., K. Deb, and L. Thiele. 2000. “Comparison of multiobjective evolutionary algorithms: Empirical results”. Evolutionary Computation 8 (2): 173-195.

Web references mentioned throughout the Thesis (last verified on February 2017):

1. www.moeaframework.org: MOEA framework. Useful resource on MOEAs.

2. https://ls11-www.cs.uni-dortmund.de/rudolph/hypervolume/start: Very interesting summary of hyper-volume-related literature.

3. https://hpi.de/en/friedrich/research/hypervolume.html: Additional hyper-volume literature.

4. http://www.aero.upm.es/LSLCWT: Access to a full wind tunnel Excel design spreadsheet developed by González et al. (2013).

A

Appendix A - Illustration of the MOST-HDS process

Illustration of the MOST-HDS process for the most complex case presented, the wind tunnel shape optimization.

1. The MOST-HDS user interface has tree simple steps, as shown in Figure 0–1

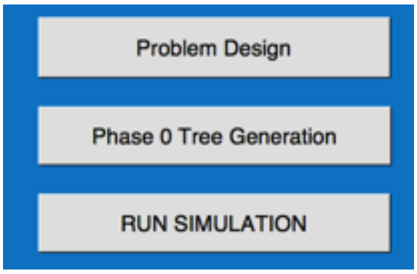

Figure 0–1 - MOST-HDS user interface.

2. Problem design: This is done via a .txt file created by the user. This file indicates the number of hierarchies of variables, the name and type of each variable, and their range of values. It also specifies number, name and type of attributes.

```
ProblemDesign
HIERARCHIES, 2
VARS_H1, 6
V1_H1, wT, 2, 1, 40
V2_H1, lTS, 2, 1, 5
V3_H1, wTS, 2, 1, 4.57
V4_H1, rP, 1, 90, 180
V5_H1, dF, 1, 6.8, 7.6
V6_H1, gTS, 2, 2, 1, 2
VARS_H2, 2
V1_H2, p1, 2, 2, 1, 2
V2_H2, s1, 2, 2, 1, 2
ATTRIBUTES, 2
A1, cost, 1
A2, delta, 1
```

Figure 0–2 - Problem design input file.

3. The Excel tool created to implement MOST-HDS can generate a very wide range of closed wind tunnel configurations, based on the value of the input variables. The geometry is generated via Bézier cubic curves and their corresponding control points. The program carries out a geometry absurdity check to validate if the geometry has negative volumes, intersections, etc. The example of Figure 0–3 illustrates a case with absurd geometry.

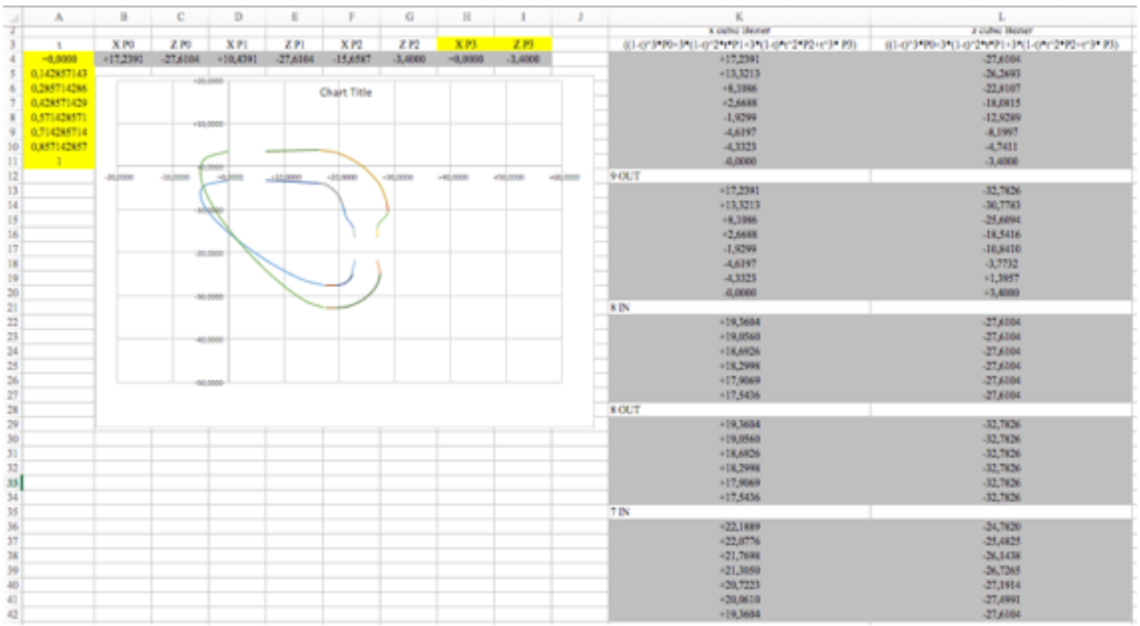

Figure 0–3 - Geometry parameterization.

4. Phase 0 tree generation: the design points for the design exploration of Phase 0 are generated. Note that the variables defined by the user (Figure 0–2) are transformed to variables used by ANSYS to generate the tunnel geometry (Figure 0–4). In ANSYS there are many more variables, hence not all are independent, and they are far less intuitive than those defined by the user, which are the variables used for the optimization process itself.

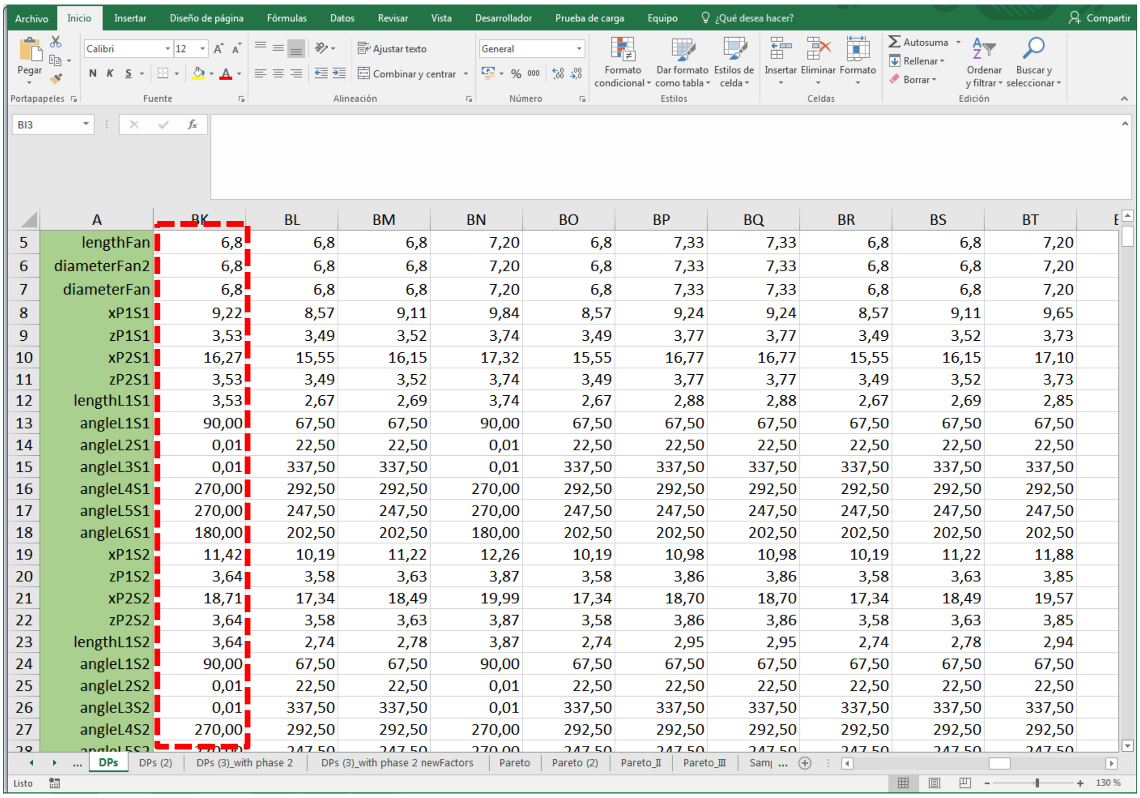

	A	BK	BL	BM	BN	BO	BP	BQ	BR	BS	BT
5	lengthFan	6,8	6,8	6,8	7,20	6,8	7,33	7,33	6,8	6,8	7,20
6	diameterFan2	6,8	6,8	6,8	7,20	6,8	7,33	7,33	6,8	6,8	7,20
7	diameterFan	6,8	6,8	6,8	7,20	6,8	7,33	7,33	6,8	6,8	7,20
8	xP1S1	9,22	8,57	9,11	9,84	8,57	9,24	9,24	8,57	9,11	9,65
9	zP1S1	3,53	3,49	3,52	3,74	3,49	3,77	3,77	3,49	3,52	3,73
10	xP2S1	16,27	15,55	16,15	17,32	15,55	16,77	16,77	15,55	16,15	17,10
11	zP2S1	3,53	3,49	3,52	3,74	3,49	3,77	3,77	3,49	3,52	3,73
12	lengthL1S1	3,53	2,67	2,69	3,74	2,67	2,88	2,88	2,67	2,69	2,85
13	angleL1S1	90,00	67,50	67,50	90,00	67,50	67,50	67,50	67,50	67,50	67,50
14	angleL2S1	0,01	22,50	22,50	0,01	22,50	22,50	22,50	22,50	22,50	22,50
15	angleL3S1	0,01	337,50	337,50	0,01	337,50	337,50	337,50	337,50	337,50	337,50
16	angleL4S1	270,00	292,50	292,50	270,00	292,50	292,50	292,50	292,50	292,50	292,50
17	angleL5S1	270,00	247,50	247,50	270,00	247,50	247,50	247,50	247,50	247,50	247,50
18	angleL6S1	180,00	202,50	202,50	180,00	202,50	202,50	202,50	202,50	202,50	202,50
19	xP1S2	11,42	10,19	11,22	12,26	10,19	10,98	10,98	10,19	11,22	11,88
20	zP1S2	3,64	3,58	3,63	3,87	3,58	3,86	3,86	3,58	3,63	3,85
21	xP2S2	18,71	17,34	18,49	19,99	17,34	18,70	18,70	17,34	18,49	19,57
22	zP2S2	3,64	3,58	3,63	3,87	3,58	3,86	3,86	3,58	3,63	3,85
23	lengthL1S2	3,64	2,74	2,78	3,87	2,74	2,95	2,95	2,74	2,78	2,94
24	angleL1S2	90,00	67,50	67,50	90,00	67,50	67,50	67,50	67,50	67,50	67,50
25	angleL2S2	0,01	22,50	22,50	0,01	22,50	22,50	22,50	22,50	22,50	22,50
26	angleL3S2	0,01	337,50	337,50	0,01	337,50	337,50	337,50	337,50	337,50	337,50
27	angleL4S2	270,00	292,50	292,50	270,00	292,50	292,50	292,50	292,50	292,50	292,50

Figure 0–4 - Generation of Excel design point table. In particular, generation of design points for Phase 0 (design exploration phase) and variable transformation to ANSYS variables.

5. ANSYS workflow for wind tunnel shape design optimization.

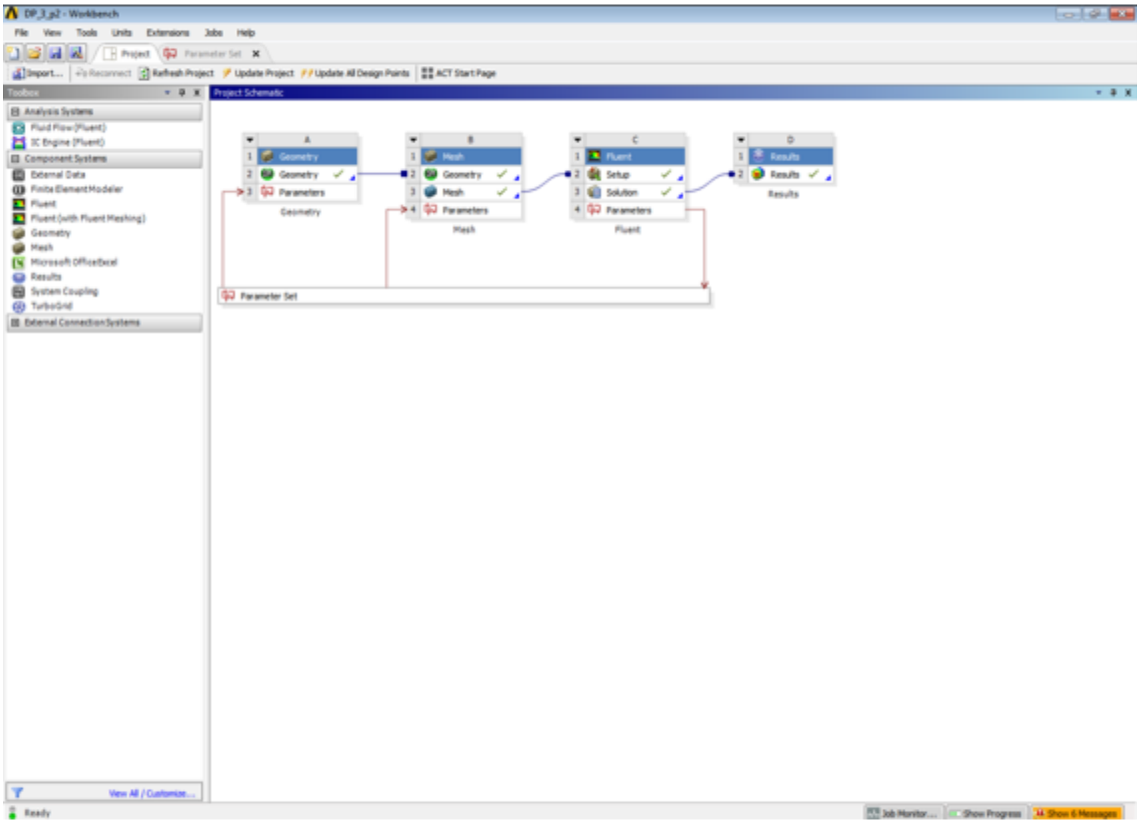

Figure 0–5 - ANSYS workflow architecture.

6. ANSYS parameter set: ANSYS receives the variable values for each design point from the Excel design point table.

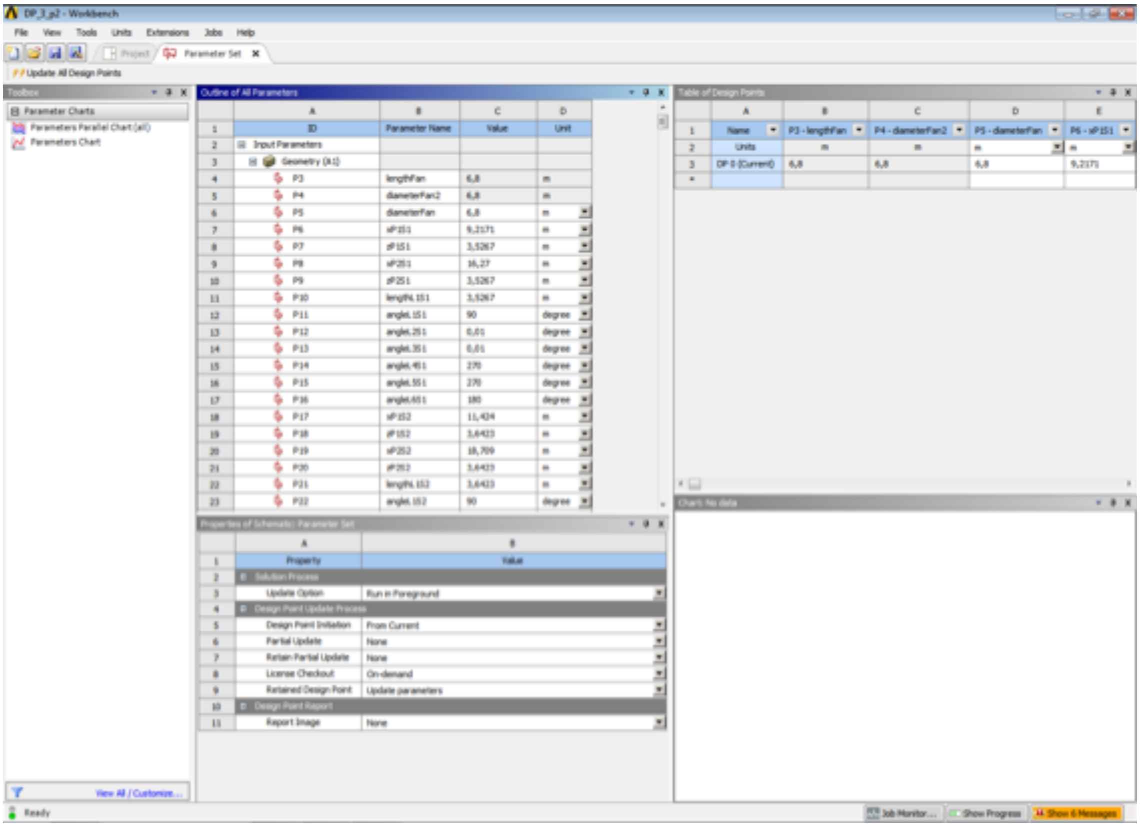

Figure 0–6 - ANSYS parameter set with values received from Excel for all the ANSYS variables.

7. The automatic workflow set up in ANSYS, based on the values of the variables of each design point, creates the geometry (Figure 0–7), generates the mesh (based on the meshing configuration) (Figure 0–8), carries out the CFD simulation for each design point (Figure 0–11) and finally feeds the values obtained for each attribute automatically back to the Excel design point table (Figure 0–12). A closer view of the mesh is presented in Figure 0–9 and information on the mesh quality (skewness) is given in Figure 0–10 (refer to the detailed justification in Appendix B regarding the occasional use of meshes with apparently unacceptable skewness values).

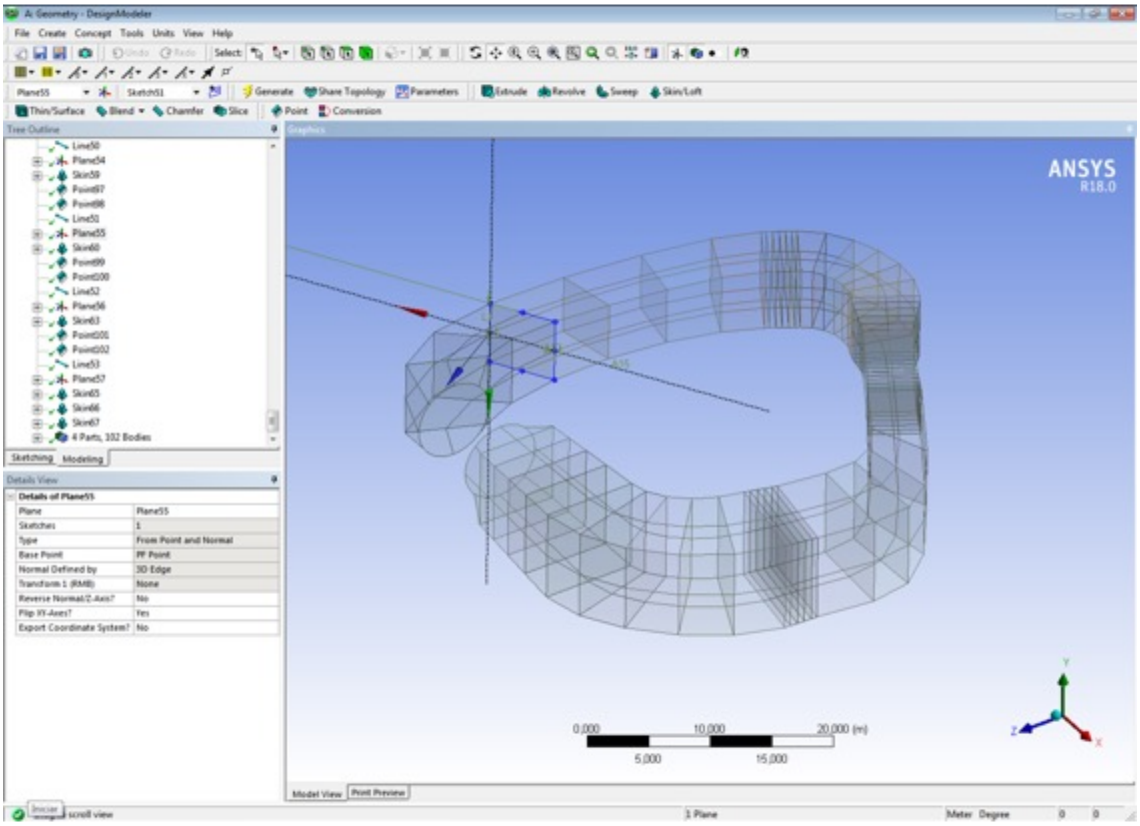

Figure 0–7 - ANSYS geometry generation.

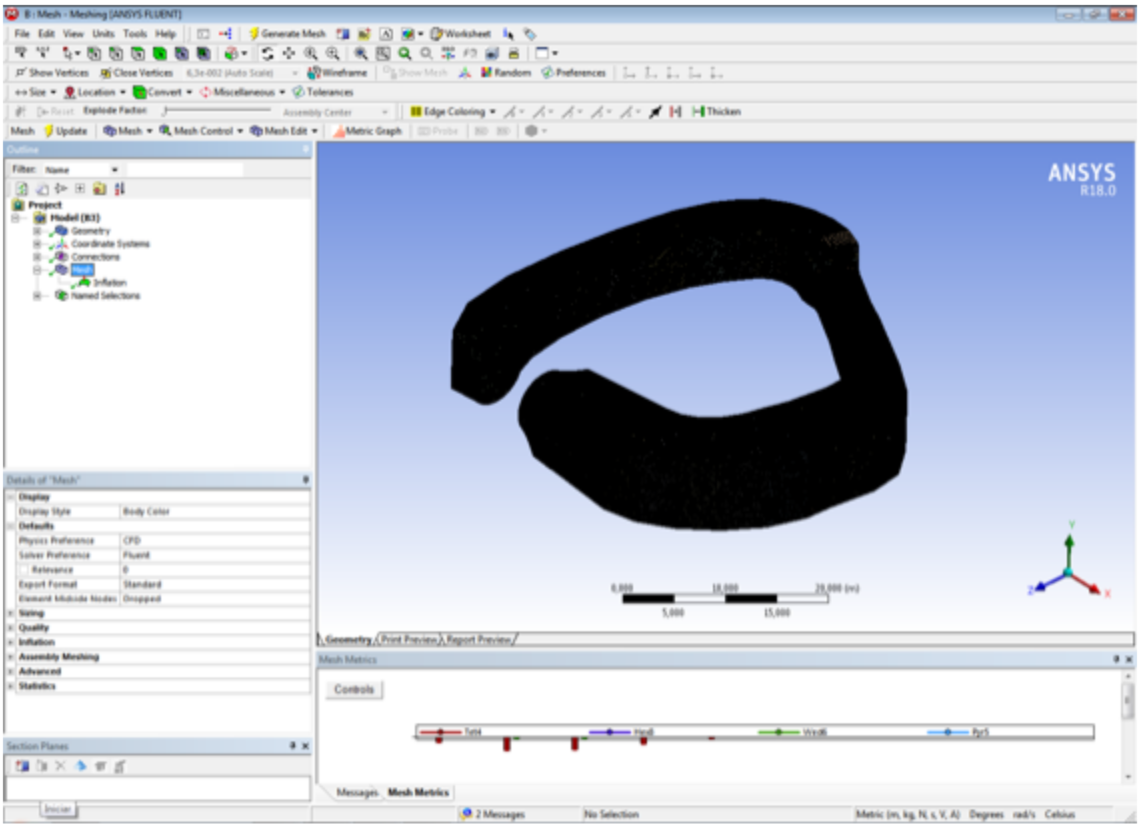

Figure 0–8 - ANSYS mesh generation.

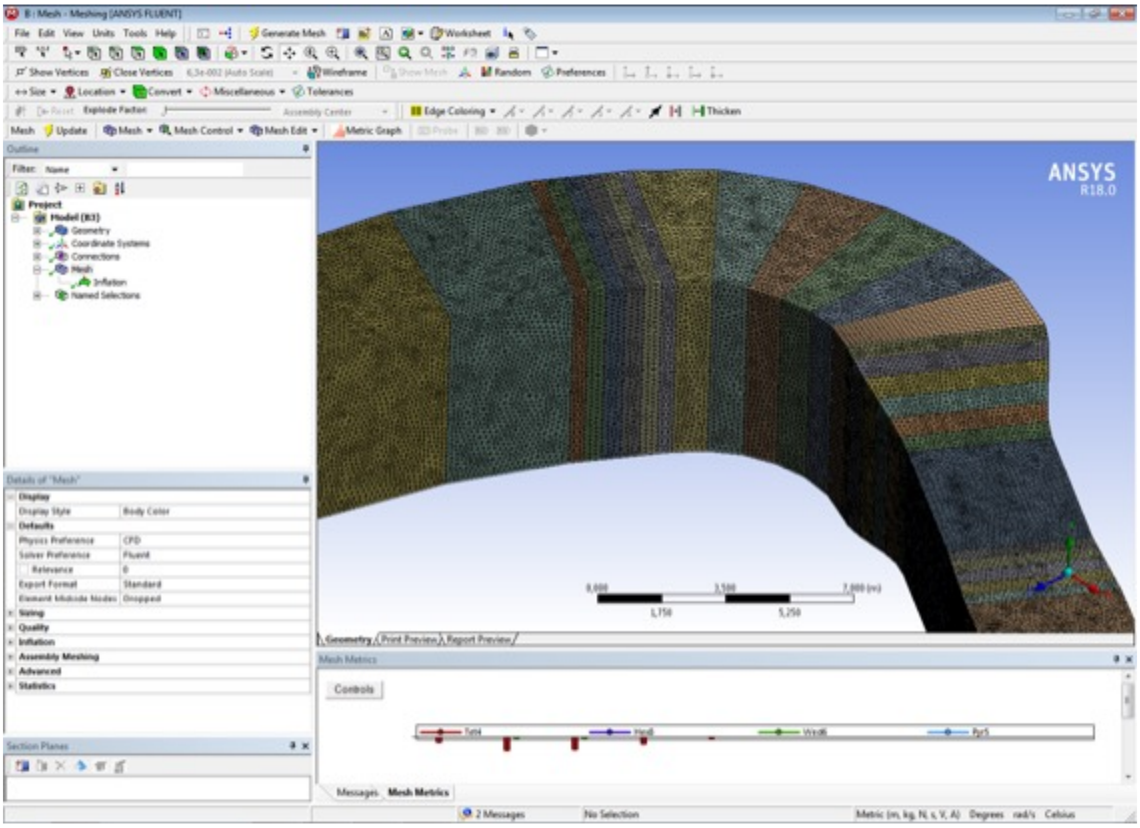

Figure 0–9 - ANSYS mesh generation (detail).

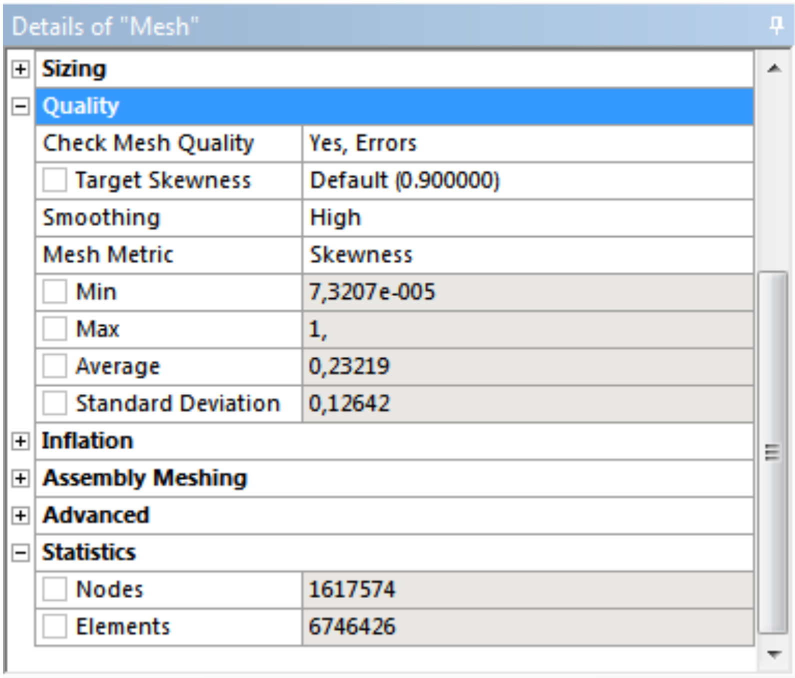

Figure 0–10 - Example mesh quality for most complex design points.

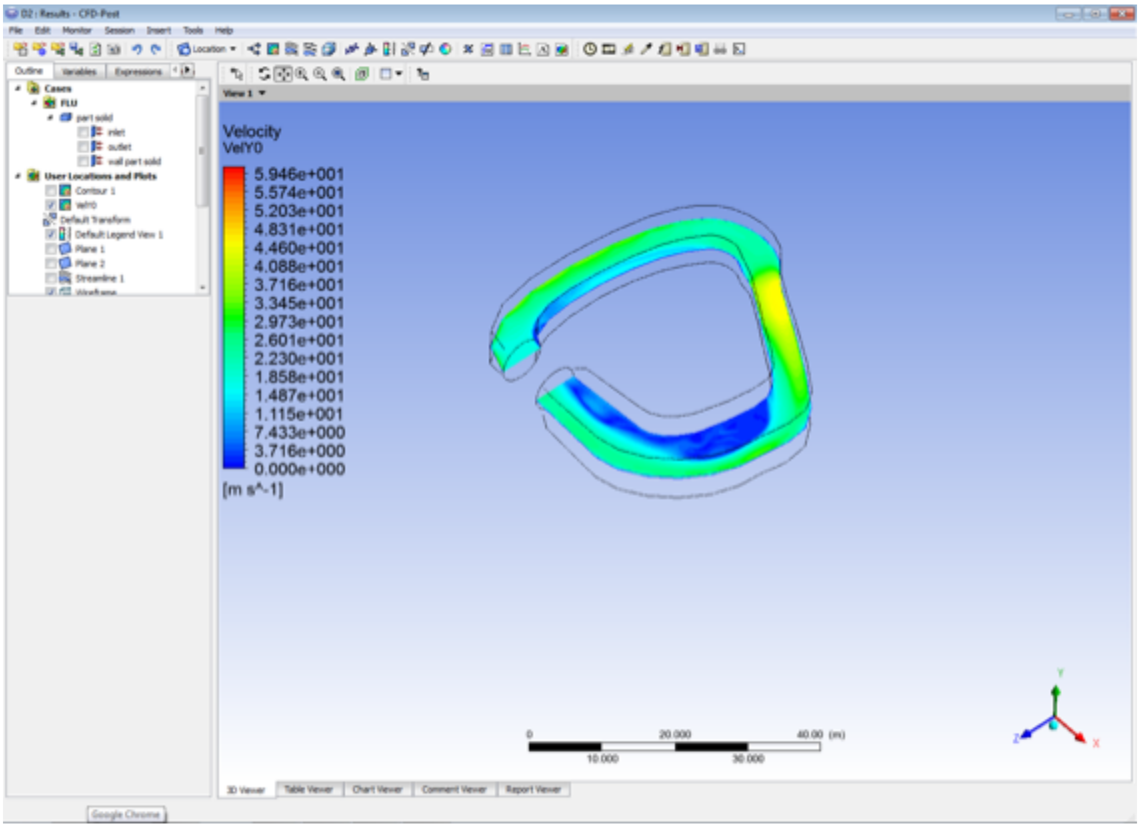

Figure 0–11 - ANSYS FLUENT CFD simulation results.

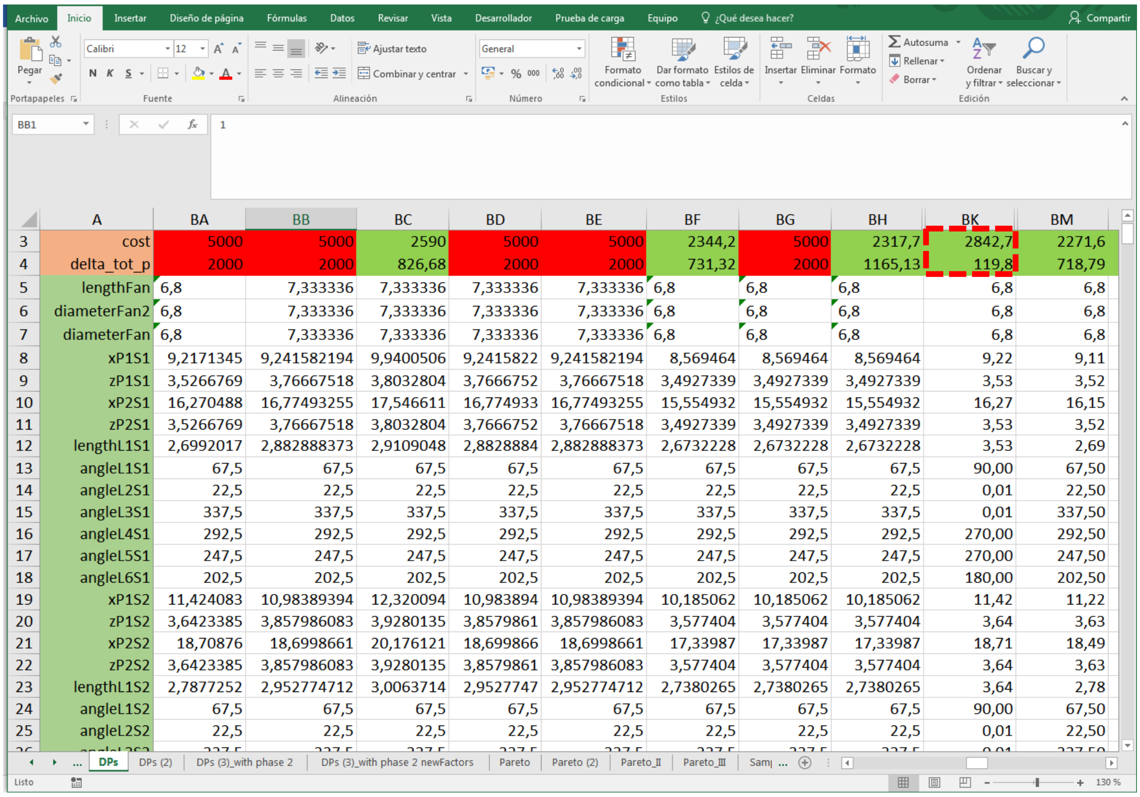

	A	BA	BB	BC	BD	BE	BF	BG	BH	BK	BM
3	cost	5000	5000	2590	5000	5000	2344,2	5000	2317,7	2842,7	2271,6
4	delta_tot_p	2000	2000	826,68	2000	2000	731,32	2000	1165,13	119,8	718,79
5	lengthFan	6,8	7,333336	7,333336	7,333336	7,333336	6,8	6,8	6,8	6,8	6,8
6	diameterFan2	6,8	7,333336	7,333336	7,333336	7,333336	6,8	6,8	6,8	6,8	6,8
7	diameterFan	6,8	7,333336	7,333336	7,333336	7,333336	6,8	6,8	6,8	6,8	6,8
8	xP1S1	9,2171345	9,241582194	9,9400506	9,2415822	9,241582194	8,569464	8,569464	8,569464	9,22	9,11
9	zP1S1	3,5266769	3,76667518	3,8032804	3,7666752	3,76667518	3,4927339	3,4927339	3,4927339	3,53	3,52
10	xP2S1	16,270488	16,77493255	17,546611	16,774933	16,77493255	15,554932	15,554932	15,554932	16,27	16,15
11	zP2S1	3,5266769	3,76667518	3,8032804	3,7666752	3,76667518	3,4927339	3,4927339	3,4927339	3,53	3,52
12	lengthL1S1	2,6992017	2,882888373	2,9109048	2,8828884	2,882888373	2,6732228	2,6732228	2,6732228	3,53	2,69
13	angleL1S1	67,5	67,5	67,5	67,5	67,5	67,5	67,5	67,5	90,00	67,50
14	angleL2S1	22,5	22,5	22,5	22,5	22,5	22,5	22,5	22,5	0,01	22,50
15	angleL3S1	337,5	337,5	337,5	337,5	337,5	337,5	337,5	337,5	0,01	337,50
16	angleL4S1	292,5	292,5	292,5	292,5	292,5	292,5	292,5	292,5	270,00	292,50
17	angleL5S1	247,5	247,5	247,5	247,5	247,5	247,5	247,5	247,5	270,00	247,50
18	angleL6S1	202,5	202,5	202,5	202,5	202,5	202,5	202,5	202,5	180,00	202,50
19	xP1S2	11,424083	10,98389394	12,320094	10,983894	10,98389394	10,185062	10,185062	10,185062	11,42	11,22
20	zP1S2	3,6423385	3,857986083	3,9280135	3,8579861	3,857986083	3,577404	3,577404	3,577404	3,64	3,63
21	xP2S2	18,70876	18,6998661	20,176121	18,699866	18,6998661	17,33987	17,33987	17,33987	18,71	18,49
22	zP2S2	3,6423385	3,857986083	3,9280135	3,8579861	3,857986083	3,577404	3,577404	3,577404	3,64	3,63
23	lengthL1S2	2,7877252	2,952774712	3,0063714	2,9527747	2,952774712	2,7380265	2,7380265	2,7380265	3,64	2,78
24	angleL1S2	67,5	67,5	67,5	67,5	67,5	67,5	67,5	67,5	90,00	67,50
25	angleL2S2	22,5	22,5	22,5	22,5	22,5	22,5	22,5	22,5	0,01	22,50

Figure 0–12 - Attribute values obtained in ANSYS are fed back to the Excel design point table.

8. Once the results of all the design points for a particular phase have been computed and fed back to ANSYS, the Pareto front is automatically calculated and drawn. The optimization intelligence coded into MOST-HDS will generate the design points to be simulated in the next phase of the optimization.

9. This process is repeated until the optimization stopping criteria are met and the final result for the optimized Pareto front is obtained (Figure 0–15).

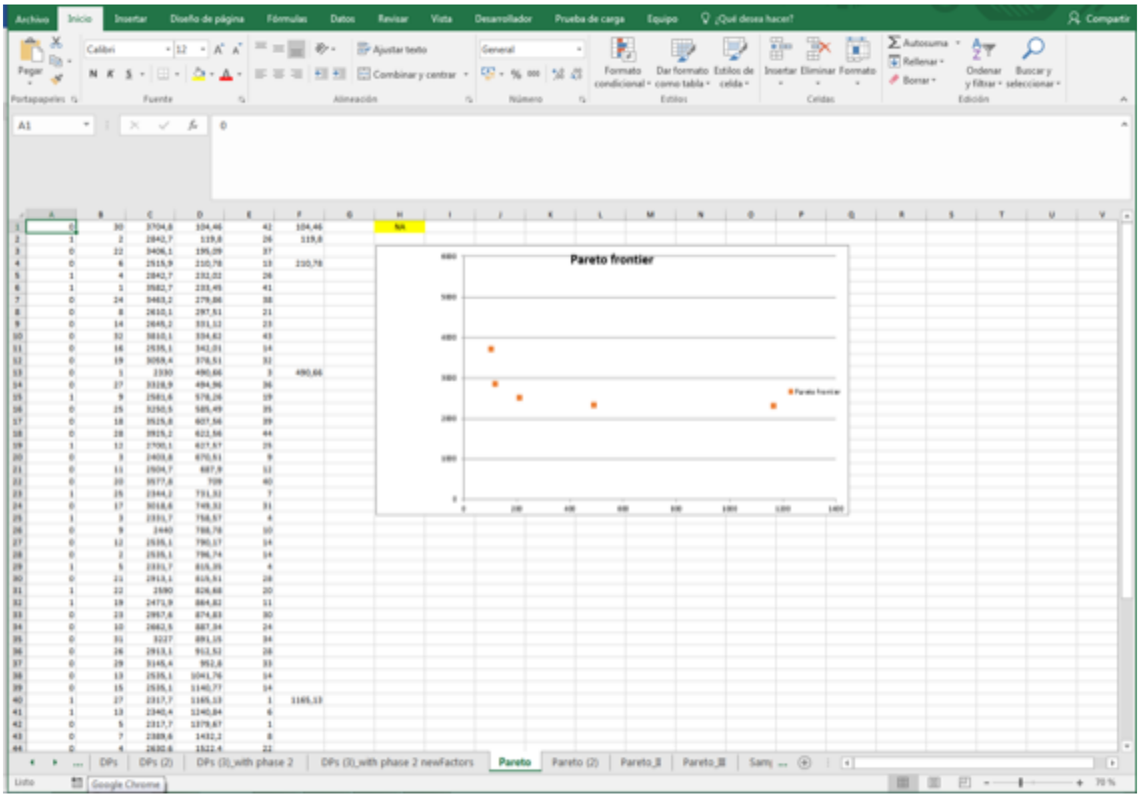

Figure 0–13 - Pareto front automatic calculation.

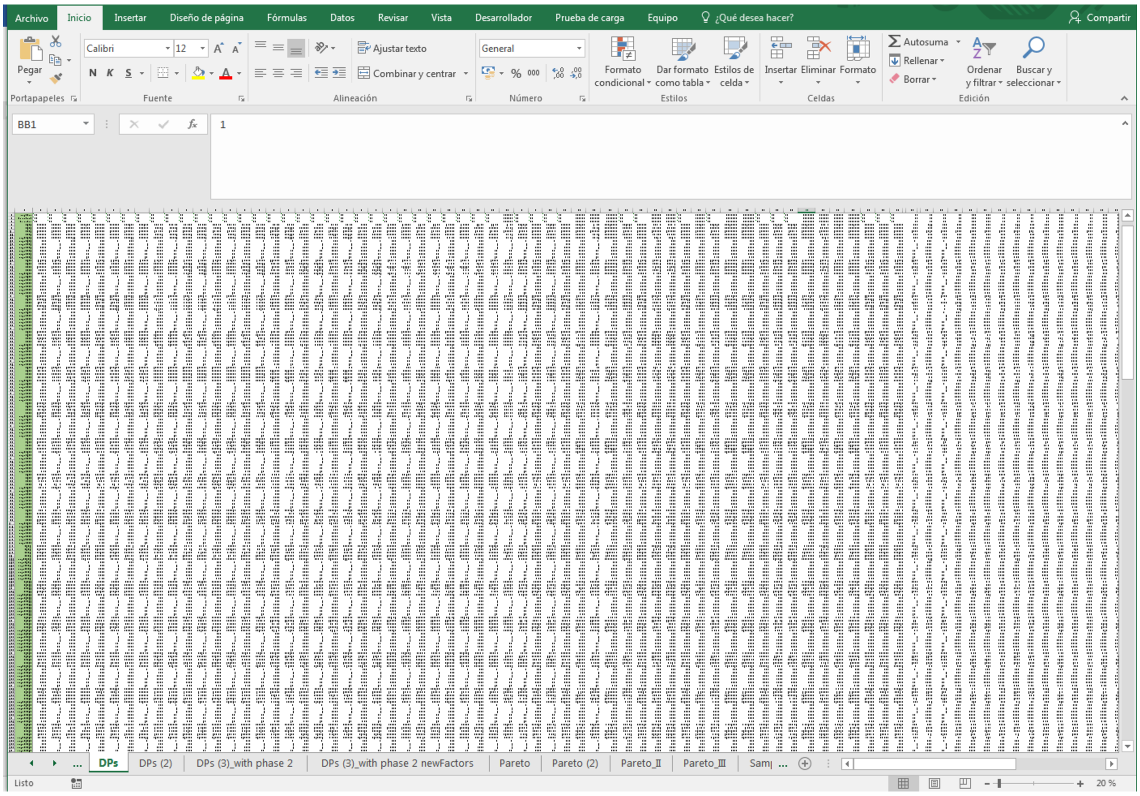

Figure 0–14 - MOST-HDS computation of the design points for the following optimization phase.

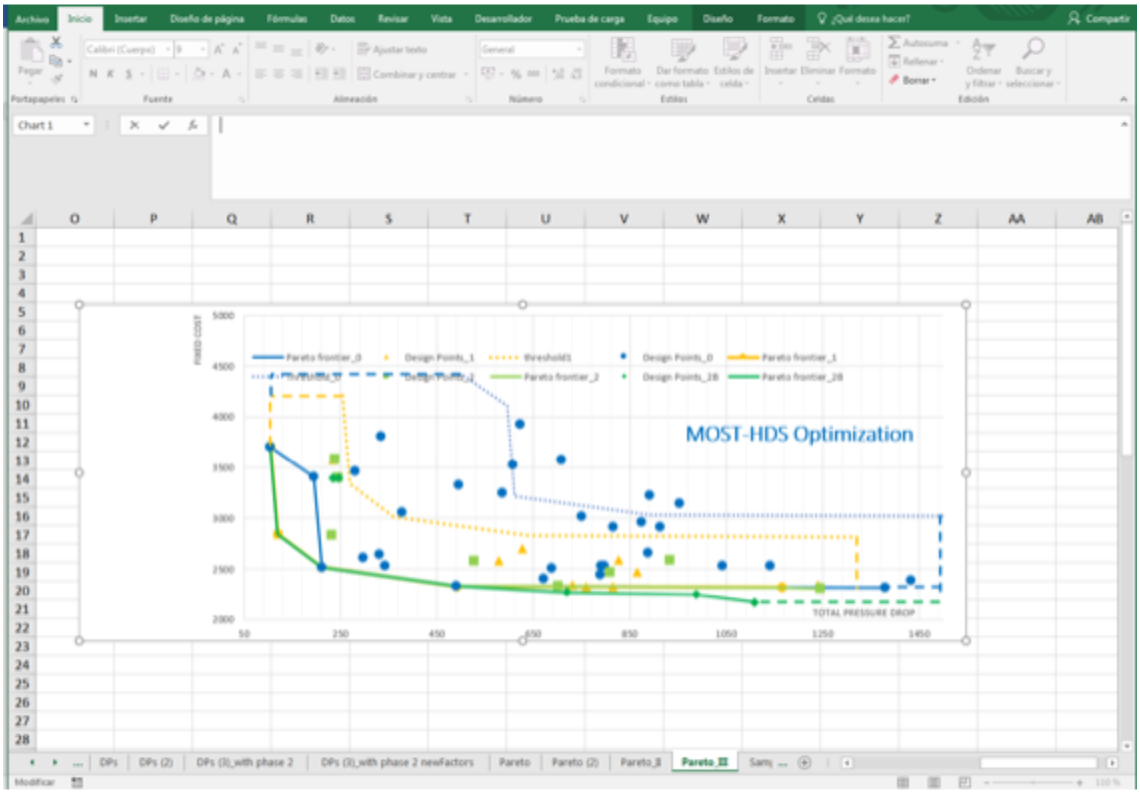

Figure 0–15 - MOST-HDS optimization final result.

B

Appendix B - Important notes on mesh sensitivity and mesh quality

Important remarks on the mesh sizes used, the sensitivity of the results to the mesh size and a general comment on mesh qualities.

B.1. Mesh sensitivity

For a direct search optimization, it is key to develop an efficient search process and to ensure the calculation time is minimized, so that the best minimum set of design candidates is evaluated in the shortest time possible. In order to achieve the objective is minimizing (or optimizing) the computation time for each design point, given that the CFD simulation was the most time consuming part of the process, an adequate range of mesh sizes had to be determined. A very coarse mesh would result in poor accuracy, whereas a very fine mesh would improve accuracy but would increase computation time. The determination of an adequate range of mesh sizes for the design configurations that were going to be considered did not aim to be mathematically strict, but instead it aimed at being reasonable from an engineering or industrial perspective. Therefore this Thesis has not followed the classical Grid Convergence Index methodology (GCI) of Roache (1994) or the more advanced methodologies of Eça and Hoekstra (2014). Instead, the sensitivity analysis carried out in this Thesis was limited to a comparison of the results obtained with increasing mesh sizes. The optimum mesh size range would be the minimum size above which the results obtained did not vary more than a reasonable threshold for the relative error (this was limited to 3-5%).

This study was carried out for the wind tunnel case, since the mesh for the industrial boilers was not as challenging and even very refined meshes computed fast.

The results of this non-exhaustive mesh sensitivity analysis are illustrated in Figure 0–1. The conclusion was that meshes in the range of 2-3 million elements marked the threshold above which the results showed no considerable variation. The meshing set-up was done so that mesh sizes for most wind tunnels would be kept within this range. This does not mean that certain design point geometries have had finer meshes (but not coarser) than this range.

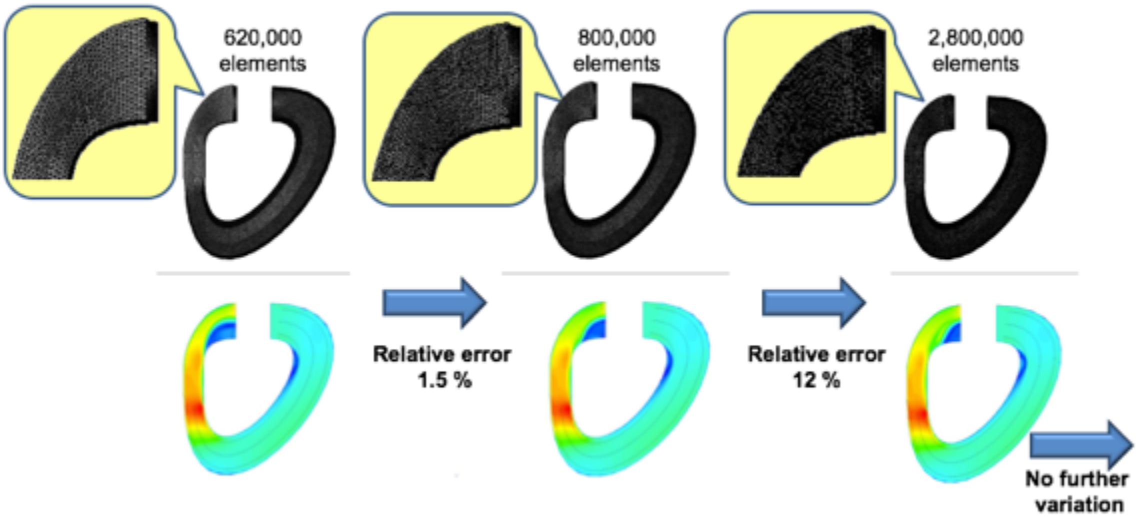

Figure 0–1 - Illustration of the non-exhaustive mesh sensitivity analysis carried out for this Thesis.

B.2. Mesh quality

As already presented in Appendix A, a typical mesh for the wind tunnel case is presented in Figure 0–2, a closer view of the mesh is shown in Figure 0–3 and information on the mesh quality (skewness) is given in Figure 0–4.

The skewness for the mesh of some design points has a maximum value close to 1 or even 1. This is commonly regarded as an indicator of an inadequate mesh. For this particular case, a trade-off must be reached between having an automatic generation of the mesh which is applicable to a very wide range of tunnel designs (therefore a very design-specific mesh set-up cannot be used) and having an adequate mesh quality. It has been checked that the mesh elements with unacceptable skewness are located in the transition from the tunnel duct to the fan and, in some cases, in a very reduced number of elements in the transition from the test section to the tunnel duct. Reducing the skewness would either mean having a design-specific mesh set-up which would not work automatically for all generated tunnel geometries, or increasing the number of elements and thus the computation time to unacceptable levels. Therefore the skewness of these very few elements has been neglected and the meshes with such a high skewness have been considered acceptable. The results obtained with these meshes have been analysed and they have been found to be coherent with the results of other tunnel geometries with meshes of much lower skewness.

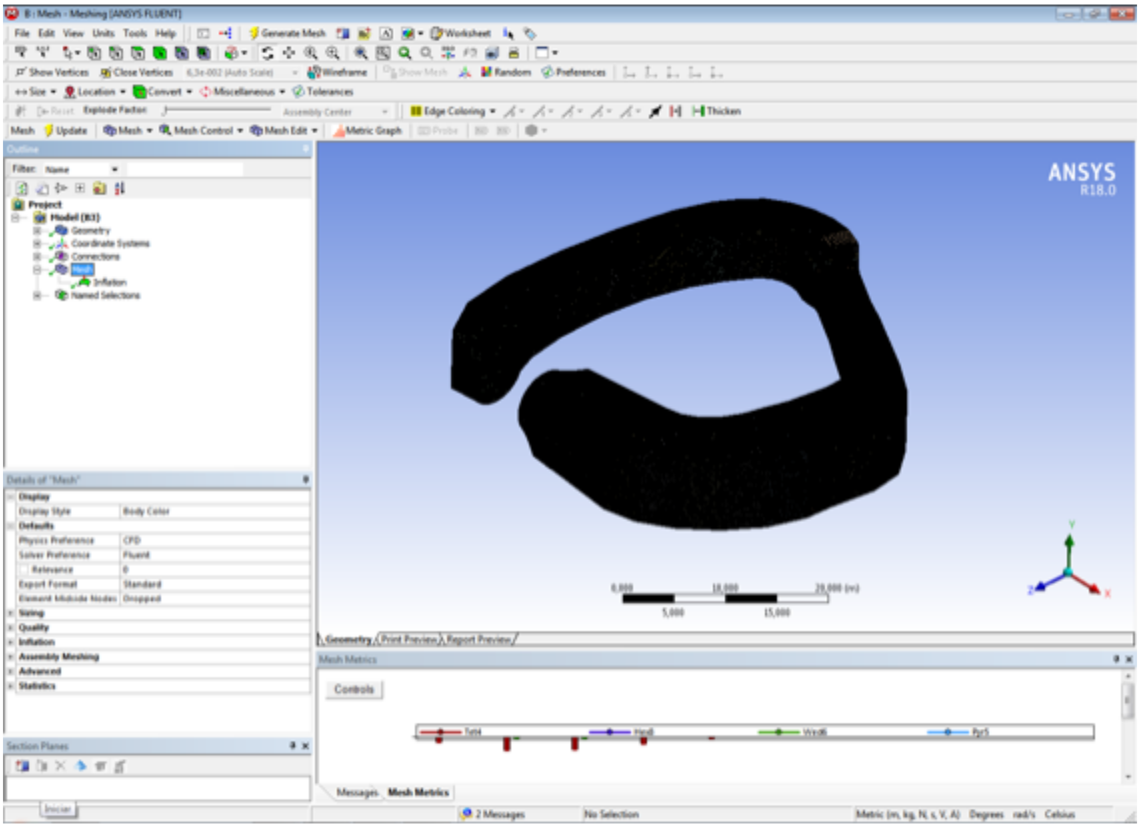

Figure 0–2 - ANSYS mesh generation.

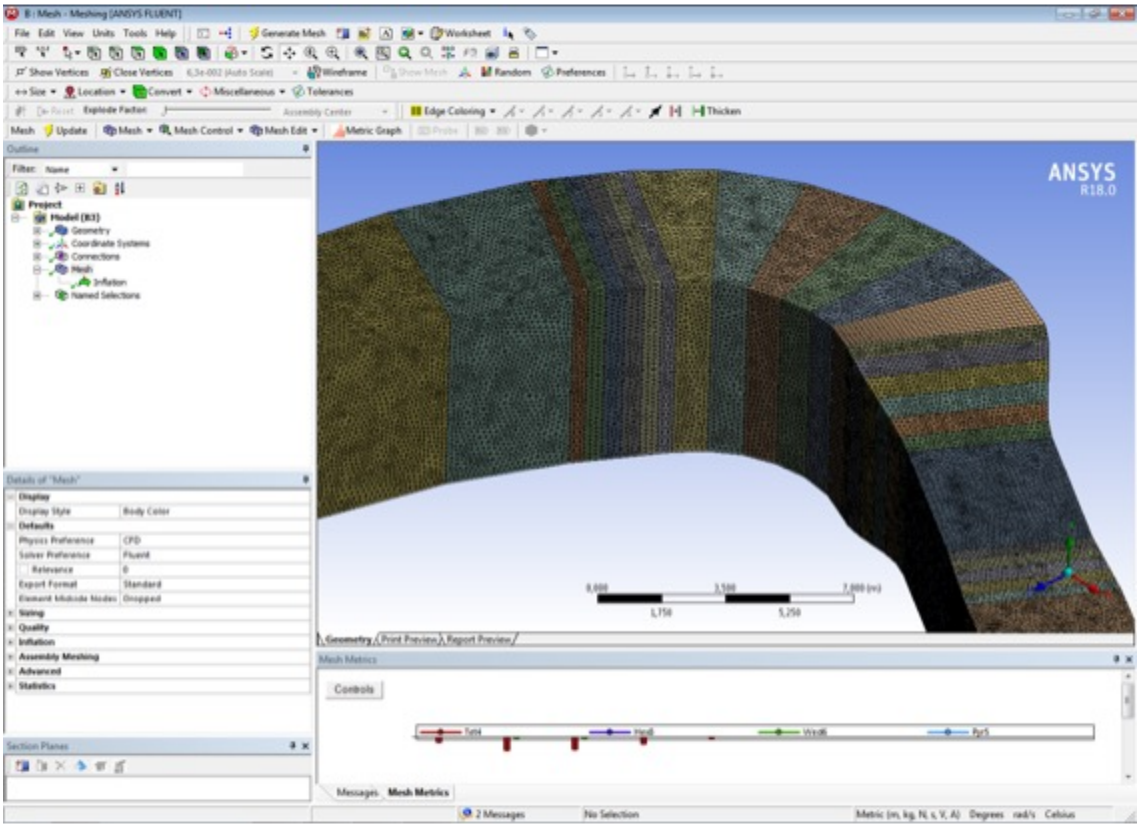

Figure 0–3 - ANSYS mesh generation (detail).

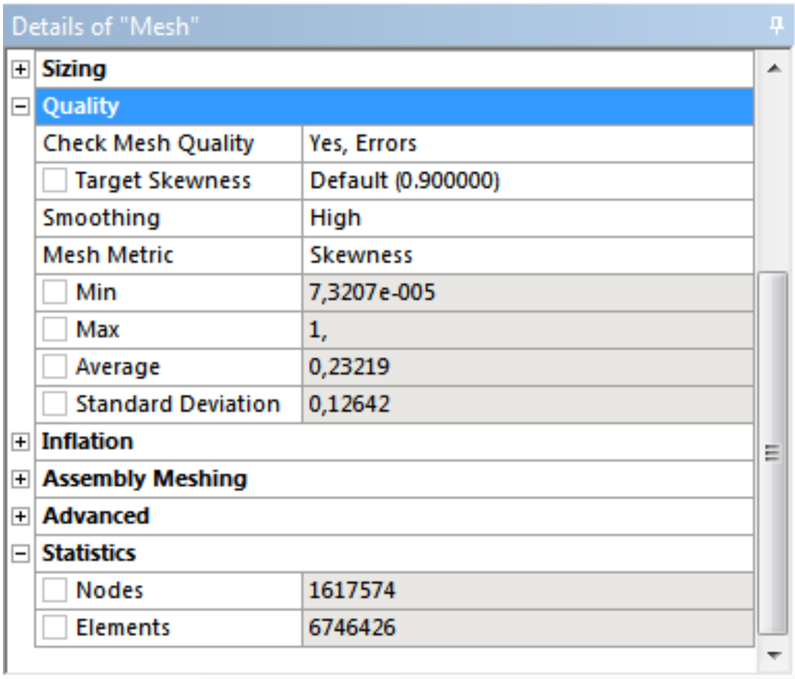

Figure 0–4 - Example mesh quality for most complex design points.